1326

DOE/NASA/0307-1
NASA CR-175058

Improved Piston Ring Materials for 650°C Service

William D. Bjorndahl
TRW Space & Technology Group
Energy Division

March 1986

Prepared for
NATIONAL AERONAUTICS AND SPACE ADMINISTRATION
Lewis Research Center
Under Contract DEN3-307

for

U.S. DEPARTMENT OF ENERGY
Office of Vehicle and Engine R&D

DOE/NASA/0307-1
NASA CR-175058

Improved Piston Ring Materials for 650°C Service

William D. Bjorndahl
TRW Space & Technology Group
Energy Division

March 1986

Prepared for
NATIONAL AERONAUTICS AND SPACE ADMINISTRATION
Lewis Research Center
Under Contract DEN3-307

for
U.S. DEPARTMENT OF ENERGY
Office of Vehicle and Engine R&D

Table of Contents

List of Figures

List of Tables

1. INTRODUCTION

The purpose of this study was to investigate the suitability of various piston ring substrate and coating materials for high temperature (650°C) application. The overall objective of the study was to identify coating and substrate combinations which will survive the operating environment of the advanced low-heat rejection diesel engine. The program was sponsored by the Department of Energy and was technically managed by the NASA Lewis Research Center.

For high temperature advanced diesel engine designs, top ring reversal temperatures at the ring/liner interface in the upper cylinder are projected to be between 590 and 650°C. Figure 1.1 shows expected in-cylinder temperature profiles for a zirconia insulated cylinder. Not only are ring/liner temperatures high in the upper cylinder, but they vary substantially between top and bottom of top ring travel.

Piston ring substrates will require thermal stability in the 480-540°C temperature range. Conventional diesel engine piston rings are cast from martensitic nodular cast irons. On the dynamometer these rings perform satisfactorily for about 600 hours at 425°C. If the temperature goes over 480°C significant loss of hardness and ring tension occurs. This leads to rapid ring wear and increased oil consumption and blow-by. Thus, cast iron rings aren't satisfactory for low heat rejection engines, where the maximum temperatures for the top ring substrate will be on the order of 540°C.

Piston ring coatings for high temperature advanced diesel engine designs will require the following characteristics:

- o high temperature wear resistance
- o low coefficient of friction
- o thermal shock resistance

Present state-of-the-art ceramic piston ring facings are capable of operating for 600 hours at 425°C on the dynamometer. Present state-of-the-art metallic facings are compatible with only a few cylinder liners, providing excessive wear rates with others.

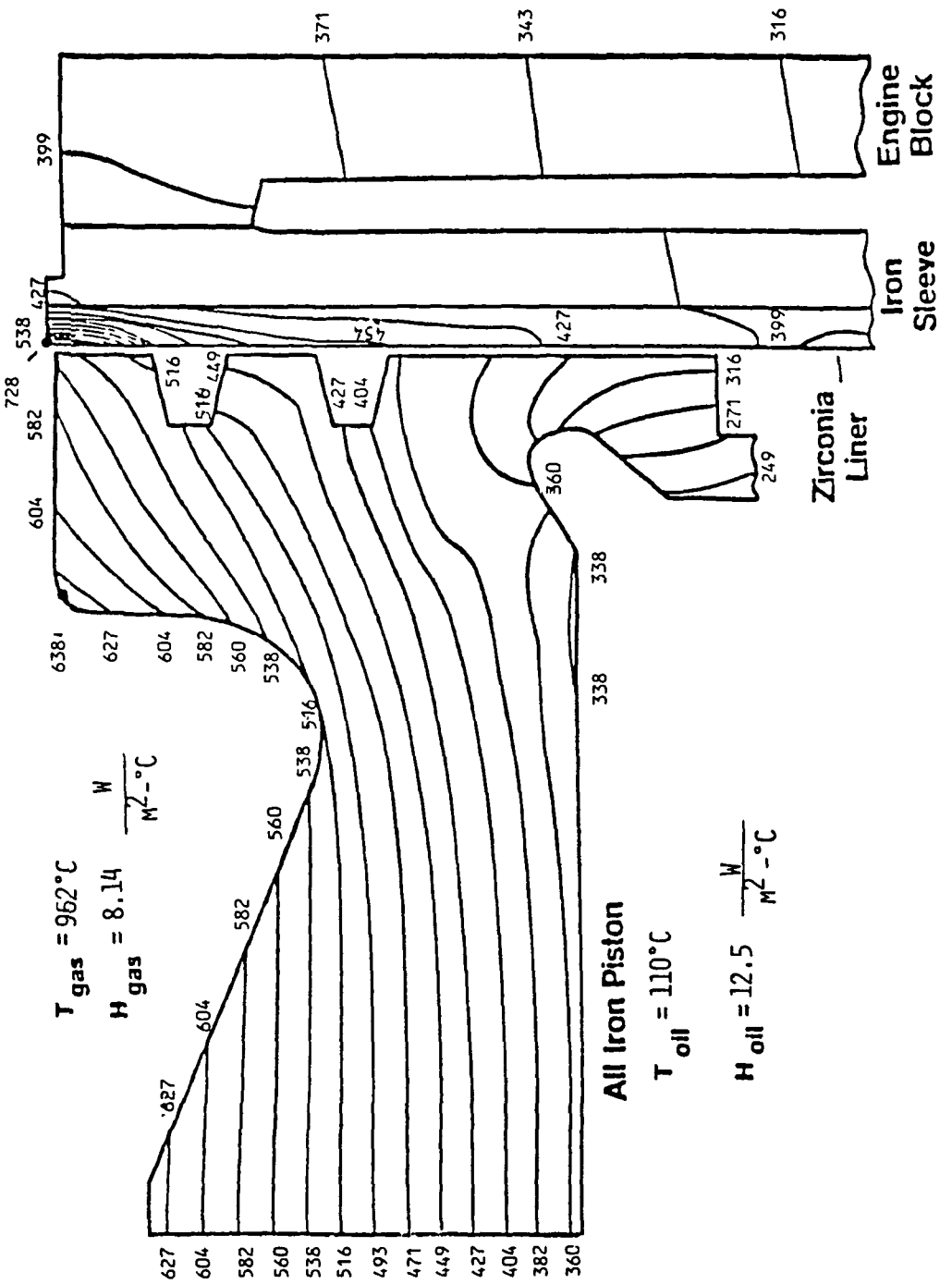

Figure 1-1. Projected In-Cylinder Temperature Profiles for a Zirconia Insulated Cylinder (from Reference 1)

Table 1.1. Candidate Substrate and Coating Materials for High Temperature Piston Rings.

Candidate Substrates	Method of Fabrication
Carpenter 709-2	Hot Forming
440 B	Hot Forming

Candidate Coatings	Method of Application
Al_2O_3/28.5-35 TiO_2/2-4 Y_2O_3	Atmospheric Pressure Plasma Spray (graded)*
ZrO_2/28.5-35 TiO_2/2-4 Y_2O_3	Atmospheric Pressure Plasma Spray (graded and ungraded)*
Al_2O_3/22 ZrO_2/18 TiO_2/5 Y_2O_3	Atmospheric Pressure Plasma Spray (ungraded)*
Mo/27 NiCrBSi	Low Pressure Plasma Spray
WC/20 Co	Plasma Transferred Arc (PTA)
Mo/27 NiCrBSi	PTA
Fe/13 Mo/3B/2Si	PTA

*Two bond coats were investigated; Ni/18-22 Cr and Ni/4.0-5.5 Al

A program was conducted to evaluate candidate piston ring substrate and coating materials for high temperature piston rings. These candidate materials are listed in Table 1.1. Also listed are the methods of fabrication or application. Coatings and substrates were developed and evaluated in separate but parallel efforts in order to save time over a serial development program. High temperature piston ring substrates were hot-formed and evaluated. Coatings were developed on nodular cast iron rings and sleeves and then subjected to thermal shock and wear evaluation. The best coatings and high temperature substrate combinations were then fabricated into rings and evaluated.

2. ATMOSPHERIC PRESSURE PLASMA SPRAY COATING

A major thrust of the coating development effort was the application, by plasma spray coating, of a number of ceramic based compositions. Initially, the program evaluated the following compositions:

- o Graded Al_2O_3/28.5-35 TiO_2/2-4 Y_2O_3
- o Not Graded ZrO_2/28.5-35 TiO_2/2-4 Y_2O_3
- o Graded ZrO_2/28.5-35 TiO_2/2-4 Y_2O_3

The graded alumina composition was chosen for development because it was felt that grading offered a mechanism to improve thermal shock resistance. The zirconia based composition was chosen for its potential high wear and thermal shock resistance.

During the course of thermal shock evaluation, the zirconia composition did not exhibit the thermal shock resistance which was desired, and another ceramic system was added for evaluation. The composiiton of this system was Al_2O_3/22 ZrO_2/18 TiO_2/5 Y_2O_3. The yttria to zirconia ratio in this composition is increased relative to the old composition in order to improve thermal shock resistance.

2.1 GRADED Al_2O_3/TiO_2

An alumina - titania - yttria powder, (Al_2O_3/28.5-35 TiO_2/2-4 Y_2O_3 by weight percent), was plasma sprayed onto cast iron ring substrates. Processing involved grading a bond coat (either Ni-Cr or Ni-Al) into the ceramic layer. The degree of bond coat grading was varied considerably. Figures 2.1 and 2.2 illustrate the extremes to which the grading occured.

Various processing parameters were investigated during coating. These were:

- o degree of grading of bond coat with ceramic
- o bond coat type
- o maximum bond coat flow rate
- o number of grading steps

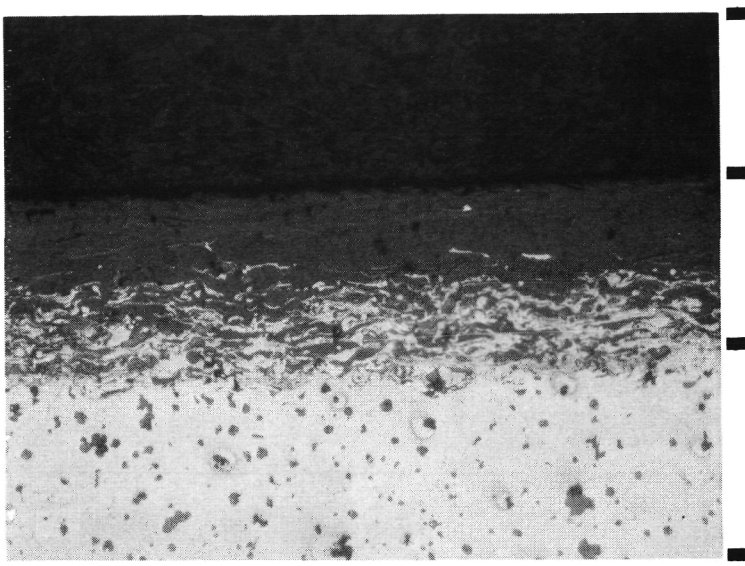

Figure 2.1. Optical photomicrograph of ring from Test #1 (100X)

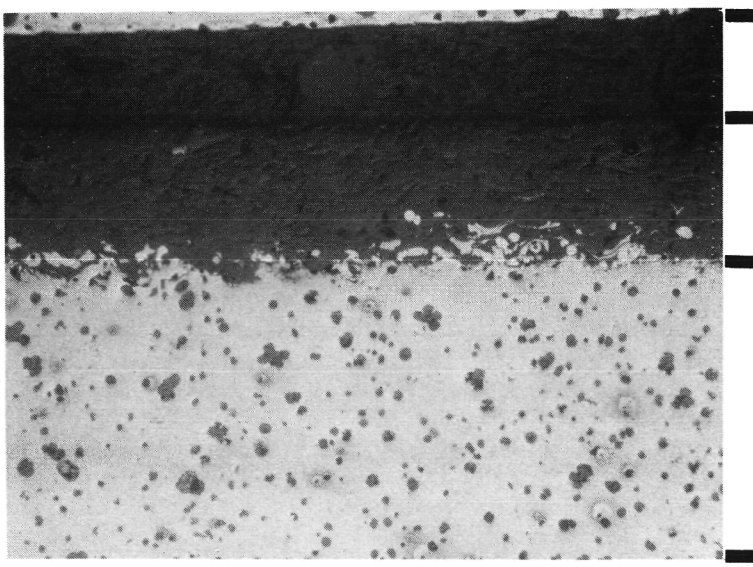

Figure 2.2. Optical photomicrograph of ring from Test #6 (100X)

Evaluation tests were then conducted to determine the effect of changing these parameters. These parameters along with their values during any one particular test are shown in Table 2.1a. The varied parameters are separately broken out and a brief description of each follows in Table 2.1b.

Both Figures 2.1 and 2.2 show the same general features. The substrate is cast iron with nodular graphite inclusions. On top of this is a mixed layer of bond coat and ceramic, with the bond coat showing up as the lighter phase. Above this is a layer of the ceramic material. The obvious difference between the two coatings is the extent of grading of bond coat with ceramic. This observation can be correlated with the parameters listed in Table 2.1a which indicate that the maximum bond coat flow rate was 60.5 g/min in test 1 while for test 6, the maximum bond coat flow rate was 30.2g/min. Therefore, the amount of bond coat observed in the photomicrograph of the test 6 sample should be less than that observed for test 1, which is indeed the case. In addition, the number of grading steps used in test 1 was 10, while the number of grading steps for test 6 was 5. This means that the extent of grading is less in test 6 than in test 1 which is also observed when the two photomicrographs are compared. Representative SEM photomicrographs are shown for tests 1 and 6 in Figures 2.3 and 2.4 respectively. This allows a closer look at the bond coat/ceramic graded region.

After the rings were coated, they were subjected to the following evaluation tests:

- o standard metallurgical section and microscopic inspection
- o microhardness
- o scanning electron microscopy (SEM)
- o thermal shock testing

The coating structures were rated on a scale of 1 to 10 with 1 being unacceptable and 10 being excellent. These results are listed in Table 2.2 along with the results of a number of other evaluation tests.

Table 2.1a. Factorial Data Sheet

Run Seq	1	16	13	3	6	12	9	8	14	4	2	15	10	7	5	11
Test Number	1	2	3	4	5	6	7	8	9	10	11	12	13	14	15	16
Flow N_2 Units	75	75	75	75	75	75	75	75	75	75	75	75	75	75	75	75
Flow H_2 Units	15	15	15	15	15	15	15	15	15	15	15	15	15	15	15	15
Spray Dist, cm	11.4	11.4	11.4	11.4	11.4	11.4	11.4	11.4	11.4	11.4	11.4	11.4	11.4	11.4	11.4	11.4
Power, KW	43.7	44.2	44.2	44.2	44.2	43.7	44.2	43.7	44.2	44.2	44.2	43.7	43.7	43.7	44.2	44.2
X_3 Feed Rate cm/min.	102	102	102	102	254	254	254	254	254	254	254	254	102	102	102	102
X_1 Car. Gas Flow Units	35	38	35	38	35	38	35	38	38	35	38	38	38	35	38	35
X_5 Arbor rpm	400	200	400	200	200	400	200	400	200	400	200	400	400	200	200	200
Arbor Wt, g, w/o caps																
Pre	10509	10506	10500	10507	10509	10514	10514	10506	10506	10503	10510	10507	10507	10504	10502	10517
Post	10555	10587	10587	10545	10543	10531	10547	10582	10570	10532	10552	10572	10562	10590	10523	10546
$X_2(X_6) + X_7$ = Total Number Passes	50	40	40	30	30	20	50	60	40	30	30	40	50	60	30	20
Time Required, sec	120	175	147	91	110	68	89	131	109	69	89	120	120	176	148	92
Hot Dia., cm	11.74	11.81	11.80	11.72	11.74	11.70	11.70	11.76	11.76	11.69	11.72	11.77	11.73	11.81	11.78	11.71
Hot Temp, °C	116	138	166	121	127	116	82	171	138	132	144	121	77	160	127	116
ATM,	1	1	1	1	1	1	1	1	1	1	1	1	1	1	1	1
X_2 Passes per Step	4	2	4	4	2	2	4	4	4	4	2	2	4	4	2	2
X_6 Number of Steps	10	10	5	5	5	5	10	10	5	5	10	10	10	10	5	5
X_7 Spray Depth #4.1 Passes	10	20	20	10	20	10	10	20	20	10	10	20	10	20	20	10
X_4 B/C Powder Type*	43F	450	450	43F	43F	450	450	43F	450	43F	43F	450	450	43F	43F	450
X_{8A} B/C Flow Max	60.5	60.5	60.5	60.5	30.2	30.2	30.2	30.2	60.5	60.5	60.5	60.5	30.2	30.2	30.2	30.2
X_{8B} 4.1 Flow Max	47.0	47.0	47.0	47.0	47.0	47.0	47.0	47.0	47.0	47.0	47.0	47.0	47.0	47.0	47.0	47.0

* Metco 43F Ni/18-22Cr

Metco 450 Ni/4.0-5.5 Al

Table 2.1b. Description of Row Labels Used in Table 3.1a

Flow N_2 Units	Flow rate of nitrogen in arbitrary units.
Flow H_2 Units	Flow rate of hydrogen in arbitrary units.
Spray Distance	Distance form work piece to spray nozzle.
Power	Power to machine.
Feed Rate	Feed rate of the arbor which holds the piston rings.
Carrier Gas	Flow rate of carrier gas in arbitrary units.
Arbor RPM	Rate at which arbor turns.
Arbor Wt G. w/o caps Pre Post	Pre and post weights of loaded arbor
Total Number of Passes	Number of passes that arbor makes during coating operation.
Time Required	Total time required for the coating operation.
Hot Dia.	Diameter of the loaded arbor immediately After a spray operation is complete.
Hot Temp	Temperature of loaded arbor immediately After spraying.
Atm	Pressure in atmospheres at which coating operation took place.
Passes per step	The term "step" refers to each independent vernier setting for the gradated coating. Passes per step is the number of passes at each setting.
Spray Depth Number of Steps	Number of steps made per gradation cycle.
Spray Depth #4.1	Passes made with overlay ceramic only composition (bond coat not included)
B/C Power Type	Type of bond coat used in the gradated coating. The bond coat is either Metco 43F. (Ni/13-22Cr) or Metco 450 (Ni/4.0-5.5 Al).
B/C Flow Max	Maximum flow rate for the bond coat during the dradation cycle.
Flow Max	Maximum flow rate for the material during the coating cycle.

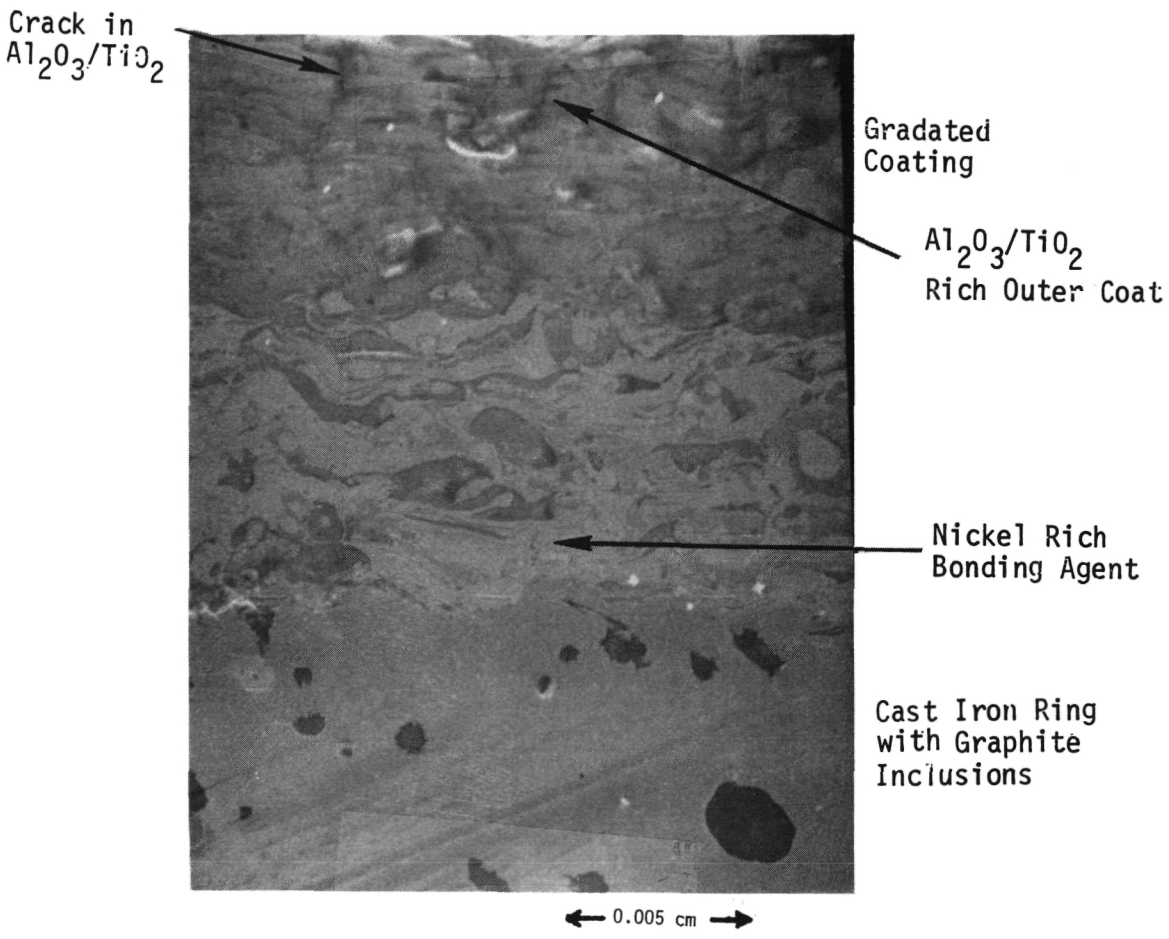

Figure 2.3. SEM photomicrograph of graded alumina coating (test 1) (500X)

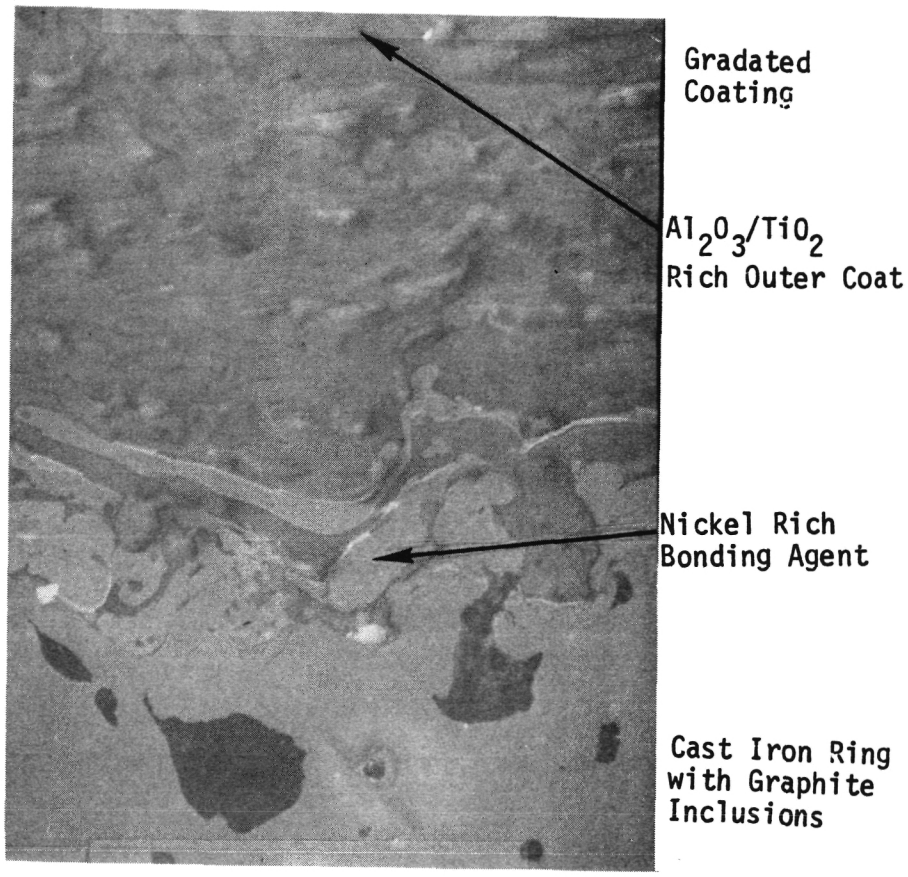

Figure 2.4. SEM photomicrograph of graded alumina coating (test 6) (500X)

Table 2.2. Results of Evaluation Tests Conducted on Graded Al_2O_3/TiO_2 Coated Rings.

Test Number	Microhardness 50g Vickers		Coating Structure Rating	% of Rings With Coating Loss After 400 Thermal Shock Cycles	% of Rings With Coating Loss After 600 Thermal Shock Cycles	% of Rings With Coating Loss After 800 Thermal Shock Cycles	% of Rings With Coating Loss After 1000 Thermal Shock Cycles
	Bond Coat	Ceramic Layer					
1	276	1485	6	0	0	0	0
2	156	1563	7	0	0	0	0
3	165	1485	3	0	0	0	0
4	285	1485	2	0	0	0	25
5	258	1485	1	0	0	0	25
6	207	1604	3	0	0	0	50
7	165	1523	4	0	0	0	50
8	296	1600	2	0	25	25	25
9	195	1485	3	0	0	0	0
10	258	1523	4	0	0	0	0
11	226	1523	5	0	0	0	0
12	165	1523	5	0	0	0	0
13	161	1604	4	0	0	25	25
14	249	1485	5	25	25	25	25
15	266	1488	2	0	25	25	50
16	165	1563	2	0	0	0	0

2.2 ZrO_2/TiO_2 COATINGS

For the zirconia system, two coating schemes were investigated. In one, the bond coat (either Ni-Cr or Ni-Al) was sprayed onto the ring prior to coating with the ceramic layer while in the other scheme, the bond coat was graded into the ceramic layer. Representative photomicrographs for each of these schemes are shown in Figure 2.5.

2.2a NON GRADED ZrO_2/TiO_2

A zirconia based powder with the composition by weight of ZrO_2/28.5-35 TiO_2/2-4 Y_2O_3 was plasma sprayed onto cast iron ring substrates. Except for bond coat grading, the processing variables investigated were the same as those for the graded alumina coating. The factorial data sheet shown in Table 2.1a, except for the grading, was followed during spray coating.

Photomicrographs of a representative ring coated for each set of processing conditions were taken and the coating structure was rated on a scale of 1 to 10. These ratings are given in Table 2.3. Hardness measurements in the bond coat region and ceramic region were also made and These values are also listed in Table 2.3.

2.2b GRADED ZrO_2/TiO_2

The zirconia based powder described in the previous section was plasma sprayed with bond coat grading onto cast iron ring substrates. The processing variables investigated and the factorial program run were the same as those studied for the graded Al_2O_3/TiO_2 coated rings. Coating structure ratings and hardness measurements are listed in Table 2.4.

2.3 THERMAL SHOCK TESTING

Representative ring samples from all the plasma spray tasks underwent thermal shock testing. The thermal shock evaluation test cycled the rings between room temperature and 650°C for 1000 cycles. The temperature cycle for the thermal shock tests is shown in Figure 2.6. Rings were loaded onto an arbor which was mechanically pulled into a tube furnace where they were heated in air to 650°C. This heating cycle took approximately 30 minutes. After

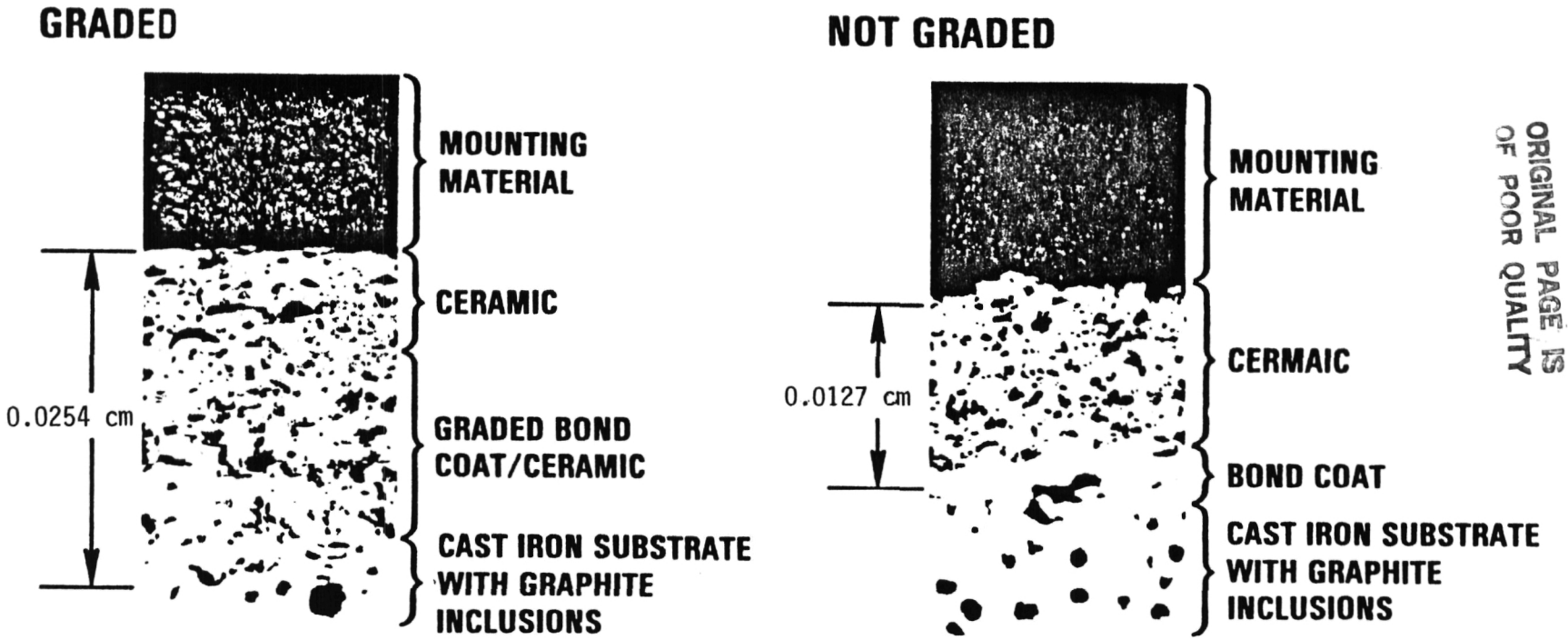

Figure 2.5. Plasma Sprayed Coatings
ZrO_2/28.5-35 TiO_2/2-4 Y_2O_3

Table 2.3. Results of Evaluation Tests Conducted on Ungraded ZrO_2/TiO_2 Coated Rings

TEST NUMBER	MICROHARDNESS 50g VICKERS		Coating Structure Rating	% of Rings with Coating Loss at 400 Thermal Shock Cycles	% of Rings with Coating Loss at 600 Thermal Shock Cycles	% of Rings with Coating Loss at 800 Thermal Shock Cycles	% of Rings with Coating Loss at 1000 Thermal Shock Cycles
	BOND COAT	CERAMIC LAYER					
1	276	1027	6	25	50	100	100
2	161	985	5	100	100	100	100
3	184	1049	7	75	100	100	100
4	258	1006	8	50	75	100	100
5	189	965	9	75	75	100	100
6	161	1006	7	50	75	100	100
7	165	965	8	0	0	75	75
8	226	1027	5	0	0	25	100
9	184	1006	7	100	100	100	100
10	266	1006	4	50	75	75	100
11	258	1049	3	75	75	100	100
12	174	1006	4	50	75	100	100
13	179	1006	6	0	25	50	100
14	258	985	8	75	75	100	100
15	258	1006	7	50	50	75	75
16	145	1006	7	0	25	50	75

Table 2.4. Results of Evaluation Tests Conducted on Graded ZrO_2/TiO_2 Coated Rings.

Test Number	Microhardness 50g Vickers		Coating Structure Rating	% of Rings With Coating Loss After 400 Thermal Shock Cycles	% of Rings With Coating Loss After 600 Thermal Shock Cycles	% of Rings With Coating Loss After 800 Thermal Shock Cycles	% of Rings With Coating Loss After 1000 Thermal Shock Cycles
	Bond Coat	Ceramic Layer					
1	276	1027	4	0	0	50	50
2	161	985	4	50	75	75	75
3	184	1049	6	50	50	75	75
4	25E	1006	5	50	75	75	100
5	18E	965	6	100	100	100	100
6	16E	1006	6	50	100	100	100
7	16E	965	8	75	75	100	100
8	22E	1027	7	50	50	75	75
9	184	1006	5	100	100	100	100
10	26E	1006	6	0	50	75	100
11	25E	1049	4	0	50	75	100
12	17E	1006	8	0	0	75	100
13	17E	1006	8	0	25	75	75
14	25E	985	7	50	50	75	75
15	25E	1006	4	50	50	100	100
16	14E	1006	9	25	25	50	50

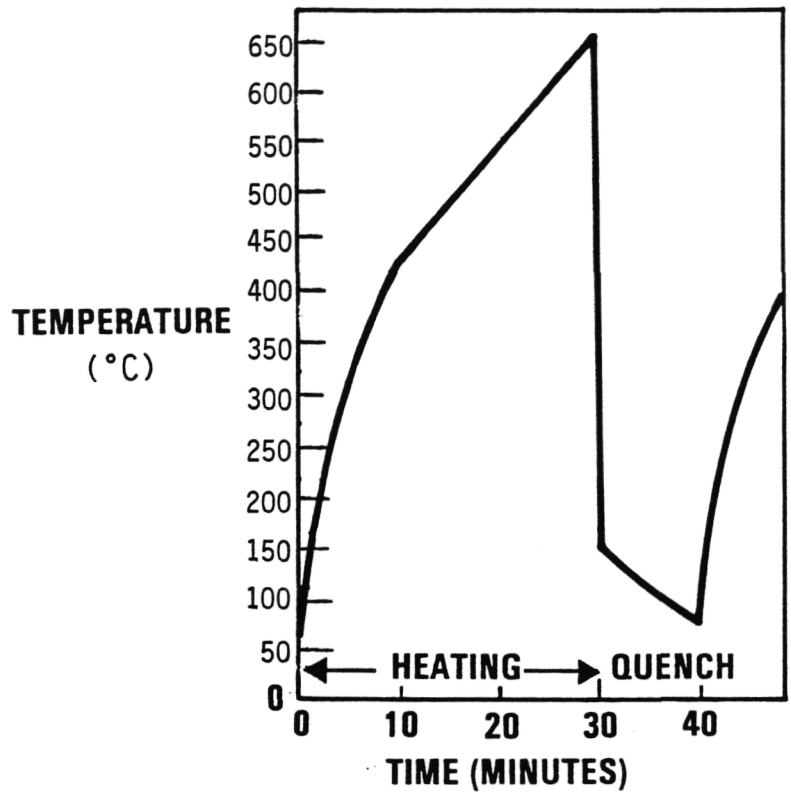

Figure 2.6. Temperature Cycle for Thermal Shock Testing

reaching 650°C, the rings were mechanically plunged into a quench medium composed of a 50/50 mixture of water and ethylene glycol.

Upon periodic visual examination, if a ring exhibited coating loss, then it was counted as a failure. The percentage of rings which failed during thermal shock testing is shown in Figure 2.7 as a function of thermal shock cycles completed.

During and after thermal shock testing, representative rings were examined using the metallograph and SEM. The alumina system exhibited better resistance to failure than did the zirconia system. Differences between the failure percentages of the graded and ungraded zirconia based systems were slight. A closer microscopic examination of cross sections of the failed portions of graded and ungraded rings did however lead to a significant observation. Failures were found to occur at the outer layer of bond coat grading, that is, separation of the oxide layer occured at the outer bond coat ceramic interface. This was found to be true regardless of the extent of the grading. Figure 2.8 shows photomicrographs taken from the good section and a failed section of a single ring, and illustrates the phenomenon. It may be that the metallic phase is undergoing some deformation and relieving thermal stresses in the ceramic which prevents the failure from extending into the bond coat/ceramic region.

Another important finding was the observation that material loss in the form of localized pitting is occurring from the coating surface of thermal shock tested rings. Photomicrographs of a before and after thermal shock tested ring surface are shown in Figure 2.9. Before thermal shock testing, there is a lot of loosely bound material on the surface, and it is expected that this material would come off during testing. Surface pitting however was not expected. This mechanism of surface material loss, i.e., loss due to thermal stresses alone was previously unrecognized. In the past, wear testing immediately followed thermal shock testing and ring surfaces were not examined until after completion of the wear tests. All the material loss which was observed at that point was attributed to wear alone. An explanation for this phenomenon is that thermal stress between particles is leading to ejection of material from the coating surface. This explanation correlates with the observation that the pits are about the same size as the individual particles.

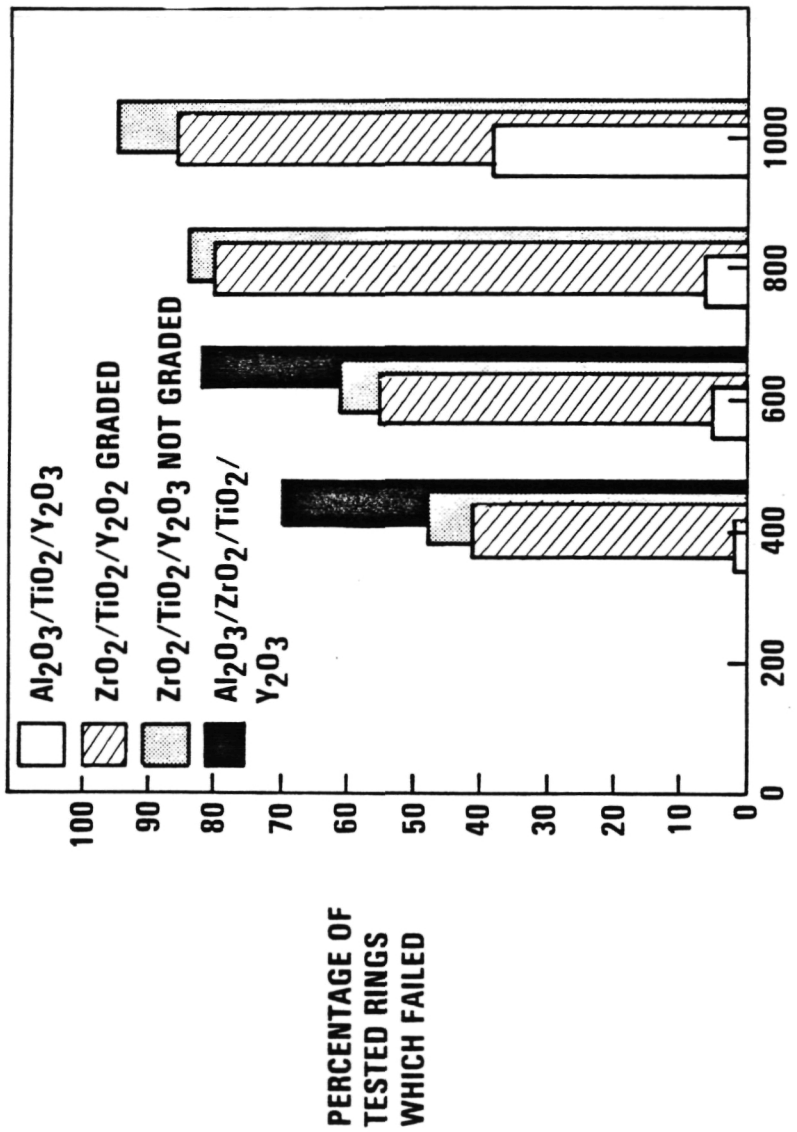

Figure 2.7. Plasma Sprayed Coatings Thermal Shock Test Results.

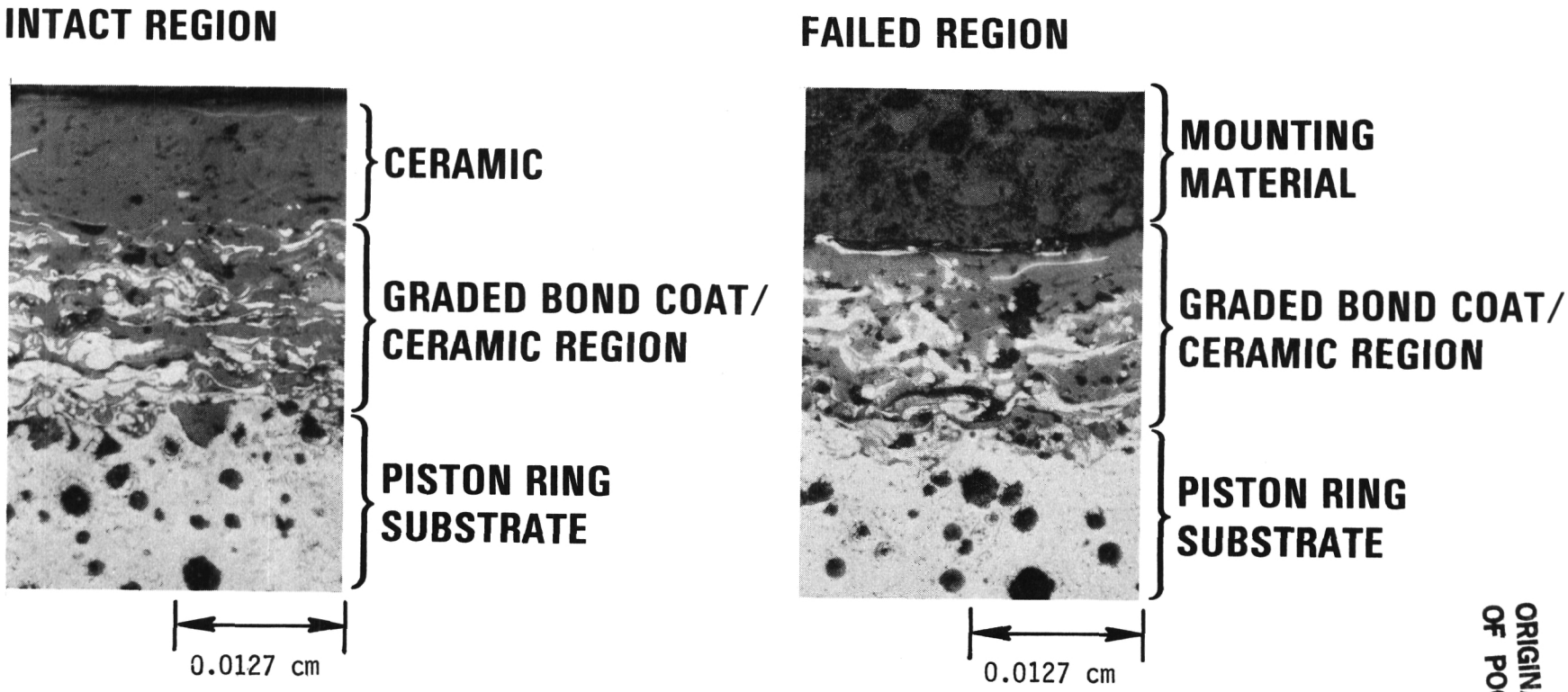

Figure 2.8. Plasma Sprayed $ZrO_2/TiO_2/Y_2O_3$
Thermal Shock Test Failure

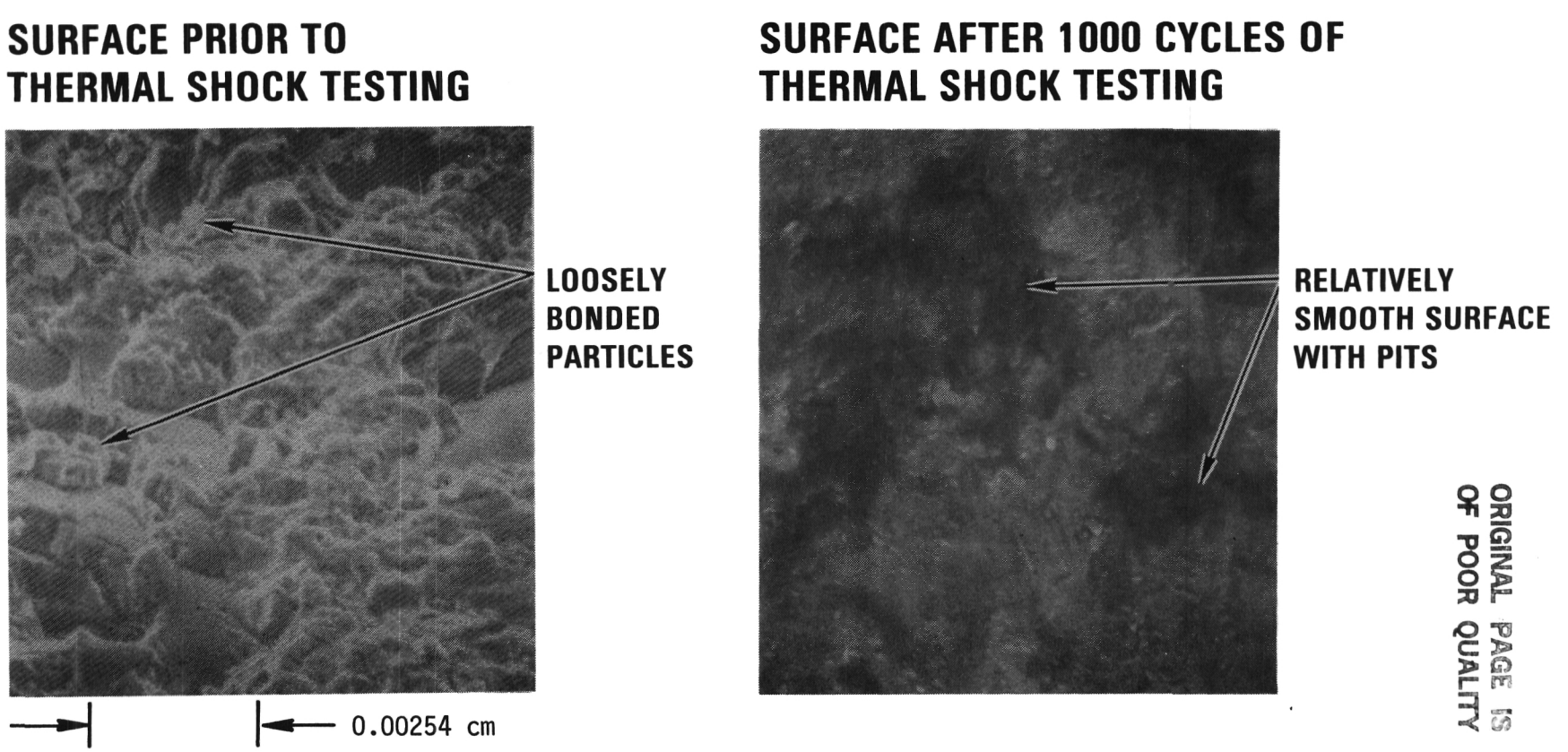

Figure 2.9. Plasma Sprayed Coatings
Loss of Surface Material Due to Thermal Shock Testing
$Al_2O_3/TiO_2/Y_2O_3$

Table 2.5 lists thermal expansion coefficients for various constituents of the mechanically mixed powders which were plasma sprayed. It is interesting to note that the alumina-titania system (for which the thermal expansion coefficients are not too greatly different) experienced fewer thermal shock failures than did the zirconia-titania system (for which the thermal expansion coefficients have a greater magnitude of difference). Another observation which was made during examination of the failed sections of thermal shock tested rings is that failure in more than 90% of the examined sections occurred at the outer edge of the bond coat grading.

Table 2.5 Mean Linear Thermal expansion Coefficients for Selected Materials (Reference 2).

Material	Mean Linear Thermal Expansion Coefficient ($cm/cm°C \times 10^6$)
Al_2O_3	8.8
TiO_2	7.8
ZrO_2 (stabilized)	10.0
Y_2O_3	9.3
Carbon Steel	9.5
440B Stainless	5.6
Nodular Cast Iron	6.6

3. MOLYBDENUM BASED LOW PRESSURE PLASMA SPRAY COATING

A molybdenum based powder with the composition Mo/27 NiCrBSi was plasma sprayed onto nodular cast iron ring substrates. The variables investigated are listed in Table 3.1 along with the two levels which were looked at for each factor in the testing. The plasma parameters and their values which were maintained constant during this testing are listed in Table 3.2. Table 3.3 shows the test variables for each of the 16 tests which were conducted. Representative photomicrographs of cross sections of the rings which were sprayed are shown in Figures 3.1 and 3.2.

The photomicrographs appear to indicate that more than one powder composition was sprayed. For example, in Figure 3.1, the dark phase (Mo) which shows up in the etched cross section appears to be present in the same amount as the light NiCrBSi phase. In Figure 3.2 however, there is considerably more NiCrBSi present than there is Mo. Another distinguishing feature observed in this last figure is the spherical nature of the dark phase indicating that complete melting of Mo did not occur during spraying. This causes some of the non-melted Mo particles to bounce off the substrate thus leading to the observed enrichment of the NiCrBSi phase. This loss of material is confirmed by the deposition effeciencies listed in Table 3.3. Test 1 had a very high deposition efficiency (100%) indicating that all the sprayed material ended up on the ring arbor, and test 3 had a very low deposition efficiency (28% due to the loss of Mo during spraying).

This problem can be explained by the relative sizes of the molybdenum and NiCrBSi particles which are sprayed and the relative times needed to heat them to their respective melting points. Gerdeman and Gecht (2) analyze this problem based on an analysis of heat transfer to a particle in a plasma, and derive the following equation for the ratio of particle diameters for two different materials.

$$\frac{D_A}{D_B} = \frac{A\ (C_p T_M + H_f)_B}{B\ (C_p T_M + H_f)_A} \qquad [1]$$

Table 3.1. Factors Evaluated in Low Pressure Plasma Spray Coating

Factor	Explanation	Low Level	High Level
X_1	Vacuum chamber holding pressure (Pa)	5.1×1^4	1.7×10^4
X_2	Gun-to-work distance (cm)	20	36
X_3	Powder feed rate (g/c)	1.0	1.3
X_4	Carrier gas pressure (Pa)	2.75×10^5	4.12×10^5
X_5	Grove depth (cm)	0.031	0.051
X_6	Preheat time (min)	1	3

Table 3.2. Plasma Parameters Maintained Constant During Low Pressure Plasma Spray

Voltage*	75 - 80 V
Current	430 - 450 A
N_2 flow rate (arbitrary units)	100
H_2 flow rate (arbitrary units)	15
Arbor Rotation Speed rpm	150

* Power level constant at 35 kW

Table 3.3. Factorial Data Sheet for Low Pressure Plasma Spray Coating.

Run Seq	Test No.	Ref Vern Set		Flow H_2 Units	Flow H_2 Units	Spray Dist (cm)	Power KW V A		Carr. Gas Flow Units (Pa x 10^{-5})	Arbor RPM				2 Arbors/10 /Test Arbor Wt. G. w/o caps Pre	Post	Net Wt. Gain	Total Powder Used	Time Req'd Sec.	Hot Dia. (cm)	2 Min. Post Spray Hot Temp °C	Pressure (Pa x 10^{-0})	Groove Depth (cm)	Pre-Heat Time Sec	Deposit Efficiency
3	1	48		100	15	20	36.9 82/450		2.75 34	150				11650 11195	11820 11370	170 180	171 N/A	3:00 3:00	11:86 11.85	237 216	1.7	0.051	60	99% 105%
13	2	48		100	15	20	36.9 82/450		4.12 34	150				11098 11103	11198 11215	180 112	228	4:00 4:00	11:82 11:83	204 274	5.1	0.031	180	44% 49%
6	3	48		100	15	36	36.9 82/450		2.75 34	150				11675 11347	11785 11475	90 188	339 473	7:00 8:30	11:70 11:72	149 177	1.7	0.051	180	28% 27%
9	4	48		100	15	36	36.9 82/450		2.75 34	150				11138 11815	11275 11887	137 72	399 399	7:00 7:00	11.81 11.72	204 204	5.1	0.031	60	34% 18%
15	5	60		100	15	20	36.9 82/450		4.12 34	150				11640 10986	11915 11270	275 284	296	4:00 4:00	11.89 11:98	271 282	1.7	0.031	180	92% 95%
1	6	60		100	15	20	36.9 82/450		4.12 34	150				11460 11547	11619 11610	159 63	356 316	4:50 4:00	11.86 11.74	177 160	5.1	0.051	60	53% 21%
10	7	60		100	15	36	36.9 82/450		4.12 34	150				11175 11517	11265 11645	90 128	399	7:00 7:00	11.72 11.76	149 149	1.7	0.031	60	17% 24%
5	8	60		100	15	36	36.9 82/450		2.75 34	150				11258 11310	11412 11480	158 170	399	7:00 7:00	11.79 11.82	188 163	5.1	0.051	180	29% 32%
12	9	60		100	15	36	36.9 82/450		2.75 34	150				11080 11550	11115 11671	035 111	399	7:00 7:00	11.68 11.79	238 204	5.1	0.031	180	6% 22%
7	10	60		100	15	36	36.9 82/450		4.12 34	150				11630 11027	11815 11270	187 243	666	9:00 9:00	11.73 11.82	149 163	1.7	0.051	60	26% 36%
16	11	60		100	15	20	36.9 82/450		4.12 34	150				11683 11108	11799 11241	116 133	296	4:00 4:00	11.83 11.86	216 260	5.1	0.231	60	38% 45%
2	12	60		100	15	20	36.9 82/450		2.75 34	150				11558 11150	11807 11305	250 155	222	3:00 3:00	11.90 11.85	188 160	1.7	0.051	180	111% 68%
8	13	48		100	15	36	36.9 82/450		4.12 34	150				11710 11115	11710 11297	210 282	513	9:00 9:00	11.85 11.87	227 204	5.1	0.051	60	40% 35%
11	14	48		100	15	20	36.9 82/450		4.12 34	150				11065 11533	11190 11705	125 172	399	7:00 7:00	11.77 11.82	204 221	1.7	0.031	180	31% 43%
4	15	48		100	15	20	36.9 82/450		4.12 34	150				11680 11232	11752 11307	52 75	188	3:00 3:30	11.89 11.78	232 221	5.1	0.051	180	42% 39%
14	16	48		100	15	20	36.9 82/450		2.75 34	150				11580 11117	11802 11355	240 238	228 278	4:00 4:00	11.89 11.92	238 232	1.7	0.031	60	105% 104%

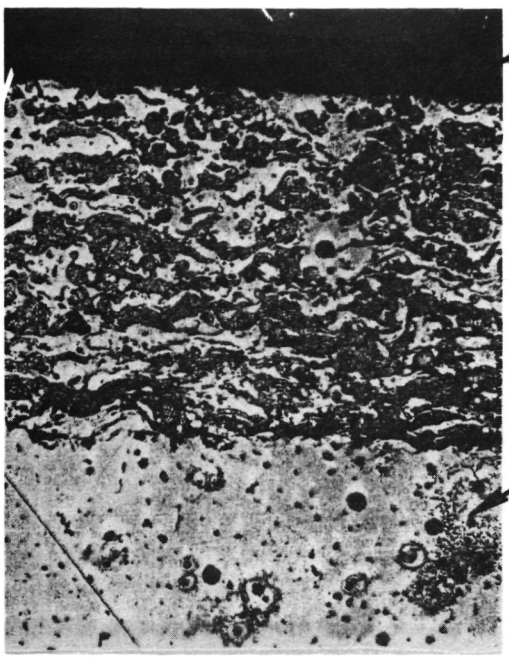

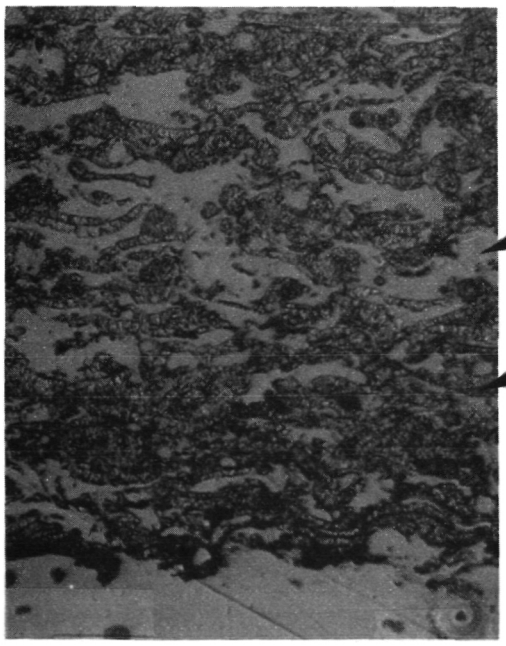

Figure 3.1. Photomicrographs of Cross Section of Ring Sprayed in Test 1 of Low Pressure Plasma Spray Coating Task.

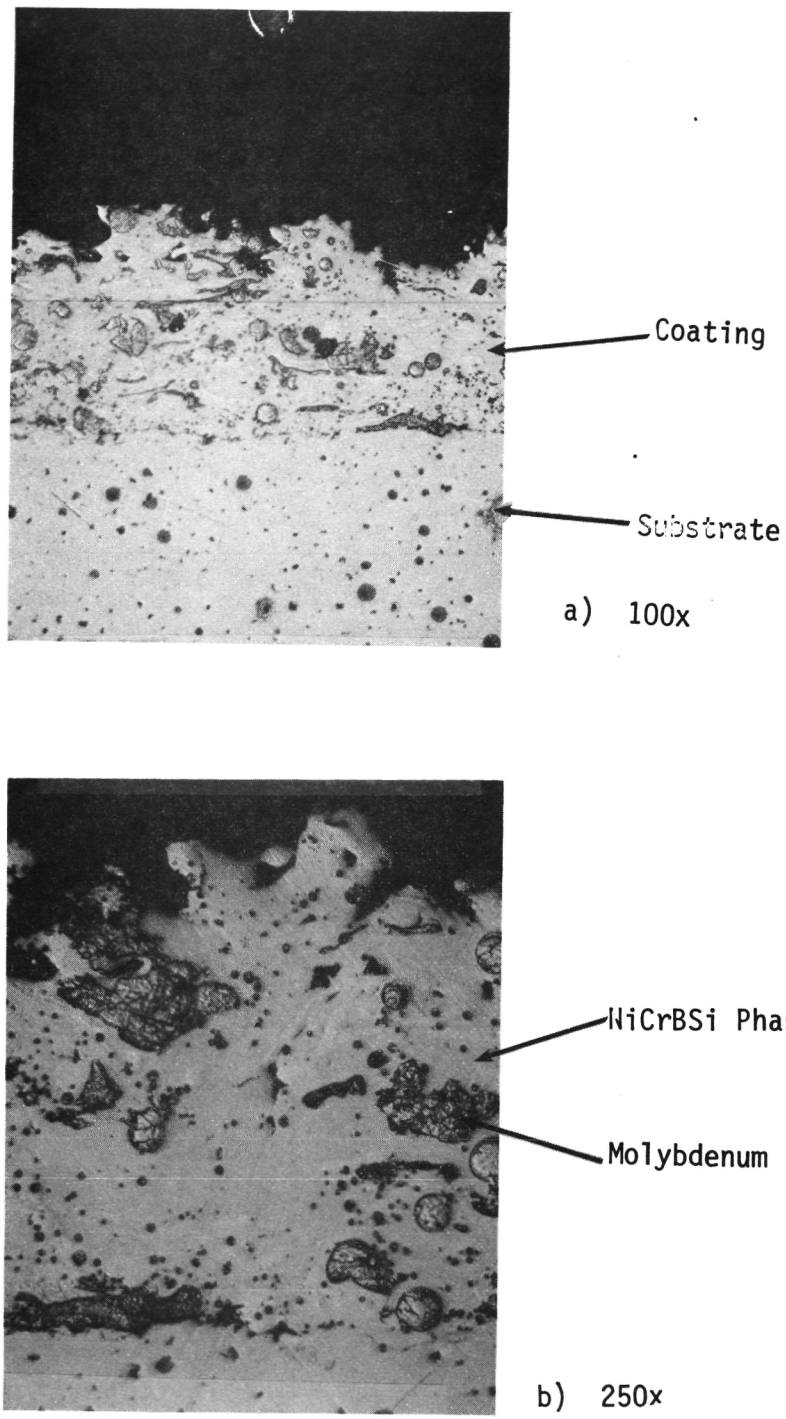

Figure 3.2. Photomicrographs of Cross Section of Ring Sprayed in Test 3. Low Pressure Plasma Spray Coating Task.

where ρ_A and ρ_B are the densities of particles A and B respectively, Cp is the specific heat, T_M is the temperature increase needed to melt the particle, and H_f is the heat of fusion.

When one substitutes physical properties for molybdenum and NiCrBSi for A and B in the above equation, one finds that the ratio of molybdenum particle diameter to NiCrBSi particle diameter should be 1.05. Photomicrographs appear to indicate a larger molybdenum particle diameter to NiCrBSi particle diameter ratio. Specification sheets on the powder were reviewed and it was found that most of the molybdenum powder fell within the size range of 44 to 105 microns while most of the NiCrBSi powder was less than 53 microns in particle size diameter. Better size control is needed to alleviate this problem.

The results of evaluation tests which were conducted on the coated rings are shown in Table 3.4. Microhardness values are given for both the Mo and NiCrBSi phases with the later giving higher hardness values. Comparative bond strengths as measured by the twist test are also shown in this Table. In the twist test, half of the ring is held in a fixture while the other half is bent until the coating parts from the ring groove. The angle through which the half ring has been bent when parting occurs is then recorded. Table 3.4 shows average values for these angles along with the observed range for these angles. The range is the difference between the high and the low value recorded for 10 tests. The coatings were rated prior to thermal shock testing and these ratings are also given in Table 3.4. A low rating indicates a coating of poor quality while a high rating indicates excellent quality.

Thermal shock testing was conducted on these rings and representative photomicrographs of tested rings are shown in Figure 3.3 and 3.4. All rings failed after 400 cycles of testing. This system exhibited a selective dissolution of the molybdenum phase rather than the coating loss observed in the plasma sprayed oxide systems. Figure 3.3 shows the disappearance of the Mo phase and the appearance of what is thought to be a breakdown product of the ethylene glycol in the quench medium. The NiCrBSi phase is retained for the most part. Figure 3.4 shows deep pitting. In this case there is also evidence that the Mo phase is selectively disappearing from the surface, but there also appears to be less of the NiCrBSi phase in the pitted regions, probably due to the loss of any surrounding Mo phase to which it might have been attached.

Table 3.4. Results of Evaluation Tests Conducted on Low Pressure Plasma Spray Coated Rings

Test No.	Microhardness Vickers 50g		Bond Meas. by Twist		Visual Coating Rating*
	Moly	NiCrBSi	Avg.	Range	
1	524	1027	59	45	8
2	655	1095	53	10	8
3	677	1049	34	10	2
4	480	1145	41	35	3
6	540	1197	56	15	5
6	501	891	30	10	10
7	566	985	30	0	4
8	549	1006	35	15	2
9	623	1049	41	5	2
10	447	1027	22	5	3
11	557	1313	34	10	5
12	524	1313	40	10	8
13	566	1120	31	5	2
14	644	985	36	5	3
15	726	1120	43	10	7
16	540	1095	53	5	6

* 10 = Excellent; 1 = Unacceptable

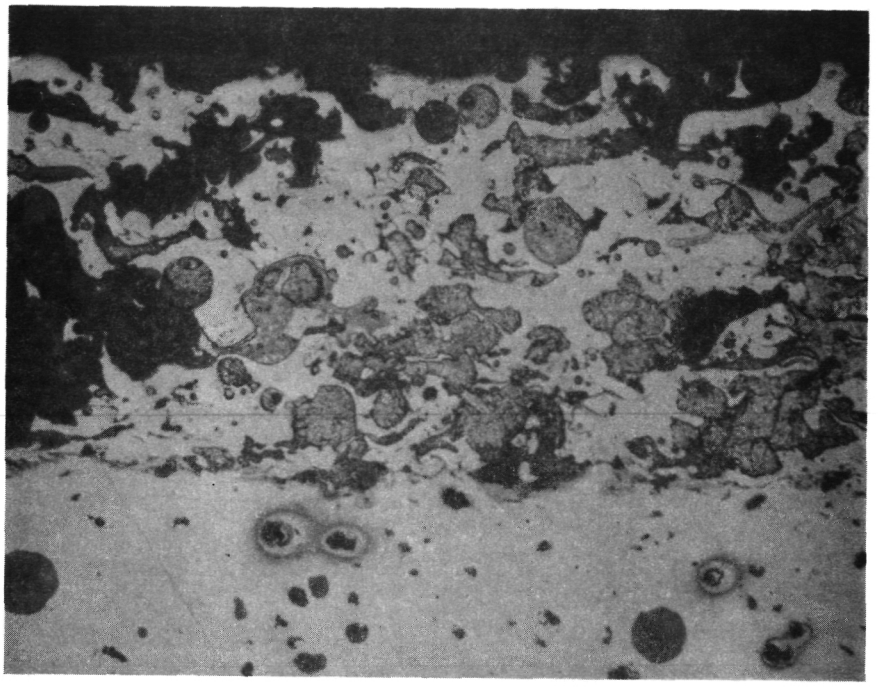

Figure 3.3. Photomicrograph of Mo Based Low Pressure Plasma Sprayed Ring from Test 6 After 400 Cycles of Thermal Shock Testing (250x).

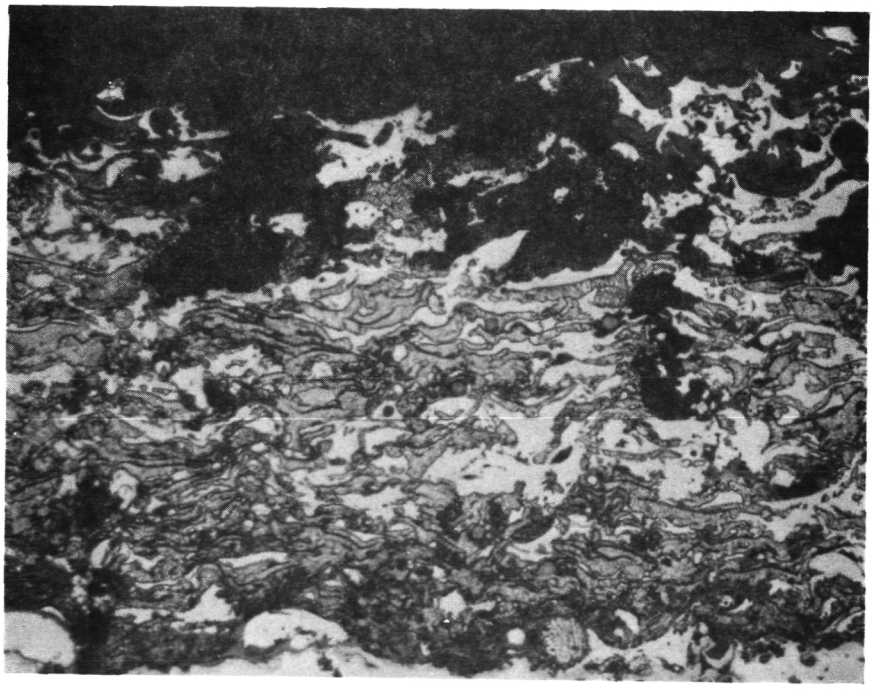

Figure 3.4. Photomicrograph of Mo Based Low Pressure Plasma Sprayed Ring from Test 4 After 400 Cycles of Thermal Shock Testing (250x).

In developing the procedures and solving initial problems in operating the system, the following items of significance have been established:

1. Organic binders which are used on a broad commercial scale to produce coated metallic particles by combining small particles to produce an agglomerated particle or to coat a center particle with an outer layer of coating, produce a significant amount of soot when sprayed in a low-pressure environment. Further work is necessary, but it appears that the soot can have a deterimental effect on properties of the final coating.

2. In previous preliminary work in developing coatings applied by low-pressure plasma spraying, control of ring temperature to avoid permanent loss of tension has been identified as a major problem in coating cast iron rings. In work conducted to date in the program, it has been established that the following approach exists to overcome this problem: use a short load length of rings (5.08 cm) rather than a normal (10.2 cm) load length and use tooling to act as a heat sink to avoid excessive temperature build-up within the rings.

4 PTA METALLIC COATINGS

In the program, three material compositions were applied to nodular iron sleeves by the plasma transferred arc (PTA) process. In this process, an arc is formed between the work piece and the plasma gun and the powdered coating material is heated and transferred to the work piece in this arc. The sleeve is rotated underneath the arc until a complete ring of the coating, which has the appearance of a weld bead, is formed around the circumference of the sleeve. Six to eight rings are coated per sleeve. Afterwards, the individual rings are separated from the sleeve and ground to the final ring shape. Three compositions were investigated: tungsten carbide in a metallic matrix (WC/40 NiCr B Al/10 Co), a molybdenum based composition (Mo/27 NiCrBSi), and an iron based composition (Fe/13 Mo/3 B/2 Si).

The major problems associated with this process are controlling the width and depth of the coating, and minimizing mixing of the coating with the substrate. Representative photomicrographs of cross sections for the tungsten carbide and molybdenum systems are shown in Figures 4.1 and 4.2 respectively. The characteristic widths and depths for these coatings, which are shown in Tables 4.1 and 4.2 are greater than one would like, particularly with respect to the depth of penetration which ideally should be between 0.254 and 0.508 mm (10 and 20 mils) in thickness. It was found during coating of the molybdenum based material that the material had a tendency to flow very easily and form wide deposits. Lower substrate temperatures would tend to alleviate this problem except that porosity and cracking develop. A minimum substrate temperature of 538°C was needed to prevent this. A single pre-heat temperature of 593°C was used for all the tests. As these problems were identified prior to this study, a number of processing parameters were varied during coating in an attempt to minimize those effects on the coating. These are shown in Tables 4.3 and 4.4. The effects of changing the processing parameters were analyzed and it was found that both coating depth and width correlated well with the parameter, (Arc current x arc voltage)/(Powder feed rate x work piece travel speed), where the work piece travel speed is the linear rotation speed of the outside surface of the sleeve. Plots of this correlation are shown in Figures 4.3 and 4.4 for the tungsten carbide and molybdenum containing coatings respectively.

Thought has been given as to what might be done to bring coating dimensions in line with what is desired. Arc current and voltage would be

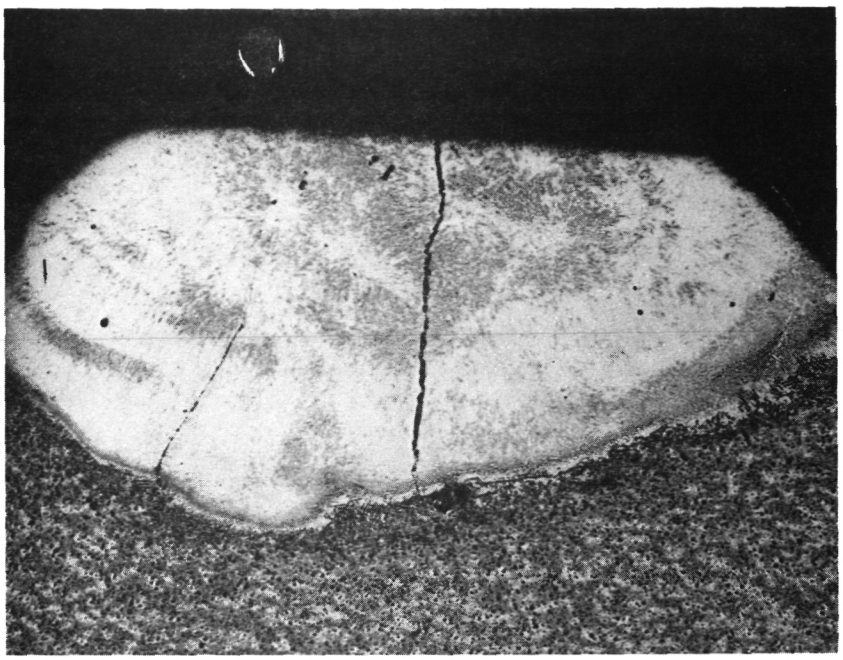

Figure 4.1. Photograph of Cross Section of Tungsten Carbide Based PTA Coated Nodular Cast Iron Ring. (20x)

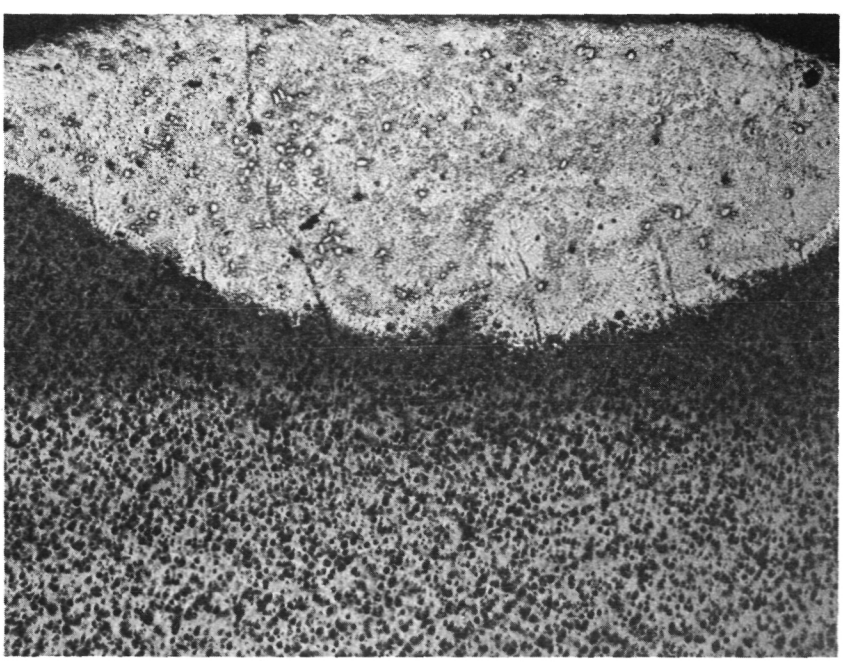

Figure 4.2. Photomicrographs of Cross Section of Molybdenum Based PTA Coated Nodular Cast Iron Ring. (20x)

Table 4.1. Characteristics of WC Based PTA Coatings

Test Number	Width of Deposit cm (mils)	Depth of Deposit	Interfacial Region
1	0.500 (197)	0.170 (66.9)	0.020 (7.9)
2	0.700 (276)	0.275 (108.0)	0.035 (13.8)
3	0.375 (148)	0.175 (68.9)	0.010 (3.9)
4	0.550 (217)	0.260 (102.0)	0.015 (5.9)
5	0.425 (167)	0.150 (59.1)	0.025 (9.8)
6	0.600 (236)	0.135 (53.1)	0.025 (9.8)
7	0.295 (116)	0.150 (59.0)	0.015 (5.9)
8	0.450 (177)	0.200 (78.7)	0.020 (7.9)

Table 4.2. Characteristics of Mo Based PTA Coating

Test Number	Width of Deposit cm (mils)	Depth of Deposit	Interfacial Region
1	0.65 (256)	0.190 (74.8)	0.010 (3.9)
2	0.800 (315)	0.315 (124.0)	0.015 (5.9)
3	0.775 (305)	0.240 (94.5)	0.010 (3.9)
4	0.750 (295)	0.250 (98.4)	0.020 (7.9)
5	0.550 (217)	0.170 (66.9)	0.010 (3.9)
6	0.725 (285)	0.185 (72.8)	0.0125 (4.9)
7	0.525 (207)	0.145 (57.1)	0.010 (3.9)
8	0.550 (217)	0.185 (72.8)	0.015 (5.9)

Table 4.3. Test Matrix Followed During PTA Coating with Tungsten Carbide Based Material.

Test No.	X_1 Arc Current (amps)	X_2 Arc Voltage (volts)	X_3 Travel Speed (cm/min.)	X_4 Powder Feed Rate (g/min.)	X_5 Preheat Temp. (°C)
1	80	24	30.5	2.1	427
2	100	24	30.5	1.6	593
3	80	22	30.5	1.6	427
4	100	22	30.5	2.1	593
5	80	24	40.6	2.1	427
6	100	24	40.6	1.6	593
7	80	22	40.6	1.6	427
8	100	22	40.6	2.1	593

Table 4.4. Test Matrix Followed During PTA Coating with Molybdenum Based PTA Coating.

Test No.	X_1 (amps)	X_2 (volts)	X_3 (cm/min.)	X_4 (g/min.)	X_5 (°F)
1	65	24	30.5	1.6	866
2	75	24	30.5	2.1	866
3	65	22	30.5	2.1	866
4	75	22	30.5	1.6	866
5	65	24	40.6	1.6	866
6	75	24	40.6	2.1	866
7	65	22	40.6	2.1	866
8	75	22	40.6	1.6	866

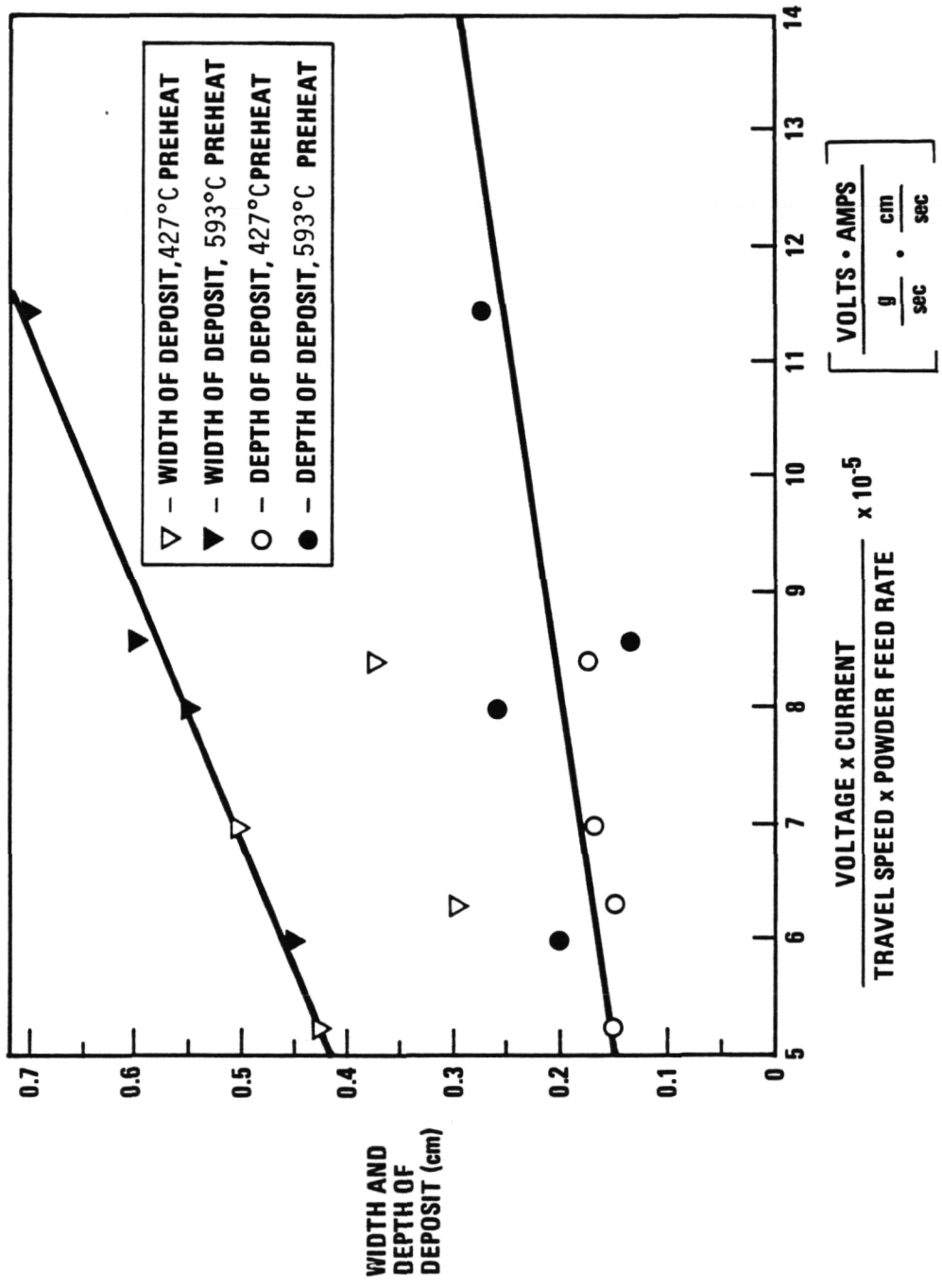

Figure 4.3. Widths and Depths of WC-Based Coatings as a Function of Processing Parameters.

Figure 4.4. Widths and Depths of Mo-Based PTA Coatings as a Function of Processing Parameter.

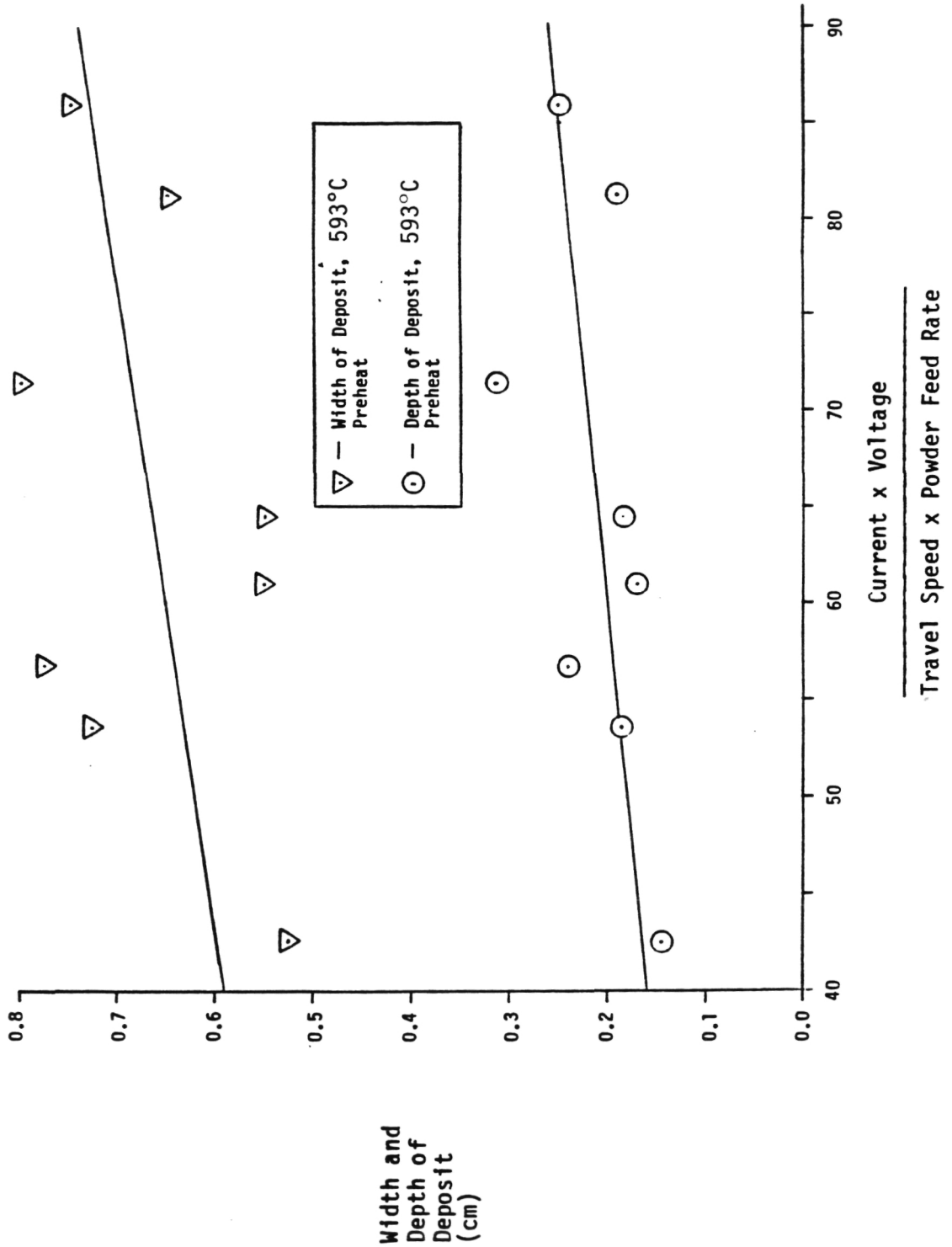

somewhat difficult to vary outside of the range which has been up to now investigated. The problems that are encountered here are similar to those found in welding in that the range of stability of an arc is limited and control of the power (IxV) is difficult to maintain precisely. Powder feed rate is another parameter which cannot be varied greatly. As powder feed rates increase, coating quality deteriorates because gases tend to become entrapped causing voids in the coatings. At this time, the parameter which appears to be the most conveniently varied and holds the most promise in controlling coating dimension is the work piece travel speed.

The depth and width of PTA applied coatings is also a function of the substrate to which they are applied. A PTA applied coating on a low melting point substrate would be expected to penetrate and spread out more than if the same coating were applied to a high melting point substrate. Figure 4.5 shows a tungsten carbide/metallic matrix coating applied to alloy steel SAE No. 9254 which is a steel containing a lower percentage of carbon than the nodular cast iron.

The potential of metallic coatings, to meet the requirements for successful piston ring/liner materials has been reviewed from a wear and thermal shock point of view. These materials show good characteristics, although, thermal shock testing in the program showed that for two phase metallic systems, material loss from the surface can occur.

The main drawback to these systems at the present time is the relatively high coefficient of friction that they exhibit. This behavior is illustrated in Figure 4.6 for stellite 31 which has the approximate composition Co-25Cr-10Ni-8W. The results shown here which were developed in experimental work performed by Stott, Stevenson, and Wood (4) show a time and temperature dependence of the coefficient of friction, with a minimum at (1073°K) of about 0.4. It is generally recognized that the goal for coefficient of friction is a number less than or equal to 0.15.

The same type of time and temperature dependence has been observed for nickel and nickel-chromium alloys. The drop in coefficient of friction and wear with time at 400°C and 800°C has been observed to be associated with the formation of low shear strength on the rubbing surface. These results

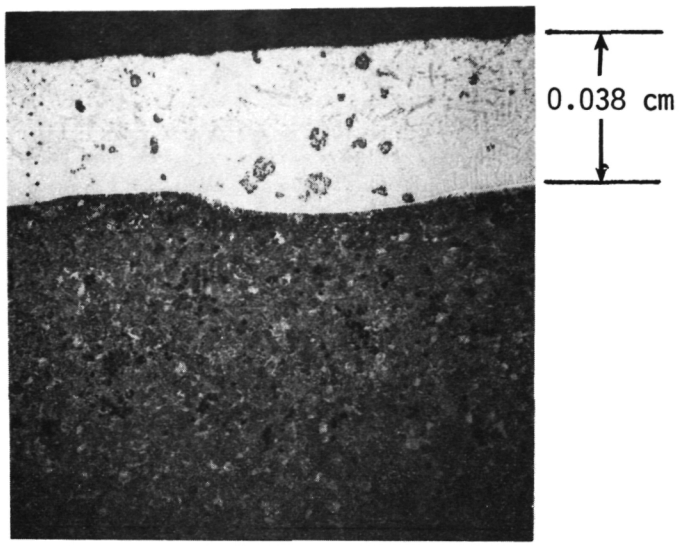

Figure 4.5. Tungsten Carbide Based Plasma Transferred Arc Coating Applied to 9254 Steel.

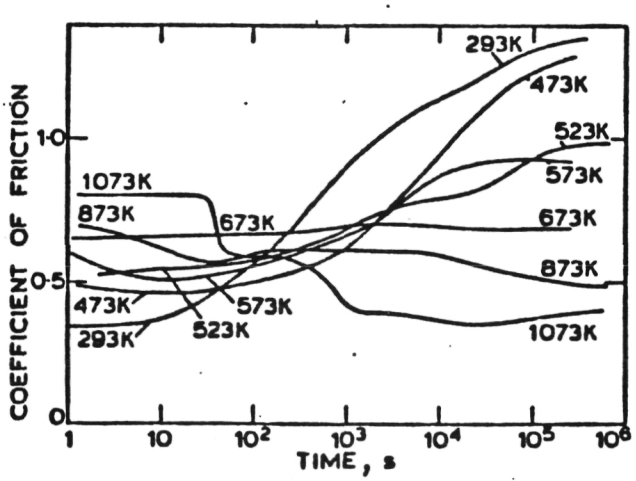

2 Plots of average coefficient of friction against time for Stellite 31 during like-on-like sliding at temperatures from 293 to 1073K

Figure 4.6. Coefficient of Friction for Stellite 31 Sliding Against Itself (from Reference 3)

indicate that further lowering of the coefficient of friction may be achieved by modification of the glaze. Two phase alloys are likely to experience more wear.

5. HOT FORMED SUBSTRATES

In this program two candidate substrate materials were selected for piston ring substrate development. These two materials (the compositions for which are shown in Table 5.1) were Carpenter 709-2, which is a low carbon steel and 440B which is a stainless steel. These substrates were hot formed into the piston ring shape. In the hot forming operation, a strip of the material is inductively heated and then wound while hot onto an arbor and quenched. The operation is illustrated in Figure 5.1. Twenty to thirty coils are wrapped onto a single arbor. These coils are then cut from the arbor and undergo subsequent heat treatment and finishing operations.

As part of the program, the effect of varying processing parameters was investigated. Table 5.2 lists these parameters. Tables 5.3 and 5.4 give the test program followed during the hot forming of the 709-2 material and the 440B material, respectively.

The formed rings then underwent a series of evaluation tests to determine their stability at temperatures to 650°C. The stability of the ring is defined as its ability to maintain its shape and tension. The factorial test data for the 709-2 is given in Tables A.1.1a-e and test data for the 440B stainless is given in Tables A1.2a-e. These tables are located in Appendix A.

Comparison of Table A1.1a with Table A1.2a indicates that the drop in hardness after tempering for the 709-2 material is greater than for the 440 B material. The average drop in Rc-hardness is 4 for the 709-2 material and 2 for the 440 B. Also, for the 709-2 material the magnitude of the drop in hardness for any one particular test can be fairly high, especially when high hardness is exhibited prior to tempering. For example, in test 16, the average hardness before tempering is 58, while after tempering it is 45, for a drop of 13 points. For tests 4 and 5, the hardness starts out low and stays low.

Visual ratings were assigned to the hot formed strips in terms of observable scale and visual coil tightness. The 440B performed better in terms of scale as would be expected because it is a stainless composition whereas the 709-2 is not. In coil tightness, the 709-2 remained tighter.

Table 5.1. Nominal Compositions of Carpenter 709-2 and 440 B.

440 B - Stainless Steel

Element	Weight %
Carbon	0.75/0.95
Maganese	1.00 max.
Phosphorus	0.040 max.
Sulfur	0.030 max.
Silicon	1.00 max.
Chromium	16.00/18.00
Molybdenum	0.75 max.
Iron	balance

709-2 - Low Carbon Steel

Element	Weight %
Carbon	0.45
Magnesium	0.55
Silicon	0.25
Chromium	1.00
Molybdenum	0.55
Vanadium	0.30
Iron	balance

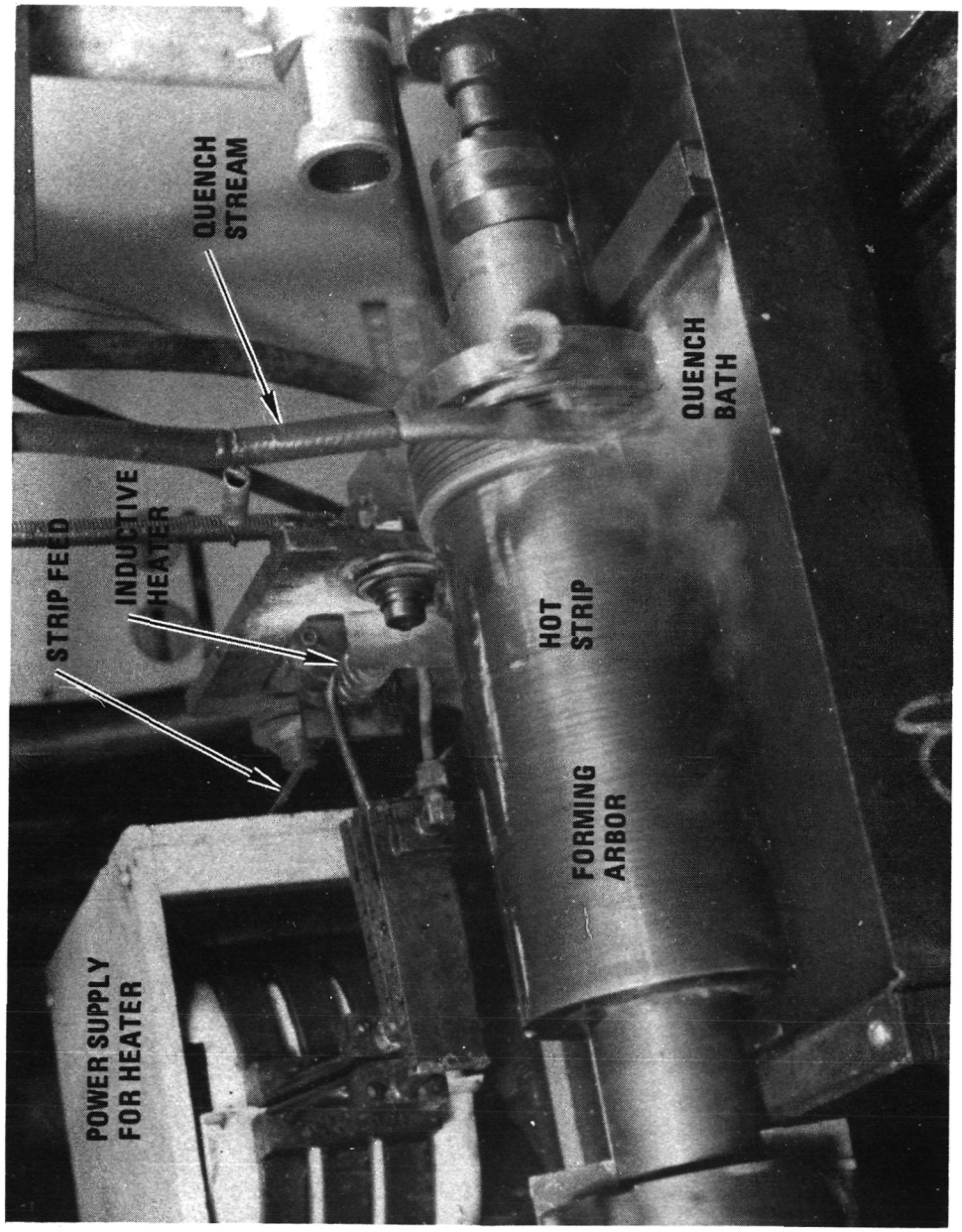

Figure 5.1. Hot Forming Equipment

Table 5.2. Explanation of Parameters Investigated During Hot Forming.

X_1 - Temperature	- This is the temperature at which the strip was hot formed.
X_2 - Quench Angle	- The quench angle refers to the position where the water and quench additive is applied to the workpiece. The quench additive used was Aquaquench 251.
X_3 - Quench Fluid	- Two quench fluids were investigated. They differed in the amount of quench additive which they contained.
X_4 - Initial Stress Relief on Coiling Arbor	- After hot forming, some ring containing arbors were placed into an oven for 30 minutes at 538°C.
X_5 - Heat Shape Temperature	- Prior to machine finishing, the hard ess of the rings must be reduced. Two oven temperatures were investigated in reducing ring hardness; 538°C and 566°C.
X_6 - Heat Shape Time	- Time (in minutes) at temperature for hardness reduction.
X_7 - Lead	- During hot forming, a distance must be kept between successive wraps in order to prevent cold welding. Lead refers to this separation distance.

Table 5.3. Test Program Followed During Hot Forming of 709-2 Material.

Test No.	X_1 Temp (°C)	X_2 Quench Angle (degrees)	X_3 Quench Fluid	X_4 Frequency	X_5 Heat Shape Temp (°C)	X_6 Heat Shape Time (min)	X_7 Lead (cm)
1	968	Tangent	2	3 kHz	566	90	0.102
2	1024	Tangent	2	450 mHz	538	90	0.127
3	968	45	2	450 mHz	568	60	0.127
4	1024	45	2	3 kHz	538	60	0.102
5	968	Tangent	10	3 kHz	538	60	0.127
6	1024	Tangent	10	450 mHz	566	60	0.102
7	968	45	10	450 mHz	538	90	0.102
8	1024	45	10	3 kHz	568	90	0.127
9	1024	45	10	450 mHz	538	60	0.127
10	968	45	10	3 kHz	566	60	0.102
11	1024	Tangent	10	3 kHz	538	90	0.102
12	968	Tangent	10	450 mHz	566	90	0.127
13	1024	45	2	450 mHz	566	90	0.102
14	968	45	2	3 kHz	538	90	0.127
15	1024	Tangent	2	3 kHz	566	60	0.127
16	968	Tangent	2	450 mHz	538	60	0.102

Table 5.4. Test Program Followed During Hot Forming of 440B Material.

Test No.	X_1 Temp (°C)	X_2 Quench Angle (degrees)	X_3 Quench Fluid	X_4 Stress Relief	X_5 Heat Shape Temp (°C)	X_6 Heat Shape Time (min)	X_7 Lead (cm)
1	941	Tangent	2	yes	566	90	0.102
2	996	Tangent	2	no	538	90	0.127
3	941	45	2	no	566	60	0.127
4	996	45	2	yes	538	60	0.102
5	941	Tangent	10	yes	538	60	0.127
6	996	Tangent	10	no	566	60	0.102
7	941	45	10	no	538	90	0.102
8	996	45	10	yes	566	90	0.127
9	996	45	10	no	538	60	0.127
10	941	45	10	yes	566	60	0.102
11	996	Tangent	10	yes	538	90	0.102
12	941	Tangent	10	no	566	90	0.127
13	996	45	2	no	566	90	0.102
14	941	45	2	yes	538	90	0.127
15	996	Tangent	2	yes	566	60	0.127
16	941	Tangent	2	no	538	60	0.102

In the drop test, attempts are made to drop the rings through a gage spacing. Whether or not the rings drop through the gage is a measure of the helix angle. Basically a low gage spacing is determined where most of the rings will not drop and then a high gage spacing is determined where most of the rings will drop. The rings are then put through a drawing operation which is a heat treatment cycle. This cycle, except for the initial stress relief on the coiling arbor, is identical to the tempering cycle. For example, the drawing operation for test 1 of the 709-2 material would consist of 90 minutes at 566°C. During this time the rings are compressed on the arbor in an attempt to remove the helix angle. After this draw operation, the high and low gage spacings are redetermined.

Table A.1.1a shows that the drawing step was fairly successful in reducing the helix angle in the 709-2 material. Not as much difference is seen for the 440B material but this material didn't in general have the initial high helix angles exhibited by the 709-2 material. The fact that the 440B helix angle did not change as much during drawing as the 709-2 helix angle may be an indication of high temperature stability for the 440B material.

The free gap before and after tempering was also measured, and these results are shown in Tables A1.1b and A.2b for the 709-2 and 440B materials respectively. The change in free gap during the drawing operation is in general greater for the 709-2 material than for the 440B material. The average change in free gap is 0.434 cm for 709-2 and 0.328 cm for 440B.

At this point, it would seem that the results show the 440B material to be a better substrate material than the 709-2. However, the thermal stability tests showed that this was not the case. Prior to these tests, the rings underwent two measurements, free gap and light transmittance. In the light transmittance test, rings are set in a circular die, and this die is placed on a light box. The amount of light which leaks between the outside edge of the ring and the die is measured.

After these measurements are made, the rings are constrained within a cylinder and heated for four hours to a temperature of either 316°C, 427°C, 538°C, or 650°C. After cooling, the free gap and light transmittance are remeasured. Results are presented in Tables A1.1c-A1.1e and A1.2c and A1.2e for the 709-2 and 440B material respectively. Figure 5.2 summarizes

representative data in a more concise way. This figure shows that as the temperature increases past 422°C, the free gap collapses for the 440B material. The free gap for the 709-2 material collapses between 538 and 650°C. This test is thought to have more weight in evaluating the suitability of the two materials as piston ring substrates. This is because as the rings are heated, they experience some stress as they expand against the sides of the cylinder. The 709-2 material can recover from this stress whereas the 440B cannot. For this reason, the 709-2 material is more suitable as a piston ring substrate beyond 422°C.

Hot formed 709-2 rings were prepared by TRW and engine tested by Cummins Engine Company. This engine testing was not part of the program, however the results are reported here because of the supporting evidence they provide on Carpenter 709-2 thermal stability. The rings were coated with Triboloy. Figure 5.3 shows some of these rings. Ring 1 has not been engine tested and has a free gap of about 2 cm. Ring 2 was engine tested at 593°C and although the ring did not fail, it experienced distortion as is evidenced by the change in free gap and the offset of the points from true circularity. Ring 3 was exposed to 650°C operating temperature and this ring failed to maintain an engine seal. These tests were run essentially without lubrication. Oil was injected during testing but it decomposed very quickly. The distortion exhibited by rings 2 and 3 indicates that the yield strength of the material is being exceeded. Changes in ring design or the use of a solid lubricant to decrease operating stress may improve the high temperature capability of the 709-2 material.

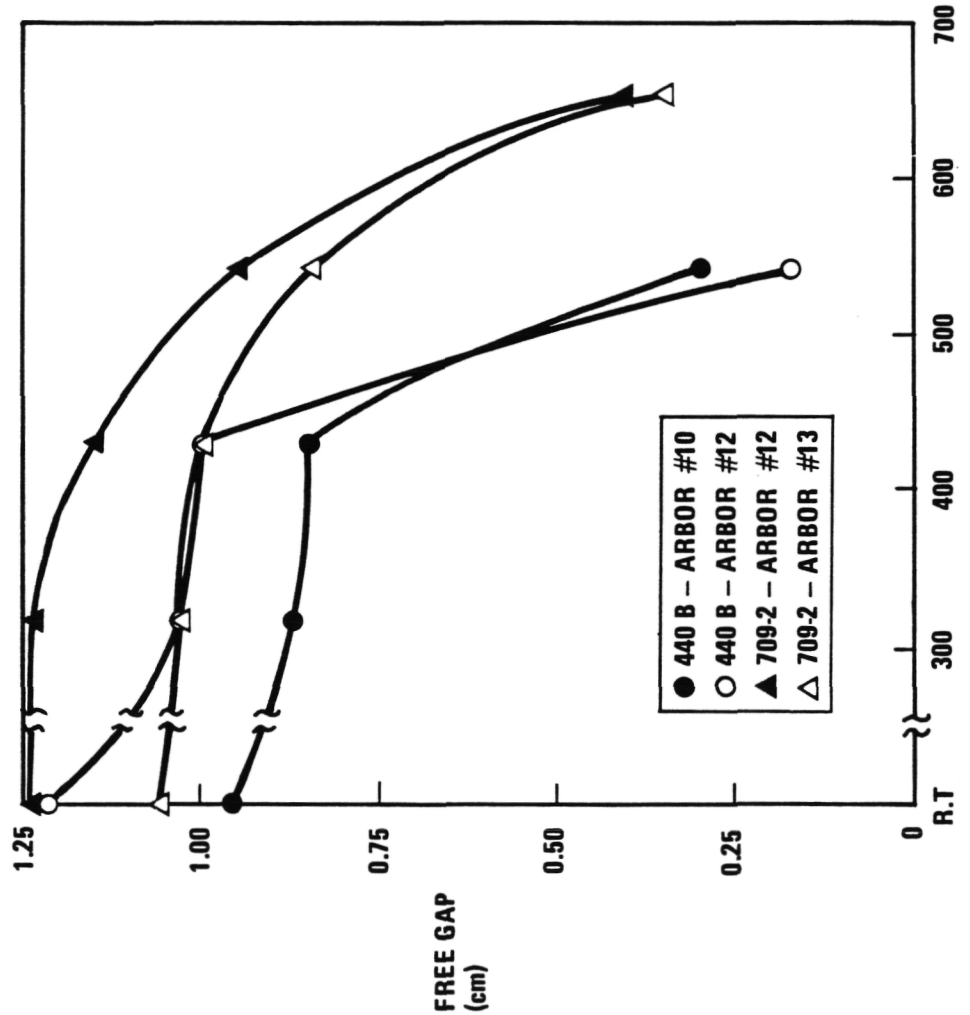

FIGURE 5.2. Hot Formed Rings – Thermal Stability Test Results-Free Gap Change

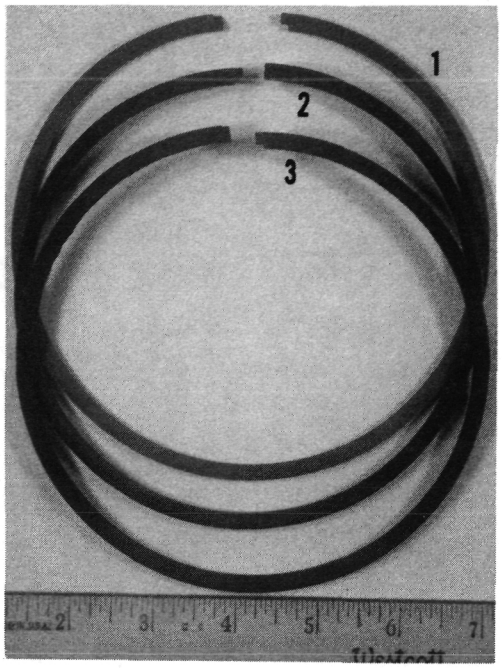

Figure 5.3. Results of Engine Tests with Hot Formed Carpenter 709-2 Base Material

Ring #1 was not subjected to engine tests

Ring #2 was exposed to 593°C. operation temperature for three hours. It maintained seal although change in free gap indicates that yield strength was exceeded.

Ring #3 was exposed to 650°C. operating temperature for three hours. yield strength was exceeded and ring failed.

6. FINISHING PROCESS

A processing scheme was developed which takes ring manufacturing from the hot forming step to the finished product. This process scheme is listed chronologically in Tables B 1a-f of Appendix B. The first step in the processing sequence is the preparation of equipment to be used in hot forming, for example, set-up of generator for conductive heating of strip, adjustment of rollers to feed strip, and quench solution make-up.

After the equipment has been prepared, the strip is hot formed onto the rotating arbor. Approximately twenty coils are wrapped onto the arbor. After the coils have cooled, a gap is cut through the coils, thus enabling their release from the arbor as individual rings. This operation is refered to as "slugging". A wrapped arbor, before and after slugging, is illustrated in Figures 6.1a and 6.1b respectively.

The rings which have been slugged from the arbor retain a helix angle which results from the fact that the wrapped coils have to be a minimum distance apart to prevent contact. A number of operations are conducted to removel this helix angle. First, the rings are bent by hand. Secondly, they are placed on an arbor and then heated to 538°C for 1 hour. Free gap and hardness are measured and then a drop test is performed to insure that the helix angle is below the maximum allowed.

The rings are then rough ground, degreased, and the end clearance is ground. The finish width is then ground, rings are again degreased, and the step gap machined on each side of the free gap according to specifications. This operation is followed by dustoff and degreasing. Dustoff consists of a very light grinding of both the top and bottom ring faces. A pipmark is placed on one face of the ring to identify the top face.

The groove is then put in the ring, and the ring is coated. The coating is ground back to the point where the rings can be broken apart from each other. A grinding operation then imparts a profile to the coated ring. After a degreasing step, the end clearance is ground and the outside diameter edges are beveled. This is followed by deburring, inspection and phosphate coating. Schematics of the finished rings are shown in Figures 6.2-6.5.

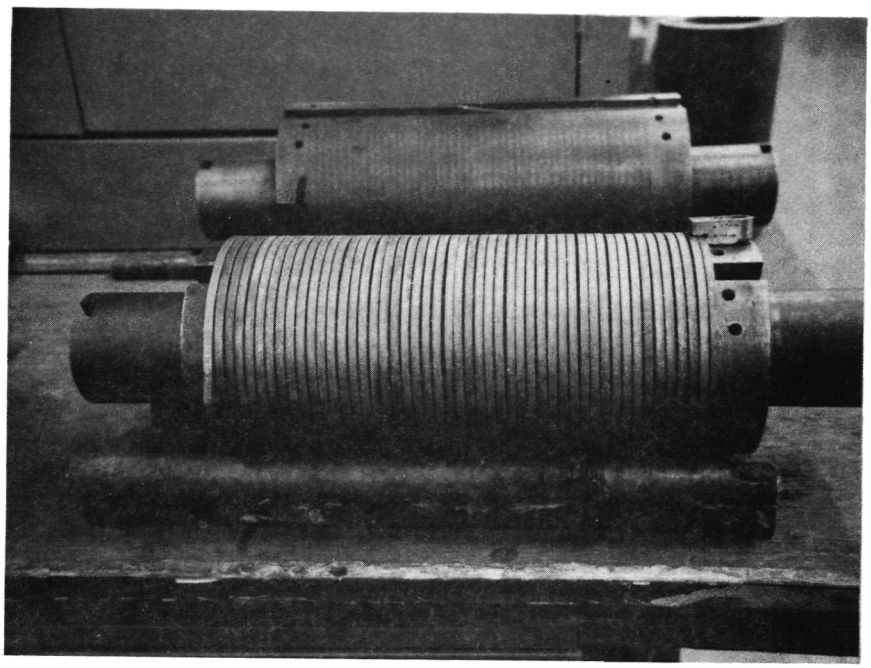

a)

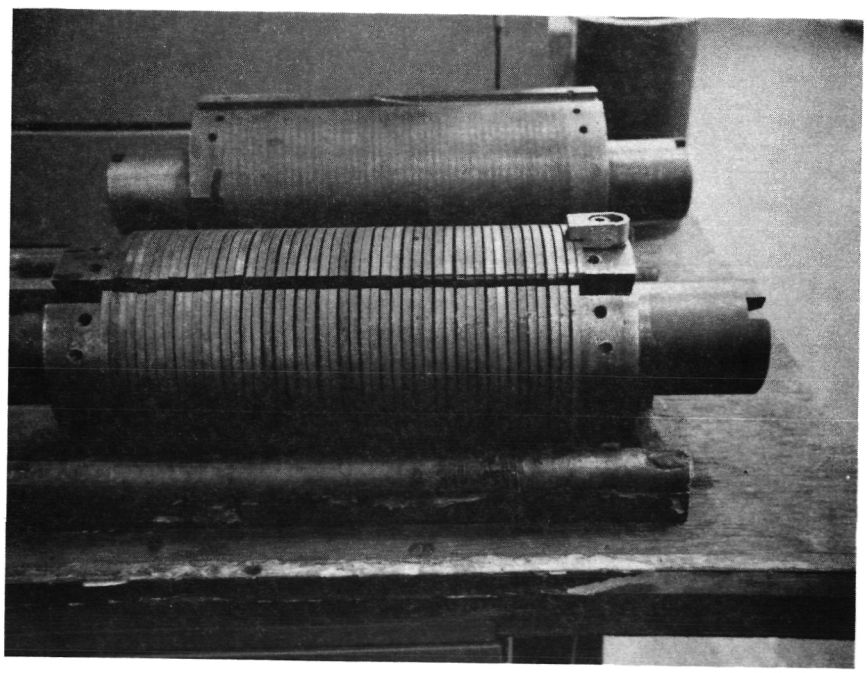

b)

Figure 6.1. Arbor Wrapped with Hot Formed Strip

a) Before Slugging
b) After Slugging

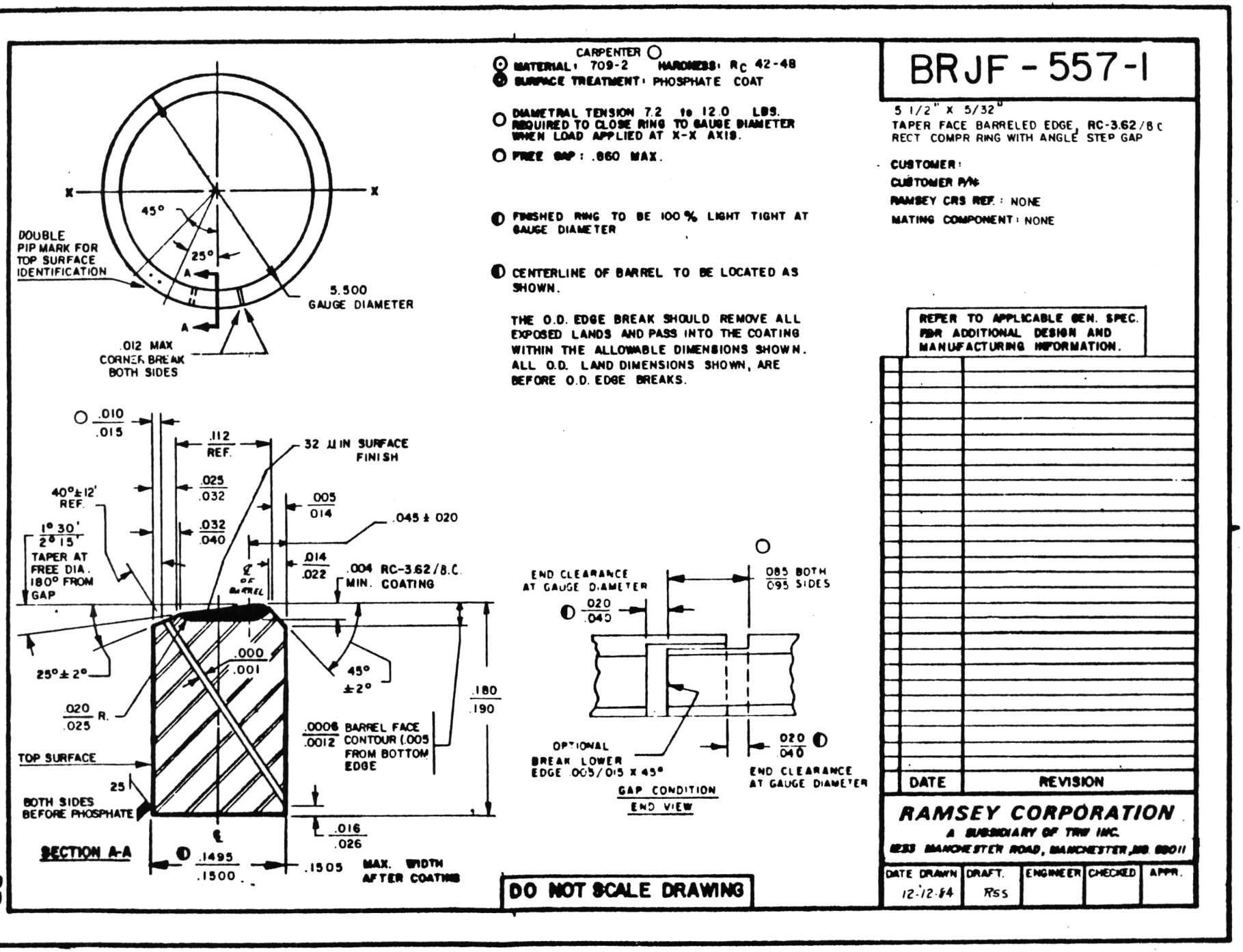

Figure 6.2. Schematic of Rectangular Plasma-Spray Coated Ring

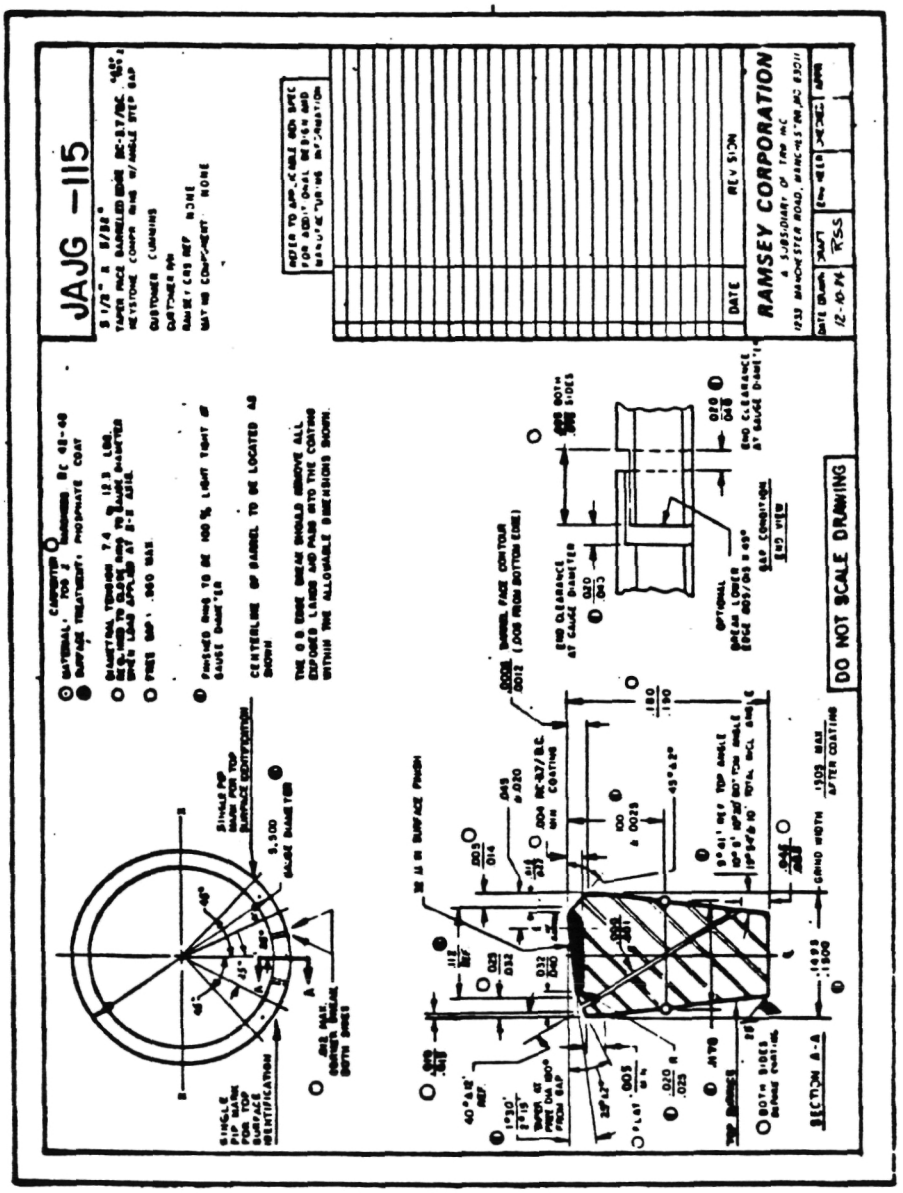

Figure 6.3. Schematic of Finished Keystone Plasma Spray Coated Ring

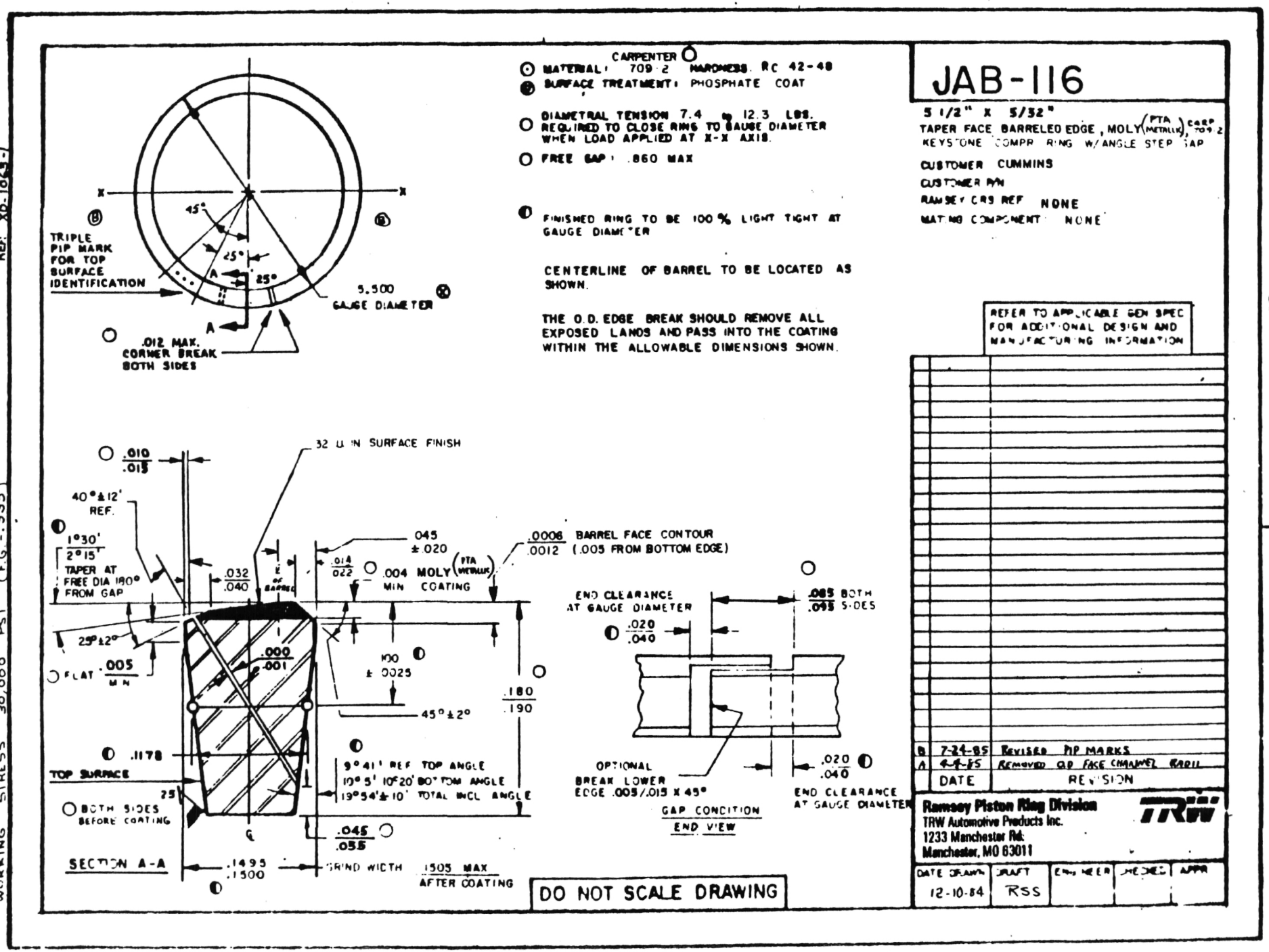

Figure 6.4. Schematic of Finished Keystone PTA Coated Ring

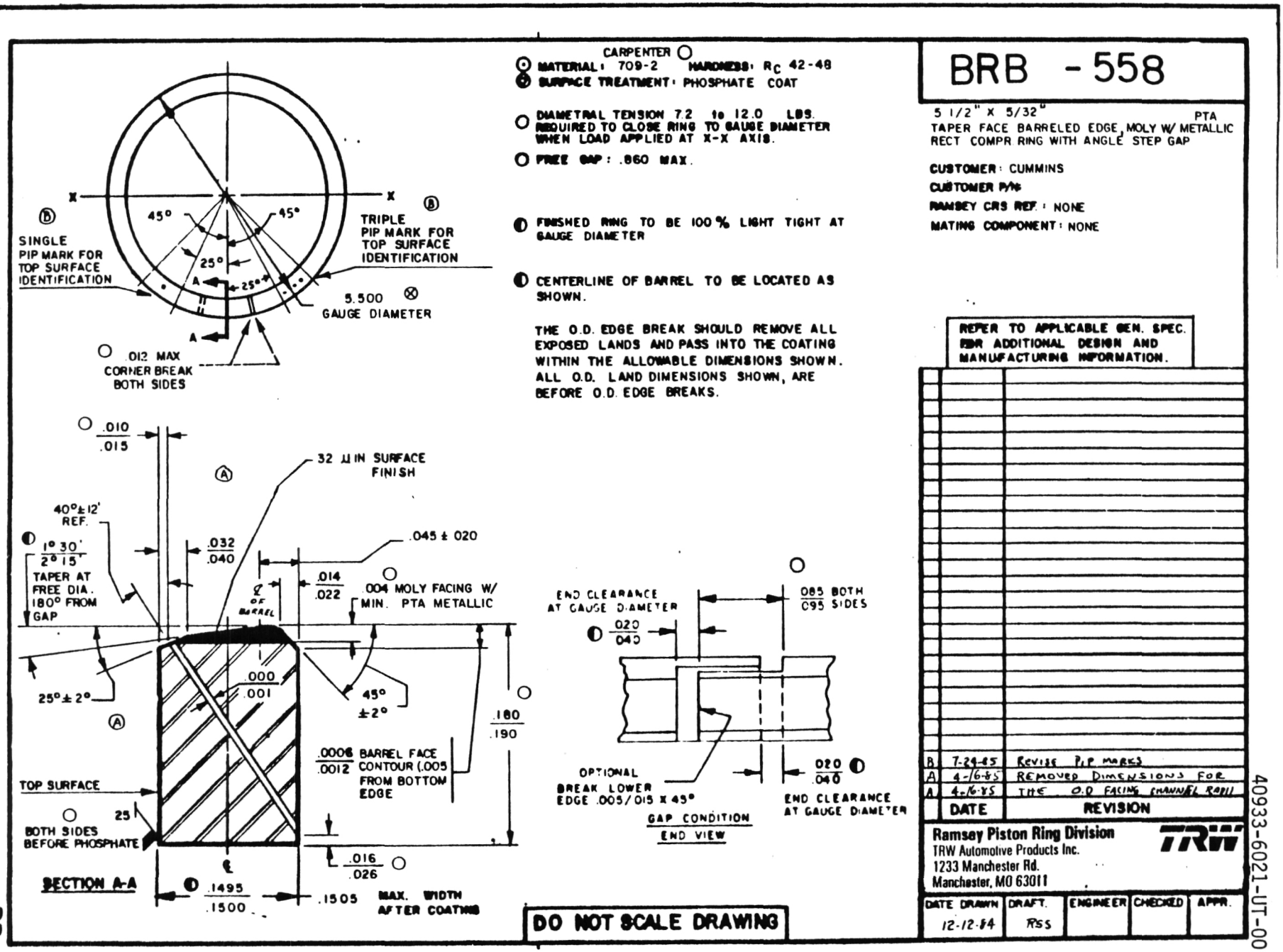

Figure 6.5. Schematic of Finished Rectangular PTA Coated Ring

7. WEAR TESTING

The coated rings were tested in a high temperature apparatus which is designed to test piston ring wear from room temperature to 566°C. The rings are loaded onto a piston (which can hold up to eight rings) as shown in Figure 7.1. The piston and piston ring assembly are then loaded onto an actuation rod which sits inside of a temperature controlled chamber. This chamber is heated by means of eight resistive heaters which are placed circumferentially around the chamber in the holes running parallel to the chambers axis. Temperature is monitored at three locations by means of thermocouples. One thermocouple is located at the liner/piston interface, one thermocouple is placed in the wall of the cylinder at the same radial distance as the resistive heaters, and the other is located on the outside of the chamber. Figure 7.2 shows a piston assembly being loaded into the wear tester. The activation rod will fit through the hole in the middle of this assembly and then be bolted into place. This actuation rod is connected to a bearing race which encompasses an eccentric cam drive. This cam drive is connected to a mechanical drive assembly which moves the piston assembly through a 0.635cm stroke at a speed of 500 r.p.m.

Lubricant supply to this apparatus is critical and is pumped from a reservoir into the temperature controlled chamber. Flow is controlled by means of a needle valve. For high temperatures, the lubricant is unstable and decomposes generating smoke and fumes. For this reason a smoke eliminator unit was installed. It consists of a blower motor, an electrostatic precipitator, a mechanical filter and air baffles.

Wear testing was performed with plasma sprayed and graded alumina, graded and non-graded zirconia, ungraded alumina/zirconia, low pressure plasma sprayed molybdenum, and molybdenum and tungsten carbide plasma transfered arc coated rings against a tungsten cylinder liner. The better performing coatings were also wear tested against a Si_3N_4 cylinder liner.

Photomicrographs of the different coatings surfaces can be seen in Figures 7.3-7.15. These photos are indicative of the range of wear that can be expected from the different coatings. Visable surface roughness and material losses shown in the figures can be used to initially evaluate the coatings' resistance to wear. For example, comparison of Figure 7.4 with Figure 7.8 would imply that the graded alumina coating wears better than the

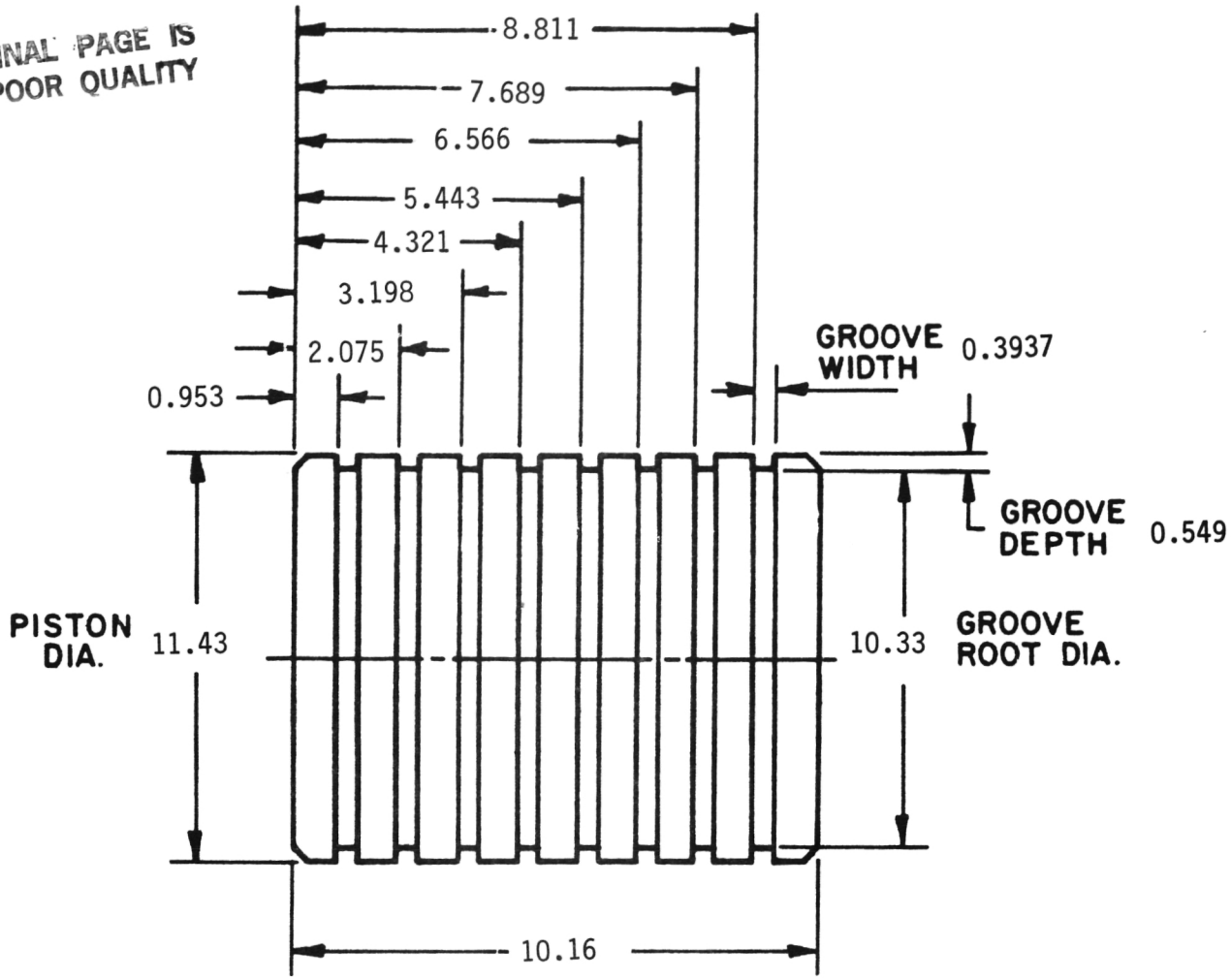

(dimensions are in centimeters)

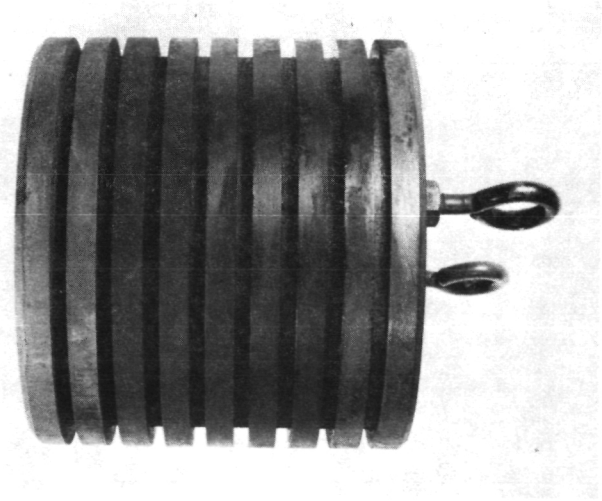

PISTON ASSEMBLY DETAIL

FIGURE 7.1

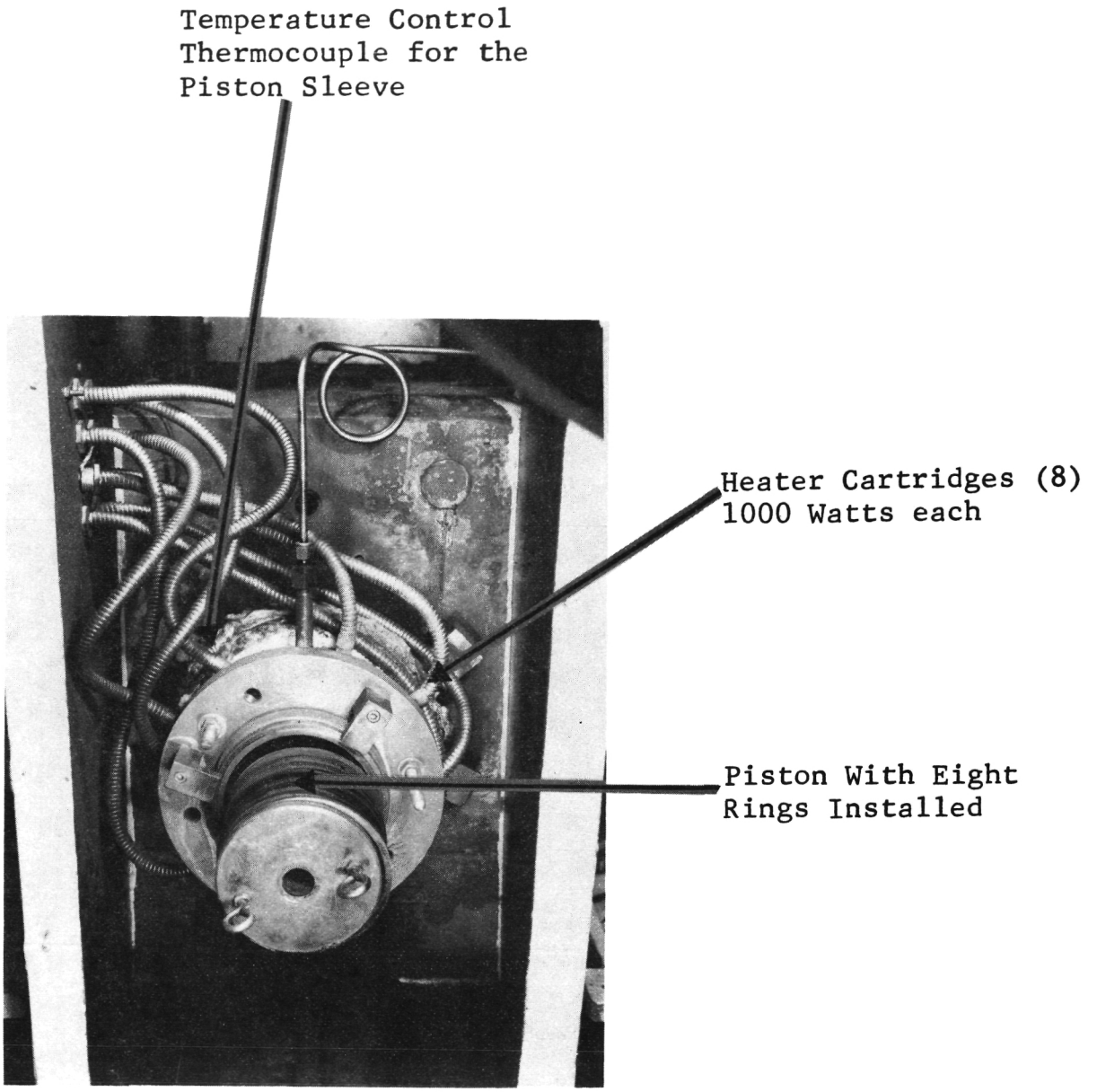

HIGH TEMPERATURE CHAMBER PISTON RING ASSEMBLY BEING LOADED

FIGURE 7.2

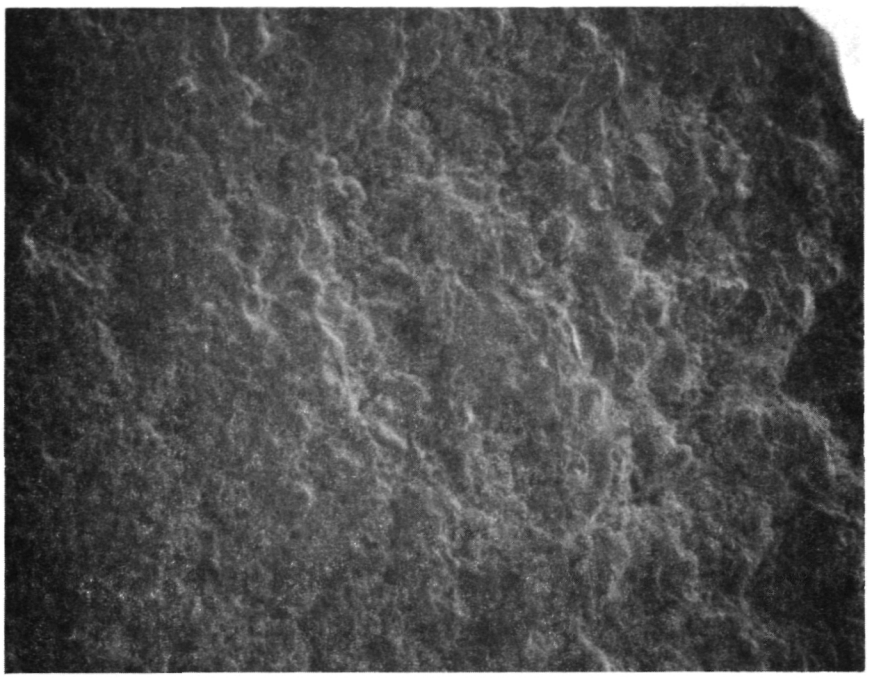

Figure 7.3. Photomicrograph of One of the Better Graded Alumina Coatings as Wear Tested Against a Tungsten Carbide Cylinder Sleeve. This Coating Performed Well in Thermal Shock Testing.

Figure 7.4. Photomicrograph of One of the Poorer Graded Alumina Coatings as Wear Tested Against a Tungsten Carbide Cylinder Sleeve.

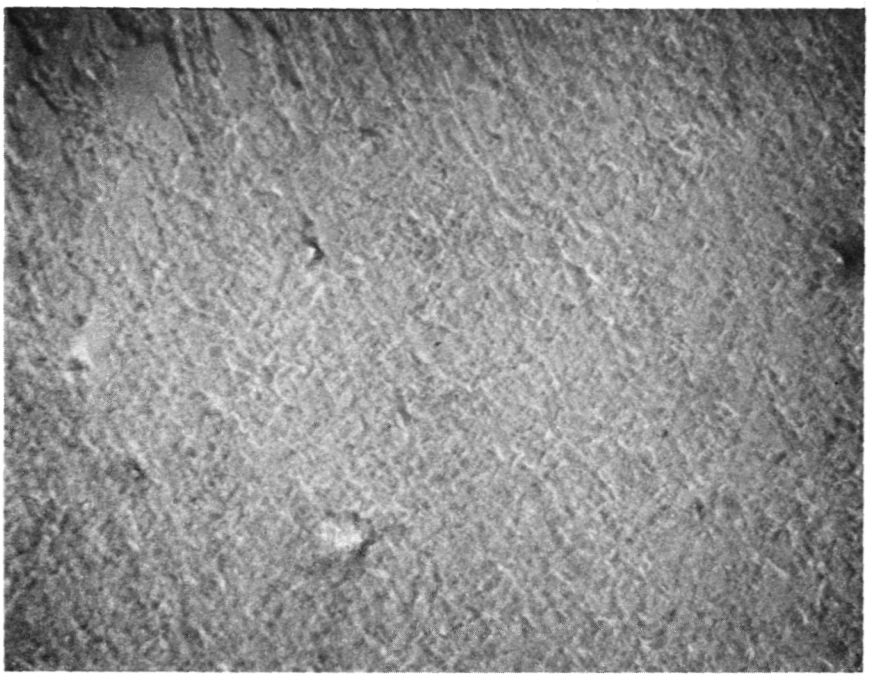

Figure 7.5. Photomicrograph of One of the Better Non Graded ZrO_2/28.5-35TiO_2/2-4 Y_2O_3 Coatings After Wear Testing Against a Tungsten Carbide Cylinder Sleeve. This Coating Performed Poorly in Thermal Shock Testing.

Figure 7.6. Photomicrograph of One of the Poorer Non Graded ZrO_2/28.5-35TiO_2/2-4 Y_2O_3 Coatings After Wear Testing Against a Tungsten Carbide Cylinder Sleeve. This Coating Performed Poorly in Thermal Shock Testing.

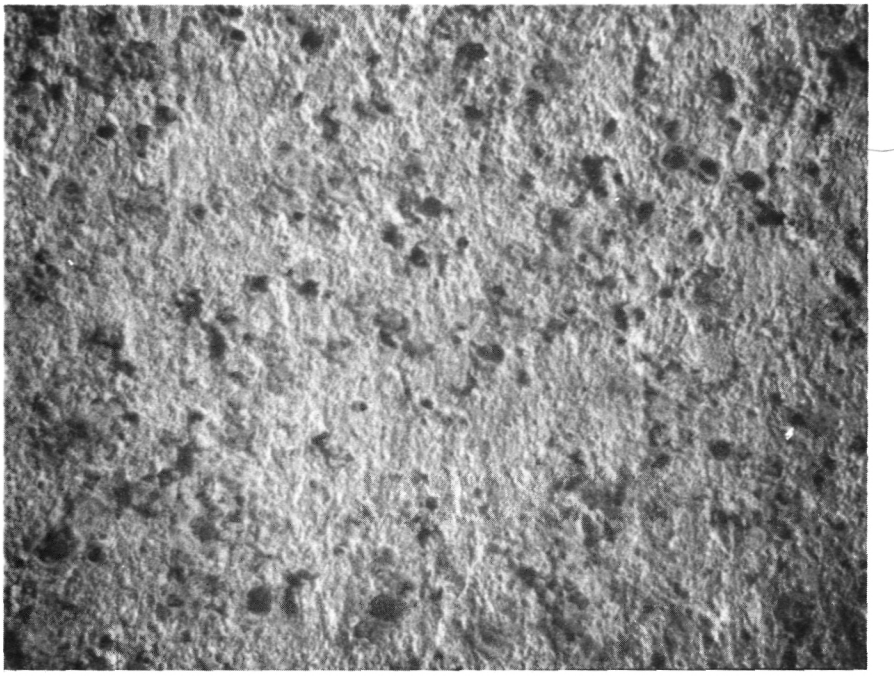

Figure 7.7 Photomicrograph of One of the Better Low Pressure Plasma Sprayed Molbdenum Coatings as Wear Tested Against a Tungsten Carbide Cylinder Sleeve. This Coating Performed Poorly in Thermal Shock Testing.

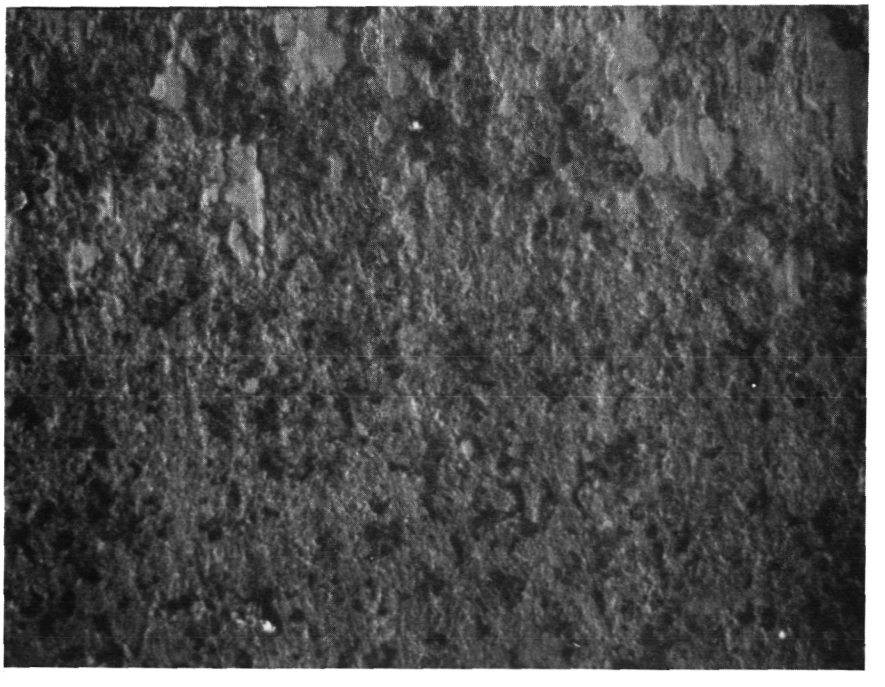

Figure 7.8. Photomicrograph of One of the Poorer Low Pressure Plasma Sprayed Molybedenum Coatings as Wear Tested Against a Tungsten Carbide Cylinder Sleeve. This Coating Performed Poorly in Thermal Shock Testing.

Figure 7.9 Photomicrograph of a Relatively Poor Portion of an $Al_2O_3/ZrO_2/TiO_2/Y_2O_3$ Ring Coating. This Coating is on the Same Ring as the Coating in Figure 7.10.

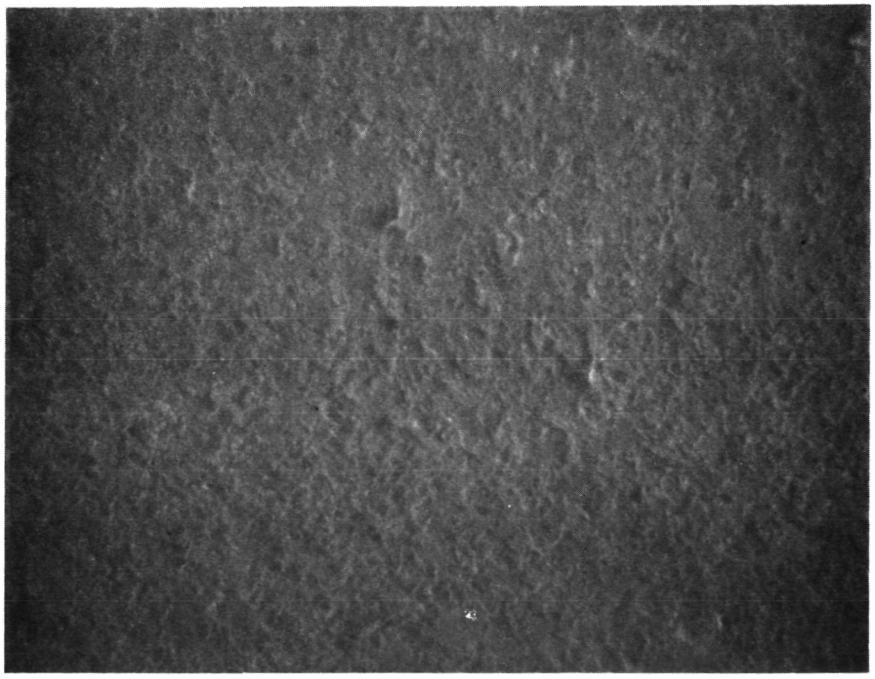

Figure 7.10 Photomicrograph of a Relatively Good Portion of an $Al_2O_3/ZrO_2/TiO_2/Y_2O_3$ Ring Coating. This Coating is on the Same Ring as the Coating in Figure 7.9.

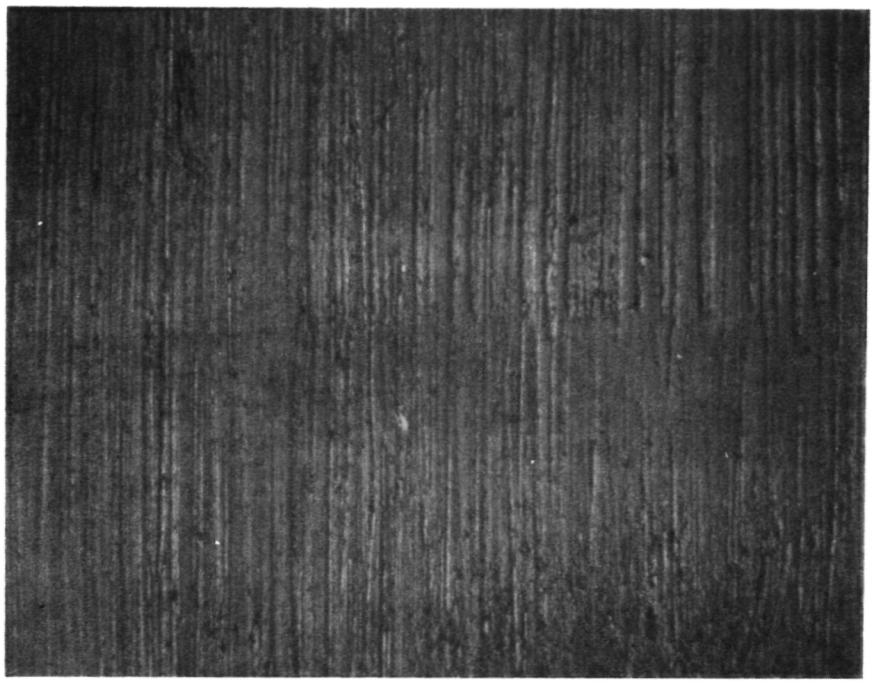

Figure 7.11 Photomicrograph of Molybdenum Based Plasma Transfered Arc Coating After Wear Testing Against a Si_3N_4 Cylinder Sleeve.

Figure 7.12. Photomicrographs of Tungsten Carbide Based Coating as Wear Tested Against a Tungsten Carbide Cylinder Sleeve.

Figure 7.13. Photomicrograph of Molybdenum Based Plasma Transfer Arc Coating After Wear Testing Against a Si_3N_4 Cylinder Sleeve.

Figure 7.14. Photomicrograph of One of the Better Graded $ZrO_2/TiO_2/Y_2O_3$ Coatings as Wear Tested Against a Tungsten Carbide Cylinder Sleeve. This Coating performed poorly in Thermal Shock Testing.

Figure 7.15 Photomicrograph of One of the Poorer Graded $ZrO_2/TiO_2/Y_2O_3$ Coatings as Wear Tested Against a Tungsten Carbide Cylinder Sleeve.

molybedenum based coatings due to less material loss. However, variance in the wear characteristics along the face of the same coated ring can also be substantial, as can be seen by comparing Figures 7.3 and 7.4. This noticable variance in the best and worst wear surfaces on the same ring can be caused by the out of roundness of the cylinder liner.

Surface profiles taken of the various ring faces were used to further evaluate the coatings' performance in terms of material loss and surface roughness (i.e., pitting). These profiles are shown in Figures C1 through C10 of Appendix C. Values for estimated wear loss and surface roughness can be found in Table 7.1a and 7.1b.

The surface profiles indicated that coating loss from the rings' face varied from 1.3 m to as much as 8.9 m. Material hardness would be expected to influence wear losses. This effect can be seen as the tungsten carbide PTA coating and the alumina/zirconia plasma sprayed coating showed the least wear. The tungsten carbide coating would be expected to perform well because it is of approximately the same hardness as the cylinder liner. The surface profiles also showed that the alumina coating and the zirconia coating had approximately the same amount of wear, but that the alumina coating had less severe pitting than the non-graded zirconia coating. This could also be due to thermal expansion effects. The low pressure plasma sprayed molybdenum based coating suffered the most shape change (i.e., material transport) compared to the other coatings. This might be expected as the molybdenum based coating is softer than the other coatings.

In conclusion, the plasma sprayed alumina/zirconia composition appeared to perform the best in the wear testing. This composition is similar to the alumina coating which offered superior thermal shock performance. Addition of the zirconia apparently increased the hardness of the coating such that it resisted wear better than the alumina coating.

Table 7.1a. Results of Wear Testing Against WC Cylinder Liner

Coating	Wear Loss (m)	Surface Texture
$Al_2O_3/TiO_2/Y_2O_3$	5.1 - 8.9	Best coating was not noticably roughened by wear testing but poorer coating was.
$ZrO_2/TiO_2/Y_2O_2$ Graded	2.5	Pits in coating before wear testing. Surface very rough after testing.
$ZrO_2/TiO_2/Y_2O_2$ Non-Graded	5.1 - 7.6	Pits in coating before wear testing. Surface very rough after testing.
$Al_2O_3/TiO_2/ZrO_2/Y_2O_3$	1.3	Moderately rough before wear testing. Same apparent roughness after wear testing.
PTA Mo-based	5.1	Surface is noticably roughened by wear testing and material is transported across ring face.
PTA WC-based	2.5	Relatively Smooth before and after wear testing.

Table 7.1b. Results of Wear Testing Against a Si_3N_4 Cylinder Liner

Coating	Wear Loss (m)	Surface Texture
$ZrO_2/TiO_2/Y_2O_2$ Graded	7.6	Surface were rough before wear testing. Wear testing did not noticably roughen surface.

8. CONCLUSIONS AND RECOMMENDATIONS

The objective of this program was to develop piston ring materials for high temperature advanced diesel engine designs. Parallel development and evaluation of substrates and coatings was carried out with the following results.

Of the two substrate materials selected for development, Carpenter 709-2 and 440B, the former exhibits greater thermal stability. The 440B material loses stability abruptly for temperatures greater than 427°C while Carpenter 709-2 exhibits potential for operation at maximum cycle temperatures of approximately 510°C. Hot forming of 709-2 was shown to be a feasible processing scheme in that the physical/mechanical properties (e.g. hardness) of the raw strip material could be controlled during processing. This control however did not enhance the thermal stability. During evaluation testing, all processing heats lost thermal stability over the same temperature range. This loss of thermal stability was confirmed in short term (3 hour) engine tests of Carpenter 709-2 at 593°C. Although engine tests were successful, considerable distortion of the ring occured and it is likely that long term operation at this temperature is not feasible.

Since current piston ring substrate materials are limited to maximum operating temperatures of 425°C, the development of Carpenter 709-2 represents a significant extension of approximately 85°C to the operating temperature limit for piston ring substrates. This result needs to be confirmed in engine testing. For future work in this area, it is recommended that nickel based superalloys, which have higher thermal stability, be developed and evaluated as substrates.

Of the plasma sprayed ceramic compositions, the Al_2O_3/28.5-35 TiO_2/2-4 Y_2O_3 exhibited the highest thermal shock resistance. An analysis of failed thermal shock test specimens for all ceramic compositions indicated that failure occured at the bond coat/ceramic interface. For graded structures, this meant that failure did not extend into the graded region. It is hypothesized that the more ductile bond coat is able to absorb the differential thermal expansions and thus reduce thermal induced stress. This suggests that thermal shock resistance may be substantially improved by grading throughout the whole ceramic region.

The low pressure plasma sprayed Mo/27 NiCrBSi exhibited problems both in processing and thermal shock testing. An examination of the deposit morphology along with a heat balance indicates that the molybdenum particles were oversized with respect to the NiCrBSi particles. Size control should improve coating quality. In thermal shock testing, the molybdenum phase was preferentially lost. It is significant to note that the PTA applied Mo/27 NiCrBSi composition did not exhibit this loss during thermal shock testing. This appears to be due to the fact that in the plasma sprayed composition, the molybdenum particles are not intimately mixed with the NiCrBSi phase but rather are stuck together with them as individual particles. In the PTA applied coating, there was more intimate mixing of the two separate compositons.

PTA application of Mo/27 NiCrBSi and WC/40 NiCrBAl/10 Co was demonstrated. Of these two, the Mo-based compositions exhibited the least amount of difficulty in application. Cracking of the substrate iron sleeve was a problem with the WC based composition. The most feasible parameter for controlling the depth and width is the rotation speed of the substrate sleeve as the weld bead is deposited. Deposition of an iron based composition Fe/13Mo/3B/2Si was attempted. The weld beads which were deposited were of very poor quality and further processing was not attempted.

It is recommended that PTA processing be further evaluated in the manufacture of piston rings which are capable of high temperature operation. This evaluation should be directed in the following areas:

- o PTA coating application on high temperature substrates like the superalloys
- o achieving smaller coating dimensions by varying the travel speed of the sleeve
- o evaluation of carbide and nitride metal matrix composites for improved high temperature wear resistance.

In wear testing, the plasma sprayed Al_2O_3/22 ZrO_2/18 TiO_2/5 Y_2O_3 coating showed the best wear resistance. This was followed by the plasma sprayed and graded ZrO_2/28.5-35 TiO_2/2-4 Y_2O_3 composition and the PTA applied WC based

composition. The metallic based PTA compositions exhibited galling and movement of the coating material to regions of low stress. The ceramic compositions in general showed a better ability to retain their original profile and are better candidate materials for high temperature (650°C) wear coatings.

Appendix A
Factorial Data Summary
Carpenter 709-2 and 440B

Table A 1.1a
FACTORIAL DATA SUMMARY
709-2 STAINLESS MATERIALS
(50 Parts Checked)

Test Number	1*	2	3	4*	5*	6	7	8*	9	10*	11*	12	13	14*	15*	16
Rc Hardness																
Average Before Tempering	44	52	53	45	45	47	50	45	50	47	48	51	44	47	46	50
Range Before Tempering	37/47	41/57	42/57	40/47	39/46	28/52	36/53	40/47	20/56	40/50	45/51	31/56	37/49	43/48	36/49	49/52
Average After Tempering	45	42	42	46	45	42	43	45	43	46	47	42	40	46	46	45
Range After Tempering	41/47	36/46	36/45	41/48	39/46	40/44	38/45	42/48	37/45	43/48	46/49	34/45	38/42	44/48	44/49	40/47
Visual Scale on Part (Heavy) 10-None	8	8	7	8	7	7	6	7	8	7	6	7	7	7	7	6
Visual Coil Tightness on Form Arbor -10-Tight; 0-Loose	8	8	7	8	7	7	7	8	8	7	6	7	7	7	8	8
Drop Test																
Gage Spacing--Low	.218	.278	.167	.187	.197	.302	.302	.197	.292	.187	.187	.302	.167	.197	.218	.218
Parts Not Dropping	45	44	46	50	50	40	35	50	50	50	50	50	50	40	50	44
Gage Spacing Before Draw-Hi	.238	.318	.172	.207	.217	.322	.322	.227	.322	.217	.207	.322	.172	.227	.238	.228
Parts Dropping Before Draw	48	49	50	49	48	50	50	50	50	50	47	50	46	49	49	50
Gage Spacing After Draw-Lo	.137	.163	.163	.177	.118	.166	.166	.118	.165	.118	.119	.166	.154	.117	.137	.117
Parts Not Dropping A/Draw-Lo	45	45	43	50	50	50	50	50	47	50	50	50	32	50	49	50
Gage Spacing After Draw-Hi	.157	.183	.169	.197	.148	.185	.186	.138	.165	.138	.138	.185	.167	.137	.157	.127
Parts Dropping After Draw-Hi	47	48	50	50	49	50	50	50	50	50	50	50	50	49	49	50

* stress relieve on the arbor

Table A 1.1b

FACTORIAL DATA SUMMARY
709-2 STAINLESS MATERIALS
(50 Parts Checked)

Test Number	1*	2	3	4*	5*	6	7	8*	9	10*	11*	12	13	14*	15*	16
Free Gap																
Before Draw Average	.238	.144	.231	.257	.237	.294	.300	.238	.259	.239	.240	.275	.159	.241	.247	.312
Before Draw Range	.230/ .245	.070/ .235	.135/ .300	.240/ .270	.225/ .245	.265/ .320	.280/ .320	.230/ .250	.230/ .285	.225/ .260	.230/ .260	.250/ .315	.135/ .180	.230/ .255	.235/ .260	.240/ .430
After Draw Average	.392	.379	.439	.318	.371	.468	.435	.404	.484	.373	.412	.452	.407	.423	.385	.499
After Draw Range	.355/ .430	.350/ .430	.430/ .453	.290/ .350	.335/ .420	.430/ .575	.465/ .545	.365/ .425	.450/ .620	.350/ .390	.375/ .500	.480/ .630	.385/ .450	.395/ .485	.305/ .490	.440/ .570
After 50 Lap Strokes Avg.	.397	.440	.420	.332	.377	.506	.525	.409	.524	.385	.427	.519	.417	.433	.395	.512
After 50 Lap Strokes Range	.360/ .440	.360/ .530	.410/ .470	.290/ .420	.340/ .440	.460/ .600	.490/ .570	.360/ .460	.480/ .530	.370/ .400	.380 .460	.480/ .580	.400/ .440	.400/ .480	.330/ .450	.460/ .590
After 1000°F Test Avg.	.360	.390	.410	.301	.382	.493	.510	.414	.505	.329	.381	.507	.381	.399	.349	.505
After 1000°F Test Range	.320/ .410	.300/ .500	.360/ .440	.260/ .390	.340/ .440	.440/ .580	.460/ .550	.370/ .480	.470/ .620	.310/ .360	.350/ .410	.490/ .570	.360/ .400	.360/ .460	.300/ .410	.430/ .590
After 25 Lap Strokes Avg.	.439	.439	.445	.307		.412	.519		.520			.515	.409	.388		.499
After 25 Lap Strokes Range	.310/ .400	.370/ .520	.420/ .470	.280/ .360		.540/ .600	.480/ .560		.480/ .580			.460/ .580	.380/ .430	.350/ .450		.420 .570
After 1200°F Test Avg.		.334	.377			.480	.487		.447			.502	.314			
After 1200°F Test Range		.230/ .420	.340/ .420			.430/ .560	.460/ .520		.400/ .520			.460/ .580	.270/ .360			
Keystone																
Average	.0041	.0059	.0036	.0038	.0034	.0061	.0056	.0034	.0057	.0035	.0035	.0058	.0037	.0038	.0036	.0038
Range	.112/ .118	.155/ .163	.156/ .163	.111/ .117	.112 .118	.155/ .164	.155/ .163	.113/ .118	.155/ .163	.112/ .119	.113/ .118	.156/ .163	.156/ .164	.112/ .118	.112/ .117	.112/ .118

Table A 1.1c

FACTORIAL DATA SUMMARY
709-2 STAINLESS MATERIALS
(50 Parts Checked)

Test Number	1*	2	3	4*	5*	6	7	8*	9	10*	11*	12	13	14*	15*	16
Open Light																
Percent Before 1000°F Test	16	12	8	28	14	6	2	20	3	20	25	3	14	15	19	12
Point Range B/4 1000°F Test	45-90	67-94	77-94	41-81	75-89	84-94	90-96	53-91	75-96	45-86	34-86	88-96	79-88	74-88	73-90	77-96
Percent After 1000°F Test	16	19	15	25	18	9	7	20	6	43	33	5	19	17	28	19
Point Range Aft 1000°F Test	40-89	63-92	67-92	42-92	73-83	76-96	82-96	53-90	78-96	25-80	24-81	84-96	71-85	57-90	26-90	46-91
Percent Before 1200°F Test	**	9	9	**		2	3		6			3	16	26		15
Point Range B/4 1200° Test	**	72-94	80-94	**		87-96	87-96		79-96			96-96	73-85	40-87		76-93
Percent After 1200°F Test		**	19			**	**		**			3	31			
Point Range Aft. 1200°F Test		**	65-93			**	**		**			85-96	52-71			
Thermal Stability Test--Percent Open Light																
Percent Open Light Before 600°F Test																
Arbor #1, Ring #1		12	2			9	0		0			4	--			
Ring #2		18	5			1	0		0			2	--			
Arbor #2, Ring #1		6	12			2	2		0			0	14			
Ring #2		4	15			2	2		0			0	12			
Arbor #3, Ring #1		17	5			1	0		6			0	11			
Ring #2		5	7			0	2		6			1	14			
Arbor #4, Ring #1		0	11			2	4		0			1	15			
Ring #2		1	4			2	2		2			2	15			
Arbor #5, Ring #1		0	7			2	0		6			1	15			
Ring #2		5	7			0	2		0			4	17			

Table A 1.1d

FACTORIAL DATA SUMMARY
709-2 STAINLESS MATERIALS
(50 Parts Checked)

Test Number	1*	2	3	4*	5*	6	7	8*	9	10*	11*	12	13	14*	15*	16
Percent Open Light After 600°F Test																
Arbor #1, Ring #1		18	2			9	0		5			7	--			
Ring #2		14	12			1	0		0			8	--			
Arbor #2, Ring #1		6	10			2	8		4			0	14			
Ring #2		4	15			2	2		0			0	12			
Arbor #3, Ring #1		17	8			4	0		6			4	11			
Ring #2		9	7			5	3		6			3	14			
Arbor #4, Ring #1		2	11			3	6		0			3	15			
Ring #2		2	11			2	3		0			5	12			
Arbor #5, Ring #1		0	8			12	2		0			1	12			
Ring #2		11	10			4	5		0			4	17			
Percent Open Light After 800°F Test																
Arbor #1, Ring #1		18	6			11	5		5			8	--			
Ring #2		16	12			4	7		2			10	--			
Arbor #2, Ring #1		7	15			3	8		4			2	16			
Ring #2		10	15			3	6		3			0	16			
Arbor #3, Ring #1		19	8			6	2		8			4	11			
Ring #2		11	7			5	4		6			3	15			
Arbor #4, Ring #1		5	12			15	11		5			6	16			
Ring #2		2	10			6	6		7			4	31			
Arbor #5, Ring #1		0	12			6	9		2			6	12			
Ring #2		14	10			9	7		3			10	23			
Percent Open Light After 1000°F Test																
Arbor #1, Ring #1		15	17			9	8		5			8	--			
Ring #2		22	17			4	7		2			8	--			
Arbor #2, Ring #1		16	15			6	9		0			7	19			
Ring #2		36	15			5	7		6			0	17			
Arbor #3, Ring #1		21	8			6	2		23			2	17			
Ring #2		11	7			4	2		24			7	15			
Arbor #4, Ring #1		10	12			7	10		23			4	20			
Ring #2		2	10			10	6		9			9	29			
Arbor #5, Ring #1		2	12			6	5		2			6	17			
Ring #2		14	10			5	7		4			10	21			

Table A 1.1e

FACTORIAL DATA SUMMARY
709-2 STAINLESS MATERIALS
(50 Parts Checked)

Test Number	1*	2	3	4	5*	6	7	8*	9	10*	11*	12	13	14*	15*	16
Percent Open Light After 1200°F																
Arbor #1, Ring #1		**	**			**	**		**			**	**			
Ring #2		**	**			**	**		**			**	**			
Arbor #2, Ring #1		**	**			**	**		**			**	**			
Ring #2		**	**			**	**		**			**	**			
Arbor #3, Ring #1		**	**			**	**		**			**	**			
Ring #2		**	**			**	**		**			**	**			
Arbor #4, Ring #1		**	**			**	**		**			**	**			
Ring #2		**	**			**	**		**			**	**			
Arbor #5, Ring #1		**	**			**	**		**			**	**			
Ring #2		**	**			**	**		**			**	**			
Thermal Stability Test--Free Gap																
Before 600°F Test																
Arbor #1, Ring #1		.430	.440			.560	.560		.500			.490	--			
Ring #2		.440	.440			.560	.560		.490			.500	--			
Arbor #2, Ring #1		.460	.440			.460	.550		.540			.570	.420			
Ring #2		.470	.420			.460	.550		.540			.570	.430			
Arbor #3, Ring #1		.400	.440			.460	.520		.520			.510	.420			
Ring #2		.480	.450			.450	.500		.510			.500	.440			
Arbor #4, Ring #1		.510	.450			.500	.490		.480			.500	.410			
Ring #2		.510	.440			.500	.480		.500			.480	.430			
Arbor #5, Ring #1		.480	.450			.520	.500		.480			.520	.400			
Ring #2		.440	.460			.530	.490		.490			.490	.400			
Free Gap After 600°F Test:																
Arbor #1, Ring #1		.480	.440			.560	.560		.500			.490	--			
Ring #2		.460	.440			.550	.560		.500			.500	--			
Arbor #2, Ring #1		.480	.440			.450	.540		.540			.550	.410			
Ring #2		.460	.420			.450	.550		.540			.580	.420			
Arbor #3, Ring #1		.400	.440			.450	.520		.510			.500	.420			
Ring #2		.490	.440			.400	.500		.500			.500	.430			
Arbor #4, Ring #1		.500	.450			.490	.490		.480			.500	.420			
Ring #2		.510	.440			.500	.480		.500			.480	.420			
Arbor #5, Ring #1		.480	.460			.520	.500		.550			.520	.400			
Ring #2		.460	.460			.520	.490		.550			.490	.400			

Table A.1.1e (Cont.)

FACTORIAL DATA SUMMARY
709-2 STAINLESS MATERIALS
(50 Parts Checked)

Test Number	1*	2	3	4*	5*	6	7	8*	9	10*	11*	12	13	14*	15*
Free Gap After 800°F Test															
Arbor #1, Ring #1		.400	.420			.540	.560		.480			.460	--		
Ring #2		.400	.420			.540	.540		.480			.480	--		
Arbor #2, Ring #1		.440	.400			.420	.500		.540			.550	.400		
Ring #2		.440	.430			.430	.510		.520			.540	.400		
Arbor #3, Ring #1		.370	.420			.430	.490		.500			.490	.400		
Ring #2		.450	.430			.420	.480		.480			.480	.430		
Arbor #4, Ring #1		.480	.430			.490	.450		.460			.460	.410		
Ring #2		.480	.420			.500	.440		.480			.460	.420		
Arbor #5, Ring #1		.460	.440			.480	.410		.520			.500	.400		
Ring #2		.430	.440			.470	.460		.520			.500	.400		
Free Gap After 1000°F Test															
Arbor #1, Ring #1		.290	.280			.400	.420		.360			.380	--		
Ring #2		.260	.280			.400	.420		.360			.390	--		
Arbor #2, Ring #1		.280	.300			.300	.350		.370			.430	.340		
Ring #2		.240	.280			.310	.350		.380			.430	.340		
Arbor #3, Ring #1		.210	.290			.300	.350		.380			.380	.210		
Ring #2		.280	.280			.310	.330		.380			.380	.330		
Arbor #4, Ring #1		.340	.280			.350	.300		.360			.360	.320		
Ring #2		.340	.280			.350	.310		.380			.360	.320		
Arbor #5, Ring #1		.310	.300			.380	.340		.380			.400	.320		
Ring #2		.300	.280			.360	.340		.370			.360	.320		
Free Gap After 1200°F Test															
Arbor #1, Ring #1		.140	.130			.160	.180		.180			.160	--		
Ring #2		.130	.140			.180	.180		.180			.160	--		
Arbor #2, Ring #1		.140	.140			.110	.150		.160			.180	.140		
Ring #2		.140	.110			.100	.180		.180			.170	.140		
Arbor #3, Ring #1		.070	.120			.110	.180		.180			.160	.070		
Ring #2		.100	.120			.110	.170		.180			.160	.120		
Arbor #4, Ring #1		.090	.120			.150	.140		.160			.160	.130		
Ring #2		.060	.110			.170	.160		.170			.150	.150		
Arbor #5, Ring #1		.080	.120			.150	.150		.160			.200	.120		
Ring #2		.100	.110			.160	.150		.160			.180	.140		

Table A 1.2a

FACTORIAL DATA SUMMARY
440-B STAINLESS MATERIALS
(50 Parts Checked)

Test Number	1	2	3	4	5	6	7	8	9	10	11	12	13	14	15	16
Rc Hardness																
Average Before Tempering	46	53	55	46	45	51	51	47	51	45	46	52	54	45	47	54
Range Before Tempering	37/49	50/55	53/56	43/51	39/49	41/54	47/53	41/50	40/55	39/47	40/48	41/54	50/57	38/48	37/49	50/57
Average After Tempering	44	49	50	48	48	48	47	48	47	46	48	48	50	47	47	49
Range After Tempering	37/49	46/50	47/52	40/50	44/50	46/50	43/48	42/50	45/50	43/49	46/50	43/49	49/51	45/49	44/50	47/51
Visual Scale on Part 0=heavy; 10=none	8	8	8	8	8	8	8	8	10	8	8	8	8	8	8	8
Visual Coil Tightness on Form Arbor -10=Tight; 0=Loose	7	8	8	7	5	4	4	7	4	4	4	4	6	7	5	7
Drop Test																
Gage Spacing	.150	.175[a]	.175[a]	.250	.250	.245	.258	.258	.258	.250	.250	.264	.140	.270	.270	.175[a]
Parts Not Dropping	32	46	36	50	50	36	38	50	30	35	37	48	40	24	50	48
Gage Spacing Before Draw-Hi	.158	.185	.180	.270	.278	.265	.274	.274	.274	.258	.266	.285	.145	.278	.290	.180
Parts Dropping Before Draw	48	48	50	50	47	48	46	48	48	47	45	50	38	48	49	50
Gage Spacing After Draw-Lo	.150	.175	.170	.202	.187	.158	.175	.180	.168	.195	.187	.143	.140	.210	.197	.170
Parts Not Dropping A/Draw-Lo	40	39	50	39	50	48	41	35	49	46	37	50	49	41	49	18
Gage Spacing After Draw-Hi	.160	.185	.175	.222	.227	.174	.185	.188	.184	.215	.203	.153	.150	.240	.217	.175
Parts Dropping After Draw-Hi	49	42	50	43	45	50	48	49	47	48	46	49	49	50	49	21

Table A 1.2b

FACTORIAL DATA SUMMARY
440-B STAINLESS MATERIALS
(50 Parts Checked)

Test Number	1	2	3	4	5	6	7	8	9	10	11	12	13	14	15	16
Free Gap																
Before Draw Average	.252	.266	.286	.251	.252	.263	.267	.251	.254	.251	.264	.252	.270	.270	.278	.268
Before Draw Range	.245/ .280	.240/ .295	.270/ .310	.230/ .272	.240/ .285	.240/ .280	.235/ .285	.235/ .270	.200/ .290	.240/ .275	.250/ .280	225/ .285	.262/ .290	.240/ .300	.250/ .320	.260/ .290
After Draw Average	.381	.426	.437	.308	.317	.443	.405	.403	.402	.355	.354	.470	.451	.351	.346	.417
After Draw Range	.340/ .435	.390/ .515	.380/ .455	.275/ .345	.300/ .330	.400/ .465	.365/ .430	.310/ .540	.340/ .440	.310/ .400	.330/ .400	.425/ .520	.420/ .490	.310/ .415	.320/ .375	.380/ .450
After 50 Lap Strokes Avg.	.388	.440	.420	.312	.317	.434	.417	.403	.424	.351	.352	.466	.457	.367	.347	.424
After 50 Lap Strokes Range	.350/ .450	.360/ .530	.410/ .470	.270/ .400	.300/ .340	.410/ .470	.400/ .430	.250/ .500	.380/ .470	.340/ .410	.340/ .380	.420/ .520	.410/ .500	.320/ .400	.320/ .380	.400/ .460
After 1000°F Test Avg.	.352	.390	.410	.289	.293	.406	.398	.395	.333	.329	.305	.454	.340	.304	.441	.410
After 1000°F Test Range	.340/ .380	.300/ .500	.360/ .440	.210/ .340	.270/ .320	.380/ .450	.380/ .430	.300/ .490	.360/ .430	.300/ .380	.270/ .340	.420/ .500	.280/ .380	.270/ .330	.380/ .500	.360/ .460
After 25 Lap Strokes Avg.	.399	.464	.441	.316	.318	.441	.422	.394	.415	.370	.361	.471	.460	.381	.358	.407
After 25 Lap Strokes Range	.360/ .460	.420/ .580	.390/ .480	.260/ .360	.300/ .350	.400/ .480	.400/ .460	.320/ .460	.360/ .460	.320/ .470	.340/ .400	.420/ .540	.420/ .500	.340/ .420	.330/ .420	.380/ .460
After 1200°F Test Avg.	.373	.457	.470	.296	.302	.422	.406	.386	.391	.346	.323	.456	.453	.343	.317	.420
After 1200°F Test Range	.360/ .410	.400/ .560	.420/ .530	.260/ .330	.280/ .340	.380/ .480	.380/ .440	.320/ .460	.350/ .430	.320/ .440	.300/ .350	.410/ .510	.410/ .500	.310/ .360	.260/ .380	.380/ .490

Table A1.2c

FACTORIAL DATA SUMMARY
440-B STAINLESS MATERIALS
(50 Parts Checked)

Test Number	1	2	3	4	5	6	7	8	9	10	11	12	13	14	15	16
Light																
Percent Before 1000°F Test	10	3	1	15	17	9	10	11	9	14	10	12	2	11	12	3
Point Range B/4 1000°F Test	72-96	84-96	94-96	74-90	72-89	79-94	82-92	80-89	83-94	78-87	79-92	81-87	90-96	82-92	77-94	84-96
Percent After 1000°F Test	10	2	3	12	14	9	6	9	10	14	11	7	14	14	1	3
Point Range Aft. 1000°F Test	62-95	89-96	87-96	79-94	76-89	83-93	83-92	79-96	82-95	77-90	80-90	82-96	79-89	74-89	87-96	88-96
Percent Before 1200°F Test	6	2	0	11	10	4	5	8	9	11	12	6	5	6	7	5
Point Range B/4 1200°F Test	84-94	89-96	91-96	80-90	82-96	85-96	84-96	81-94	83-89	81-91	79-89	79-96	83-96	84-95	81-95	80-96
Percent After 1200°F Test	8	3	3	8	11	5	6	3	10	7	7	5	8	11	12	6
Point Range Aft. 1200°F Test	84-95	89-96	83-96	83-94	77-93	84-96	82-96	87-95	77-93	83-95	84-96	82-96	74-96	77-94	76-94	82-96
Thermal Stability Test--Percent Open Light																
Percent Open Light Before 600°F Test																
Arbor #1, Ring #1	16			5	9			5		19	21	15	6			1
Ring #2	17			4	25			15		8	12	6	4			2
Arbor #2, Ring #1	6			11	10			17		8	19	0	7			2
Ring #2	6			12	10			18		11	17	2	2			0
Arbor #3, Ring #1	15			1	9			6		12	15	10	1			2
Ring #2	11			7	16			3		12	16	3	0			0
Arbor #4, Ring #1	0			4	17			5		17	8	8	0			5
Ring #2	5			8	15			0		8	9	15	1			6
Arbor #5, Ring #1	3			9	18			10		9	2	1	2			4
Ring #2	3			9	16			9		2	2	4	0			0

ORIGINAL PAGE IS
OF POOR QUALITY

Table A 1.2d
FACTORIAL DATA SUMMARY
440-B STAINLESS MATERIALS
(50 Parts Checked)

Test Number	1	2	3	4	5	6	7	8	9	10	11	12	13	14	15	16
Percent Open Light After 600°F Test																
Arbor #1, Ring #1	9			10	9	5				11	21	8	8			0
Ring #2	12			8	10	14				10	16	6	8			1
Arbor #2, Ring #1	4			16	10	12				7	9	1	0			2
Ring #2	5			11	10	14				11	14	2	1			0
Arbor #3, Ring #1	10			0	10	6				9	15	10	1			3
Ring #2	11			9	9	7				12	15	2	0			0
Arbor #4, Ring #1	0			8	12	5				12	7	7	7			8
Ring #2	0			8	13	0				9	11	15	2			7
Arbor #5, Ring #1	3			9	10	10				10	2	2	6			4
Ring #2	4			9	16	9				7	2	2	4			5
Percent Open Light After 800°F Test																
Arbor #1, Ring #1	14			21	16	8				22	23	14	8			12
Ring #2	19			17	27	19				19	21	14	10			3
Arbor #2, Ring #1	15			20	16	17				20	20	4	16			7
Ring #2	8			20	15	17				17	21	12	8			5
Arbor #3, Ring #1	16			17	25	15				17	23	12	7			8
Ring #2	17			20	19	14				15	21	12	15			6
Arbor #4, Ring #1	8			18	15	18				22	26	16	3			14
Ring #2	8			14	19	5				19	19	21	4			10
Arbor #5, Ring #1	11			18	29	15				17	15	9	9			10
Ring #2	15			10	22	16				12	15	14	12			7
Percent Open Light After 1000°F Test																
Arbor #1, Ring #1	**			**	**	**				**	**	**	**			**
Ring #2	**			**	**	**				**	**	**	**			**
Arbor #2, Ring #1	**			**	**	**				**	**	**	**			**
Ring #2	**			**	**	**				**	**	**	**			**
Arbor #3, Ring #1	**			**	**	**				**	**	**	**			**
Ring #2	**			**	**	**				**	**	**	**			**
Arbor #4, Ring #1	**			**	**	**				**	**	**	**			**
Ring #2	**			**	**	**				**	**	**	**			**
Arbor #5, Ring #1	**			**	**	**				**	**	**	**			**
Ring #2	**			**	**	**				**	**	**	**			**

** denotes ring collapse

Table A 1.2e

FACTORIAL DATA SUMMARY
44C-B STAINLESS MATERIALS
(50 Parts Checked)

Test Number	1	2	3	4	5	6	7	8	9	10	11	12	13	14	15	16
Thermal Stability Test--Free Gap																
Free Gap Before 600°F Test																
Arbor #1, Ring #1	.440			.280	.320			.420		.380	.360	.480	.480			.460
Ring #2	.420			.320	.260			.350		.380	.360	.480	.480			.450
Arbor #2, Ring #1	.410			.340	.320			.380		.390	.340	.580	.440			.400
Ring #2	.410			.340	.320			.360		.360	.340	.520	.480			.390
Arbor #3, Ring #1	.400			.300	.380			.460		.380	.360	.460	.420			.400
Ring #2	.410			.280	.330			.460		.380	.340	.460	.420			.400
Arbor #4, Ring #1	.350			.320	.300			.400		.340	.360	.360	.490			.400
Ring #2	.360			.340	.310			.400		.340	.370	.460	.460			.400
Arbor #5, Ring #1	.370			.310	.330			.450		.380	.380	.480	.460			.460
Ring #2	.360			.310	.310			.460		.440	.380	.480	.460			.420
Free Gap After 600°F Test																
Arbor #1, Ring #1	.360			.310	.300			.400		.350	.340	.410	.400			.430
Ring #2	.360			.250	.340			.330		.340	.350	.400	.400			.440
Arbor #2, Ring #1	.360			.270	.310			.310		.360	.320	.480	.420			.390
Ring #2	.350			.280	.300			.310		.340	.330	.440	.420			.370
Arbor #3, Ring #1	.370			.310	.320			.380		.370	.340	.410	.380			.380
Ring #2	.370			.300	.360			.370		.360	.330	.400	.390			.380
Arbor #4, Ring #1	.310			.300	.300			.310		.320	.320	.430	.360			.380
Ring #2	.300			.310	.290			.320		.310	.320	.410	.370			.370
Arbor #5, Ring #1	.320			.300	.300			.380		.360	.360	.400	.460			.320
Ring #2	.320			.300	.300			.380		.420	.360	.400	.460			.400
Free Gap After 800°F Test																
Arbor #1, Ring #1	.380			.300	.300			.400		.340	.340	.400	.460			.440
Ring #2	.360			.240	.240			.340		.340	.340	.400	.460			.440
Arbor #2, Ring #1	.350			.280	.320			.300		.350	.330	.480	.360			.400
Ring #2	.360			.270	.310			.310		.340	.320	.430	.360			.390
Arbor #3, Ring #1	.370			.300	.300			.380		.370	.330	.380	.380			.380
Ring #2	.370			.300	.300			.380		.360	.320	.380	.380			.390
Arbor #4, Ring #1	.300			.290	.300			.320		.300	.320	.400	.400			.380
Ring #2	.300			.310	.320			.330		.320	.320	.390	.380			.380
Arbor #5, Ring #1	.300			.300	.280			.380		.360	.360	.380	.400			.420
Ring #2	.300			.300	.300			.370		.420	.360	.400	.420			.400

Table A 1.2e (Cont.)

FACTORIAL DATA SUMMARY
440-B STAINLESS MATERIALS
(50 Parts Checked)

Test Number	1	2	3	4	5	6	7	8	9	10	11	12	13	14	15	16
Free Gap After 1000°F Test																
Arbor #1, Ring #1	.160			.110	.060			.080		.120	.069	.070	.125			.130
Ring #2	.160			.070	.050			.090		.130	.074	.080	.130			.090
Arbor #2, Ring #1	.130			.090	.080			.060		.080	.073	.110	.115			.100
Ring #2	.130			.080	.060			.070		.080	.076	.120	.100			.100
Arbor #3, Ring #1	.100			.110	.080			.120		.100	.120	.100	.095			.100
Ring #2	.080			.110	.070			.120		.100	.125	.100	.091			.110
Arbor #4, Ring #1	.080			.060	.100			.090		.100	.085	.130	.085			.120
Ring #2	.090			.080	.100			.090		.070	.075	.130	.097			.180
Arbor #5, Ring #1	.120			.080	.070			.130		.120	.100	.120	.120			.140
Ring #2	.130			.090	.080			.120		.120	.098	.120	.125			.150

Appendix B
Ring Forming and Finishing
Process Sequence

Table B 1.a. Ring Forming and Finishing Process Sequence

HOT-FORMED ROLLED-STEEL STEP-GAP PLASMA WEDGE COMPRESSION RING

PRODUCT ENGINEERING SAMPLE ROUTING

SAMPLE PART NO _____ SAMPLE LINE NO _____ CHARGE NO _____

START DATE _____ QUANTITY _____ MATERIAL _____ SPECIAL OPERATIONS 3 6

CUSTOMER _____ MFG PART NO _____ 1 4 7 2 5 8

SEQ NO	OPERATION DESCRIPTION	DEPT NO	MACHINE NO	OPER CODE	TOOLING DESCRIPTION & SPECIFICATION	OPERATOR INSPECTOR INSTRUCTIONS	OPER	READINGS 2	3	OPER NO	DATE	PCS IN	PCS OUT	OPER ACCEPT	INSPECT ACCEPT
	Material				Chrome vanadium alloy steel										
	Raw stock size				160 x .200										
	Cam form/heat shape arbor				C-33754-702-191										
	Annealing mandrel				D-36231-147										
	Closing band				D-36231-640										
	Arbor major diameter				5 392										
	Arbor minor diameter				5 260										
	Distortion				132										
	Annealing mandrel major diameter				5 500										
	Annealing mandrel minor diameter				5 315										
	Distortion				.185										
	Average OD after cam form				5.726										
	Length of ring				17 989"										
010	Setup	639	HI-25		Groom machine										
		639	HAM-2		Straighten stock										
		639	LE-65		Set crossfeed										
					Use 50/23 sprocket 195/rev										
					Set HI-25 parameters on generator										
					See operation 020 or run sheet on generator										
					Adjust feed rollers and clearances to allow stock to										
					feed freely through roller system										
					Quench solution Cp-2750F 1 5 Detrex										
					Refractometer reading (12.5 to 1) pH 8.5 to 9 5										
					Process spec PR-1052										

Table B 1.b. Ring Forming and Finishing Process Sequence

HOT-FORMED ROLLED-STEEL STEP-GAP PLASMA NITRIDE COMPRESSION RING

PRODUCT ENGINEERING SAMPLE ROUTING

SAMPLE PART NO _____ SAMPLE LINE NO _____ CHARGE NO _____

START DATE _____ QUANTITY _____ MATERIAL _____ SPECIAL OPERATIONS 1 2 3 4 5 6 7 8

CUSTOMER _____ MFG PART NO _____

SEQ NO	OPERATION DESCRIPTION	DEPT NO	MACHINE NO	OPER CODE	TOOLING DESCRIPTION & SPECIFICATION	OPERATOR INSPECTOR INSTRUCTIONS	OPER READINGS 1	2	3	OPER NO	DATE	PCS IN	PCS OUT	OPER ACCEPT	INSPECT ACCEPT
020	Cold form	639	HI-25		Arbor-C-33754-702-191										
	Harden & slug				Stock 160 x .200										
					Set generator RF grid										
					Control--83										
					P'ate KV--12										
					Grid current-- 65										
					Plate--4										
					Power control--60										
					-ater pressure (coil)--48 to 50#										
					Plate to grid 3--16 2%										
					Water temperature--80°F										
					Frequency--360/400KC										
					Hardness--Rc 38+ (see note)	NOTE for higher hardness, higher temperatures are required. A pyrometer is required for temperature accuracy. Temperature is controlled by speed adjustment on generator adjustment									
					Adjust arbor speed to achieve pyro temp 1825+@ ±25°F										
					Arbor speed--12 RPM										
					Cutoff wheel--A-12D6S										
					RSS Norton 16" x 1" x 2.0"										
					Slug-- 2.0" + .020										
					Adjust height of wheel										
					.020 + .020 FC in 32-0-5 625 3858										
030	Remove nails				Remove nails by hand										
	Heat shape and draw				Use heat shape arbor >-36231										
					Collar 21H51-1A										
					Clamp band D-36231-S2)										
					Heat treat temp 1000°F										
					Heat treat time 1 hr										
					Air cool										
					Free gap .860 min										
					Hardness Rc 28-34 (see note)										
					Drop all rings through parallel holder 32-H-4										
					Parallel block 32-H-3										
					Gage block 32-626										
					Nails .006 min										

C - 2

ORIGINAL PAGE IS
OF POOR QUALITY

Table B 1.c. Ring Forming and Finishing Process Sequence

HOT-FORMED ROLLED-STEEL STEP-GAP PLASMA WEDGE COMPRESSION RING

PRODUCT ENGINEERING SAMPLE ROUTING

SAMPLE PART NO _____ SAMPLE LINE NO _____ CHARGE NO _____

START DATE _____ QUANTITY _____ MATERIAL _____ SPECIAL OPERATIONS 1 2 3 4 5 6 7 8

CUSTOMER _____ MFG PART NO _____

SEQ NO	OPERATION DESCRIPTION	DEPT NO	MACHINE NO	OPER CODE	TOOLING DESCRIPTION & SPECIFICATION	OPERATOR INSPECTOR INSTRUCTIONS	OPER READINGS 1	2	3	OPER NO	DATE	PCS IN	PCS OUT	OPER ACCEPT	INSPCT ACCEPT
040	Rough grind	107			First grind .156 ± .005										
					Second grind .1537 ± .0004										
					Third grind .153 ± .0003										
050	Degrease														
060	Grind EC	639			.030 ± .003 end clearance										
					32-0-5 565										
					Remove equal amounts from each side										
					Deburr gap ends										
					Wheel BA-600155										
					BMJA Cincinnati										
070	Grind to finish width	111	GRS 29		Grind in retainers to .1507$ ± .0002$ (This operation is to reduce the pinch marks from the grind operation. We can go to two up width variation)										
080	Degrease														
090	Step cut				See ID-1063 print										
	deburr				.030 ± .003 end clearance in 32-0-5565 ring gage before										
	inspect				step gap machining										
					Cut step .108 ± .003 each side of gap										
					Deburr gap ends										
					Gap ends should not stick up more than .003" or .002"-										
					Check rings 100%										
100	Dustoff	111	GRS 18		Grind in retainers to .1505 ± .0002$										
					67-6-1 retainers NOTE This operation is to true up ring in step gap area										
110	Degrease														
120	Pigmark	639			Pigmark if required										
					See print										

Table B 1.d. Ring Forming and Finishing Process Sequence.

HOT-FORMED ROLLED-STEEL STEP-GAP PLASMA WEDGE COMPRESSION RING

PRODUCT ENGINEERING SAMPLE ROUTING

SAMPLE PART NO _____ SAMPLE LINE NO _____ CHARGE NO _____

START DATE _____ QUANTITY _____ MATERIAL _____ SPECIAL OPERATIONS 1 2 3 4 5 6 7 8

CUSTOMER _____ MFG PART NO _____

SEQ NO	OPERATION DESCRIPTION	DEPT NO	MACHINE NO	OPER CODE	TOOLING DESCRIPTION & SPECIFICATION	OPERATOR INSPECTOR INSTRUCTIONS	OPER READINGS 1	2	3	OPER NO	DATE	PCS IN	PCS OUT	OPER ACCEPT	INSPECT ACCEPT
130	Turn OD		LE-204		Tape no 0077-Rc9										
					Bushing 12-N 5 530										
					Collars 21-MR-5 5295										
					Tools-Kennametal DNMG 432-KC 910										
					Tool holder DDPNN-161 1" x 1" x 6"										
					Rough turn 5 515 + 010 dia										
					Groove depth .014										
					Face land top .023										
					Face land bottom 003										
					Turn speed 92 RPM										
					Infeed 002										
					Stagger gaps										
					Free gap 860 max										
				*	Fill gaps with lead before turn										
					Hot dia 5.851										
					Grind dia 5 510 ± 0005										
140	Dustoff	111	GRS 18		Dust off in retainers .14975 ± 00025										
150	Degrease														

* After this step, the coating operation occurs.

Table B 1.e. Ring Forming and Finishing Process Sequence.

HOT-FORMED ROLLED-STEEL STEP-GAP PLASMA WEDGE COMPRESSION RING

PRODUCT ENGINEERING SAMPLE ROUTING

SAMPLE PART NO _____ SAMPLE LINE NO _____ CHARGE NO _____

START DATE _____ QUANTITY _____ MATERIAL _____ SPECIAL OPERATIONS 3 _____ 6 _____

CUSTOMER _____ MFG PART NO _____ 1 _____ 4 _____ 7 _____

2 _____ 5 _____ 8 _____

SEQ NO	OPERATION DESCRIPTION	DEPT NO	MACHINE NO	OPER CODE	TOOLING DESCRIPTION & SPECIFICATION	OPERATOR INSPECTOR INSTRUCTIONS	OPER 1	READINGS 2	3	OPER NO	DATE	PCS IN	PCS OUT	OPER ACCEPT	INSPECT ACCEPT
160	Katanoka grind	111			Closing sleeve 69TM-EXP-1-5 512-D-2										
					Clamp pad headstock 21GM-1-16										
					Clamp pad tailstock 21GM-1-26										
					Guillotine blade 28TM-1-1R										
					Guillotine guide 28TM-1-2R										
					Locating fingers 28TM-1-10										
					Degrease template 78GM-X01073 (located in Samples)										
					Diamond 05-A19										
					Gage 5 510										
					Profile template 1°30'/2°15'										
					Ring specifications										
					Grind dia ref 5 510										
					End clearance .020 + .003										
					Barrel height .006/ .0012										
					.005 from bottom edge										
					Crown surface opposite pipmark										
					- .030 from C/L + .020										
170	Degrease	111													
180	Grind EC	639			Bevel gap ends before size to prevent chipping coating										
					when sizing rings .005/ .015 x 45° as specified										
					Remove overspray in gap ends by hand with diamond hone (see Foreman)										
					Check end clearance										
					32-0-5 500 gage .320 + .003--specified EC .020/.040										
					Remove stock equally from each end										
					Each step should be .085/ .095 in length.										
185	Bevel OD edges	639			Bevel bottom edge 45° + 2°										
					Stone and bright boy edges										
					Stone ID edge to remove burr and scale										

Table B 1.f. Ring Forming and Finishing Process Sequence.

HOT-FORMED ROLLED-STEEL STEP-GAP PLASMA WEDGE COMPRESSION RING

PRODUCT ENGINEERING SAMPLE ROUTING

SAMPLE PART NO _____ SAMPLE LINE NO _____ CHARGE NO _____

START DATE _____ QUANTITY _____ MATERIAL _____ SPECIAL OPERATIONS 1 2 3 4 5 6 7 8

CUSTOMER _____ MFG PART NO _____

SEQ NO	OPERATION DESCRIPTION	DEPT NO	MACHINE NO	OPER CODE	TOOLING DESCRIPTION & SPECIFICATION	OPERATOR INSPECTOR INSTRUCTIONS	OPER	READINGS 1	2	3	OPER NO	DATE	PCS IN	PCS OUT	OPER ACCEPT	INSPECT ACCEPT
190	Radius lap	639			Pot 69-L-2 & 500 ID											
					Collars 21-LA-5											
					Spacers 21-LA-5											
					Lap arbor 6-M-5											
					Gage 32-0-5.500											
					Barrel face contour .0006 to .0012, .005 from bottom											
					See print											
210	Degrease															
220	Nylon brush				Bushing 12-M-5 500											
					Collars 21-M-5 4995											
					Spacers 72-M-5 450 x .125											
					Remove burrs and sharp edges											
230	Grind side angles				Wall ass'y 88-MH-2 (AR)											
	Deburr and demag				"A" dia & 500											
					Angle measurement 32-R-1 10-D 8682 10°13'											
					Width measurement fixture 32-M-9-1 with gage											
					Spacer 32-M-10-1R- 1178											
					Gage master 32-M-12-1F 14560											
					Set dial ind + 0055											
					Ring reading .000+ 103											
					Flatness spec 32-A-1-5.500											
240	Finish inspect															
250	Phosphate coat															
	Demag															
	Oil dip (dry oil)															

Appendix C
Wear Test Profiles

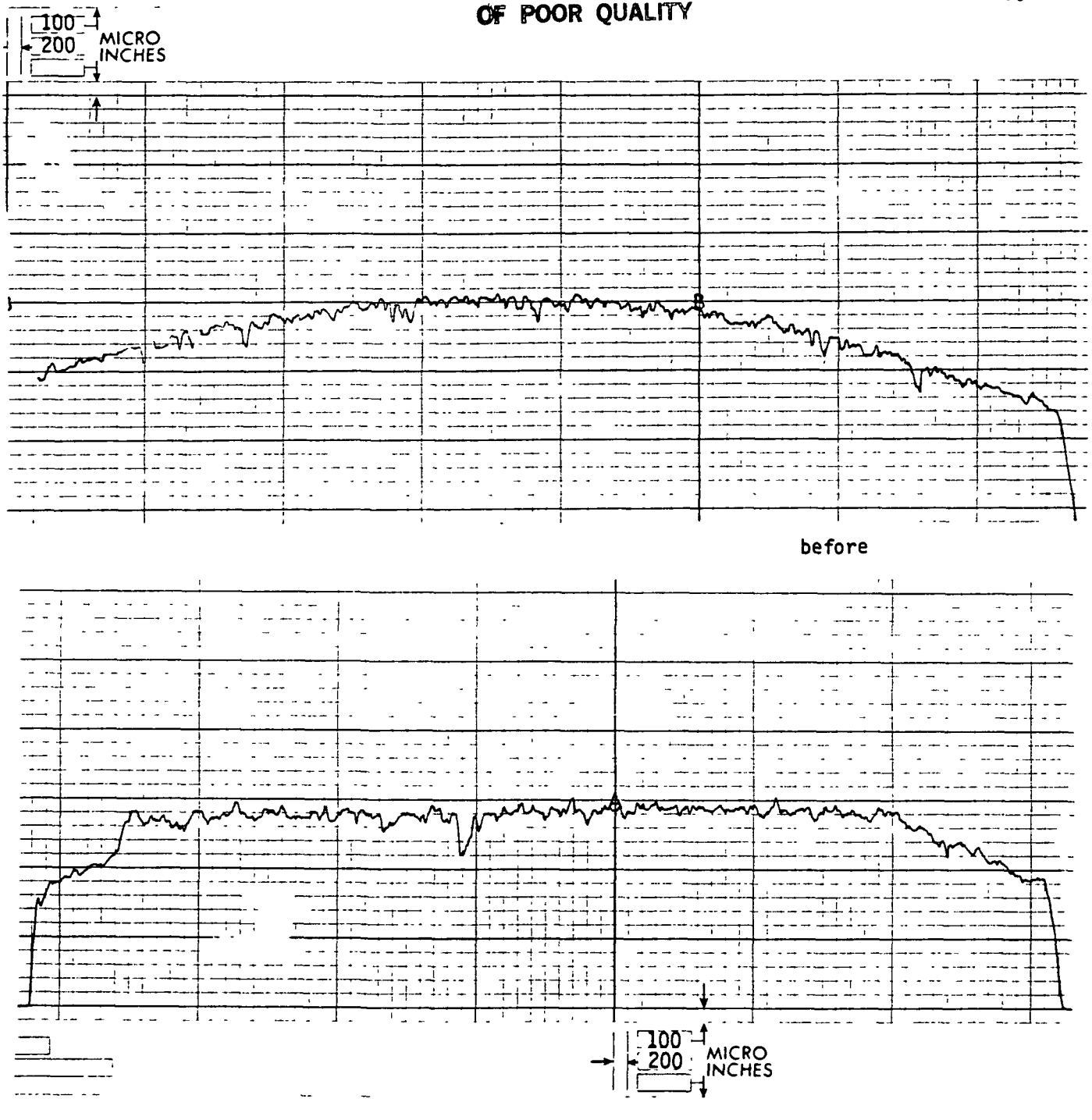

Figure C 1. Profiles of Plasma Sprayed and Graded ZrO_2/28.5-35 TiO_2/2-4 Y_2O_3 Coating Before and After Wear Testing.

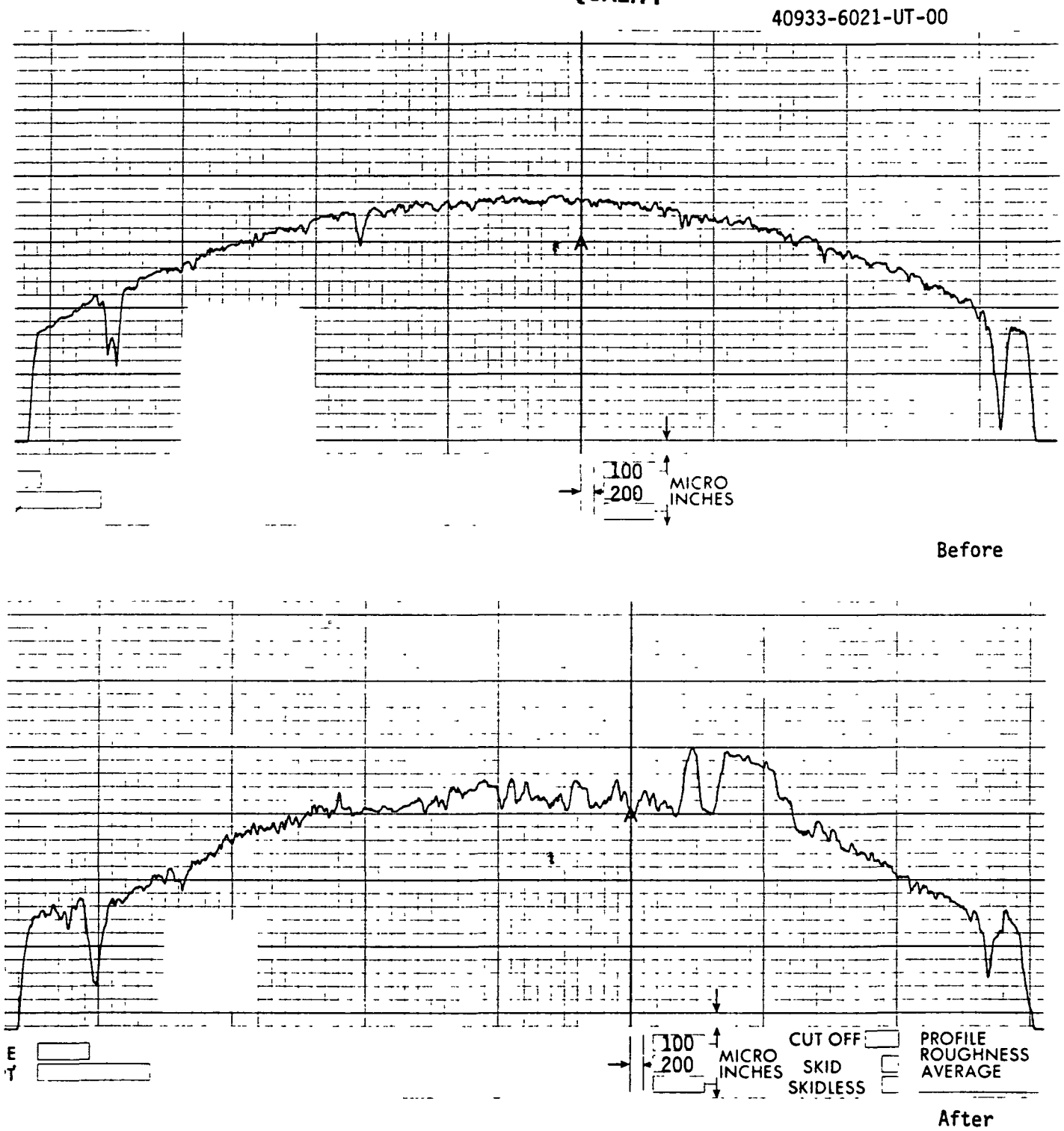

Figure C 2. Profiles of Plasma Sprayed Non-graded $ZrO_2/TiO_2/Y_2O_2$ Coating Before and After Wear Testing Against a Tungsten Carbide Cylinder Sleeve. This is an Example of One of the Better Non-graded $ZrO_2/TiO_2/Y_2O_2$ Coatings. However, this Coating Performed Poorly in Thermal Shock Testing.

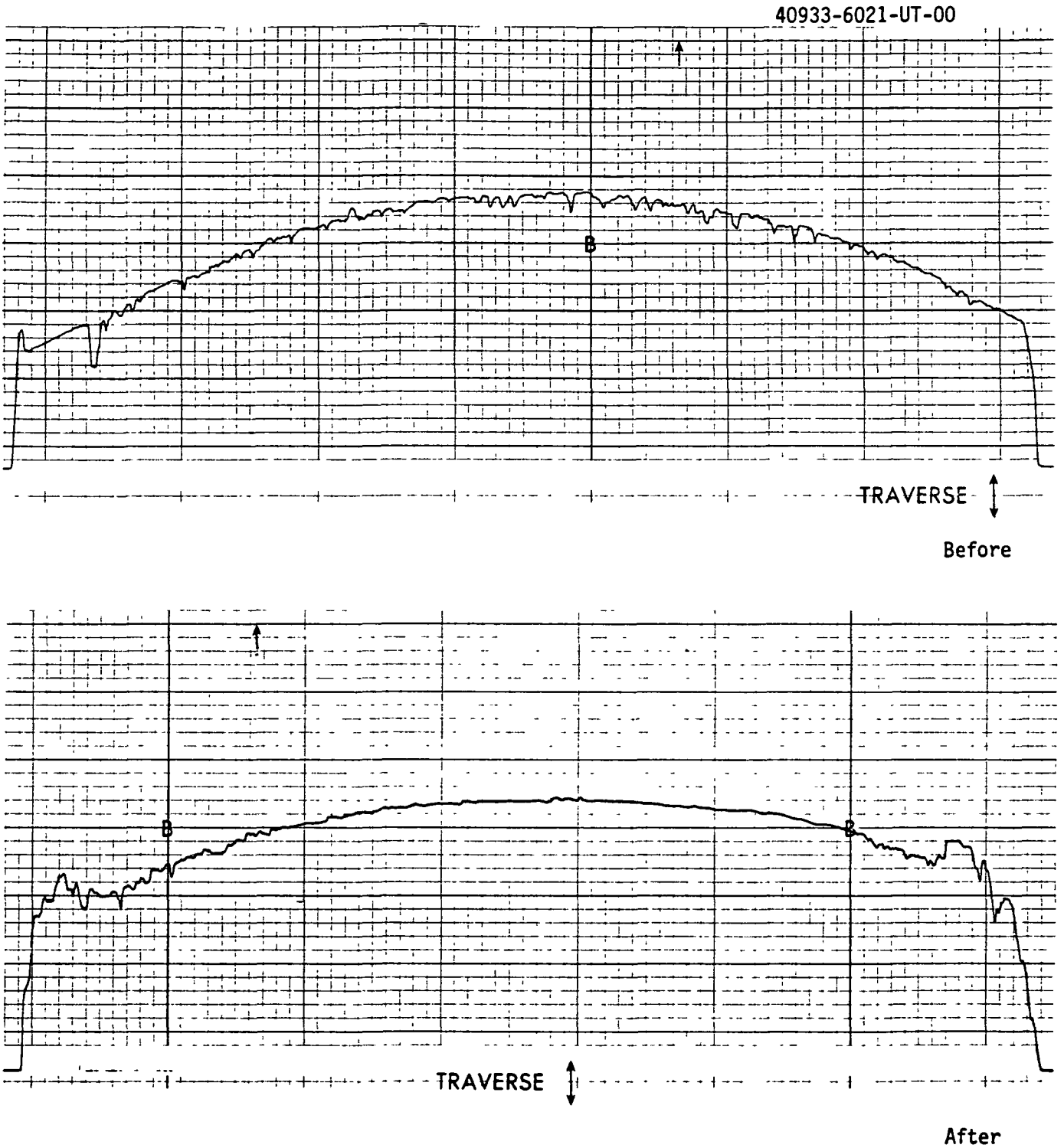

Figure C 3. Profiles of Plasma Sprayed $Al_2O_3/TiO_2/Y_2O_3$ Coating Before and After Wear Testing Against a Tungsten Carbide Cylinder Sleeve. This is an Example of One of the Better $Al_2O_3/TiO_2/Y_2O_3$ Coatings. This coating performed well in thermal shock testing.

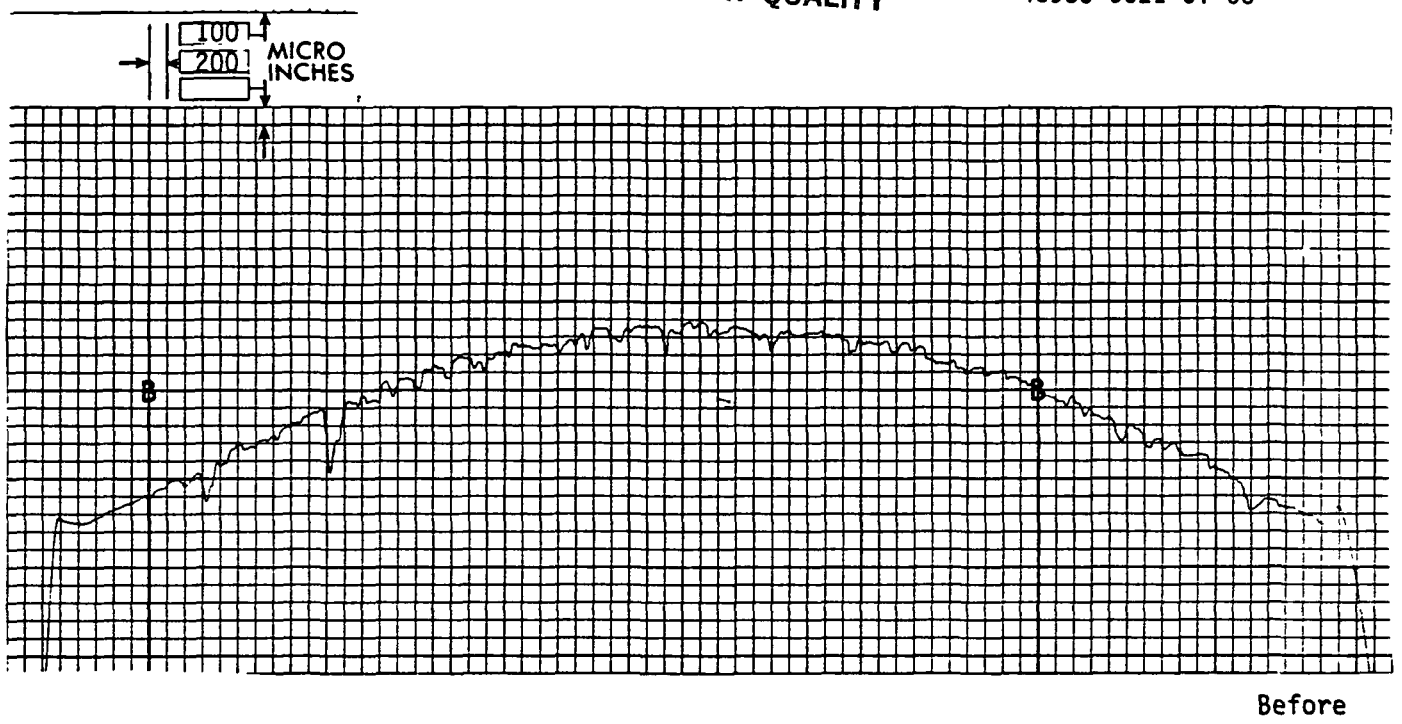

Before

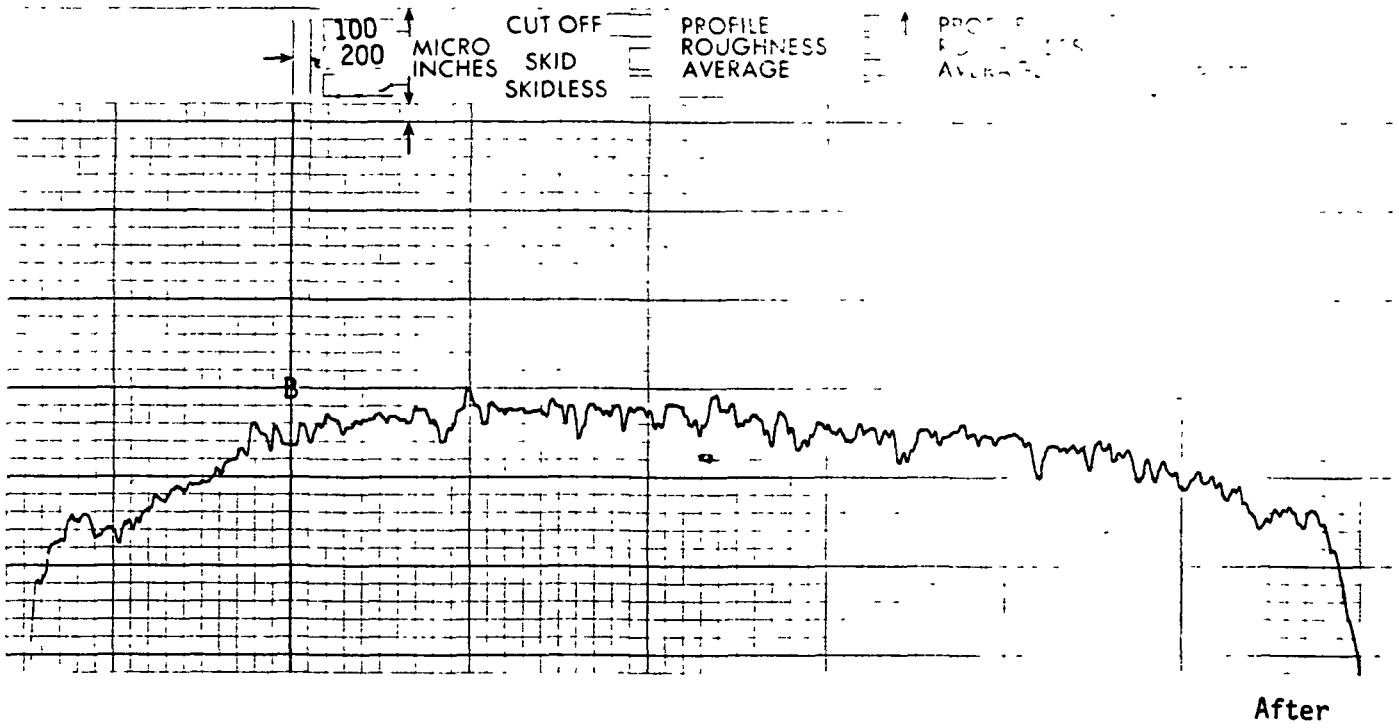

After

Figure C 4. Profiles of Plasma Sprayed $Al_2O_3/TiO_2/Y_2O_3$ Coating Before and After Wear Testing Against a Tungsten Carbide Cylinder Sleeve. This is an example of one of the poorer $Al_2O_3/TiO_2/Y_2O_3$ Coatings. This Coating Performed Well in Thermal Shock Testing.

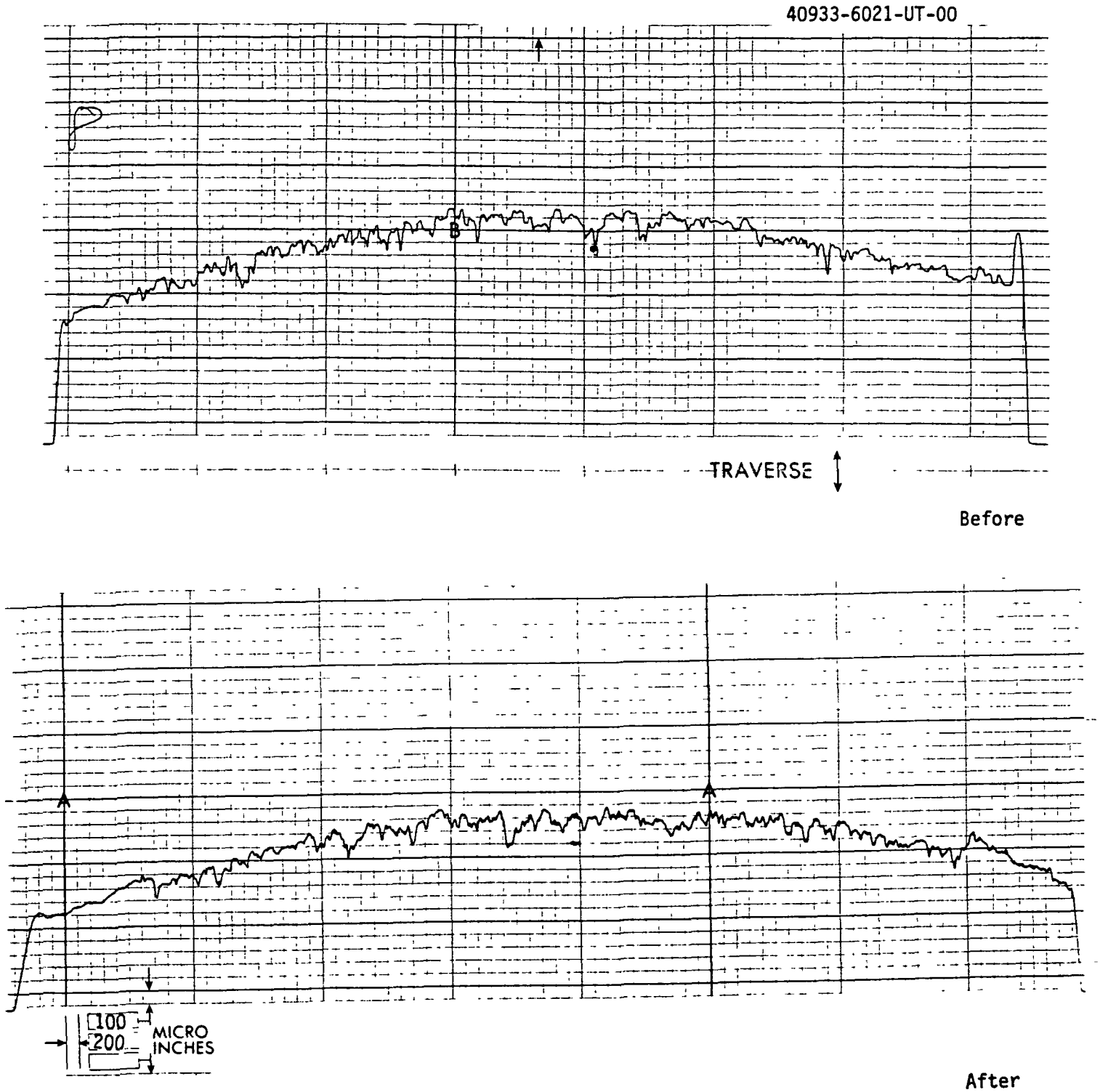

Figure C 5. Profiles of Plasma Sprayed Non-graded $ZrO_2/TiO_2/Y_2O_2$ Coatings Before and After Wear Testing Against a Tungsten Carbide Cylinder Sleeve. This is One of the Poorer Non-graded $ZrO_2/TiO_2/Y_2O_2$ Coatings. This Coating Performed Poorly in Thermal Shock Testing.

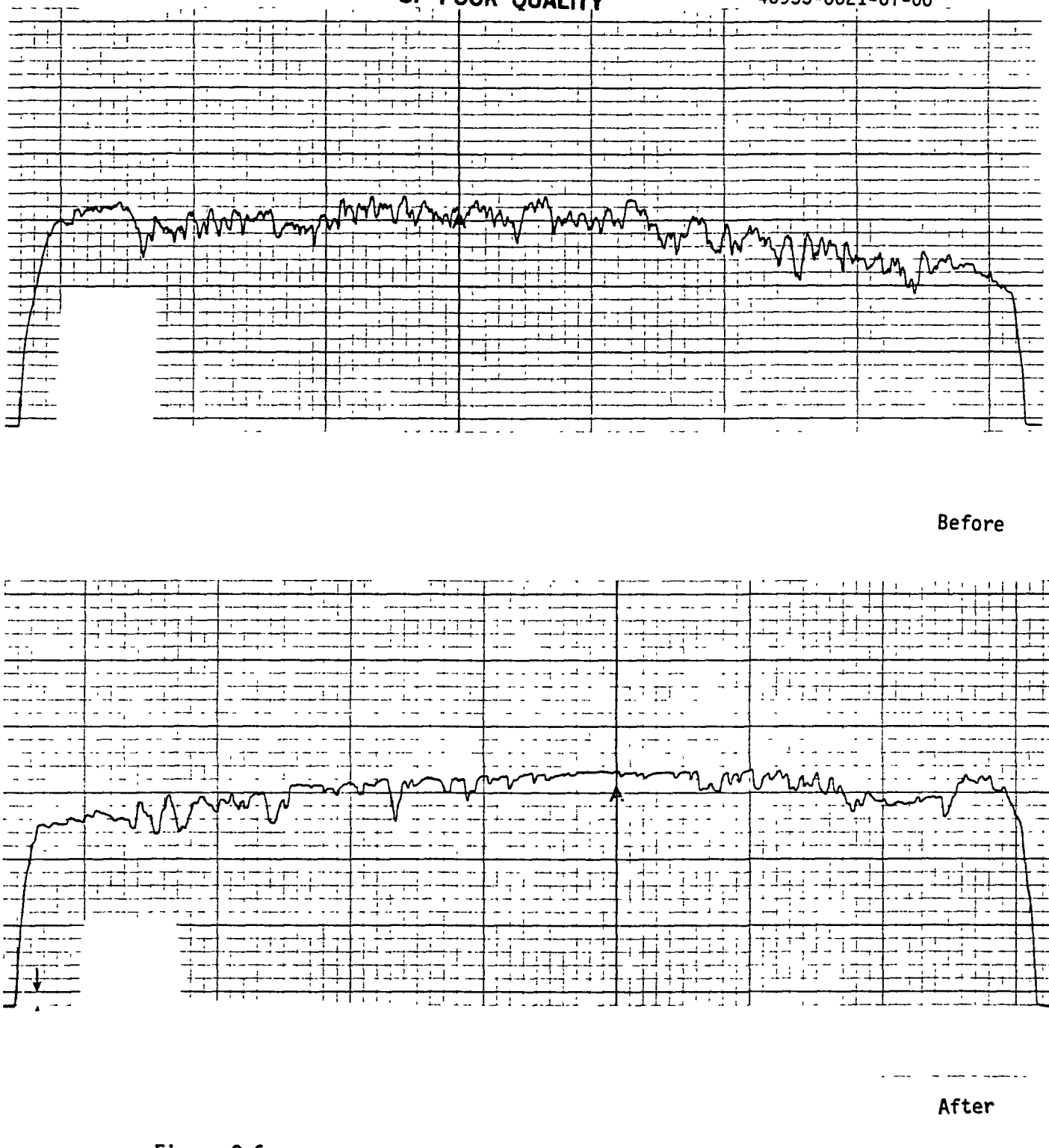

Figure C 6. Profile of Plasma Sprayed $Al_2O_3/TiO_2/ZrO_2/Y_2O_3$ Coating Before and After Wear Testing Against a Tungsten Carbide Cylinder Sleeve. This Coating Performed Poorly in Thermal Shock Testing.

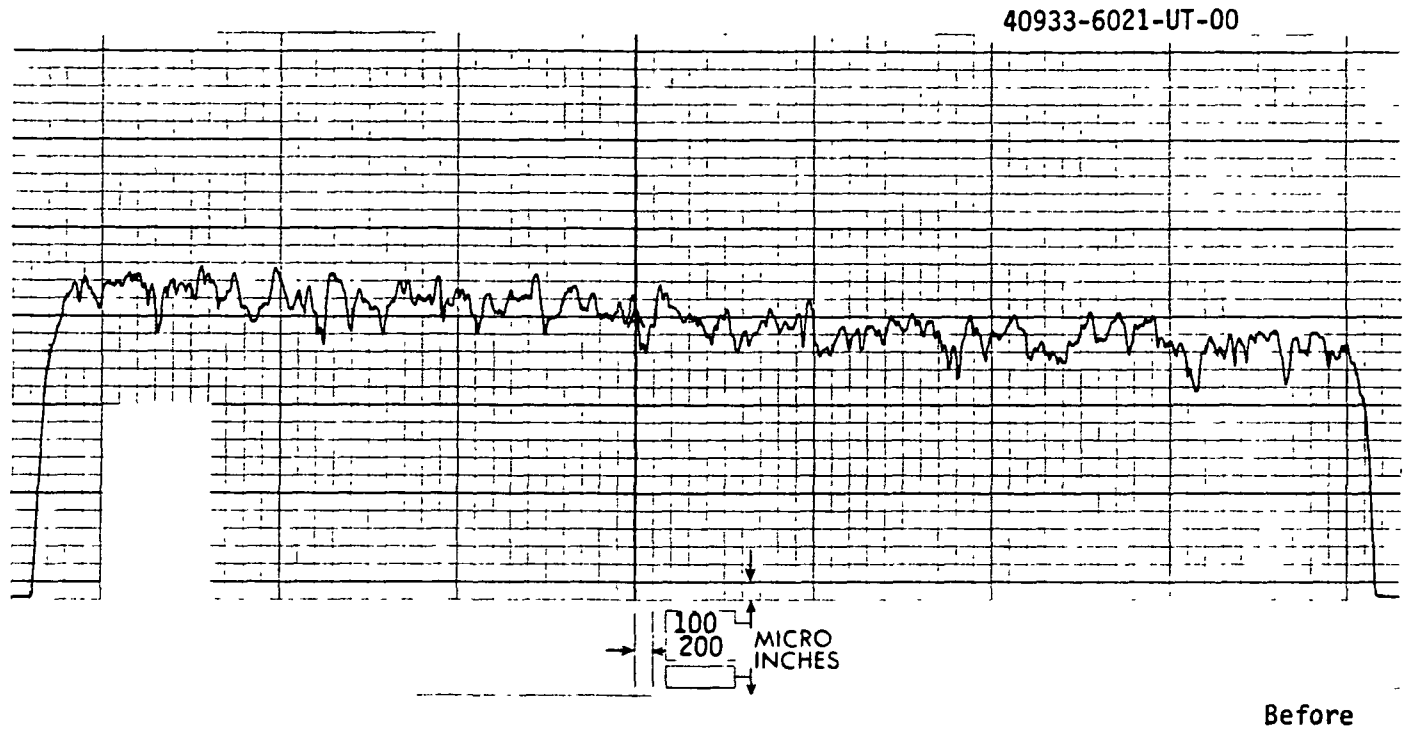

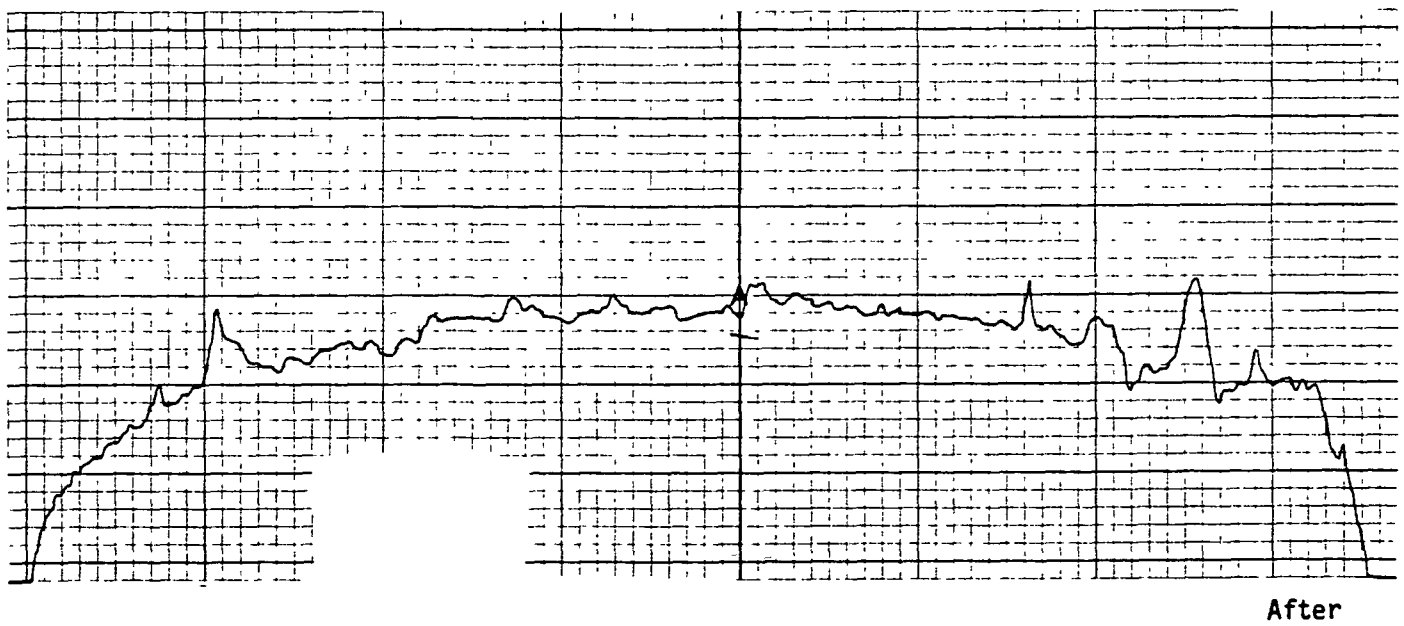

Figure C 7. Profiles of Low Pressure Plasma Sprayed Molybdenum-based Coating Before and After Wear Testing. This Coating Performed Poorly in ThermalShock Testing.

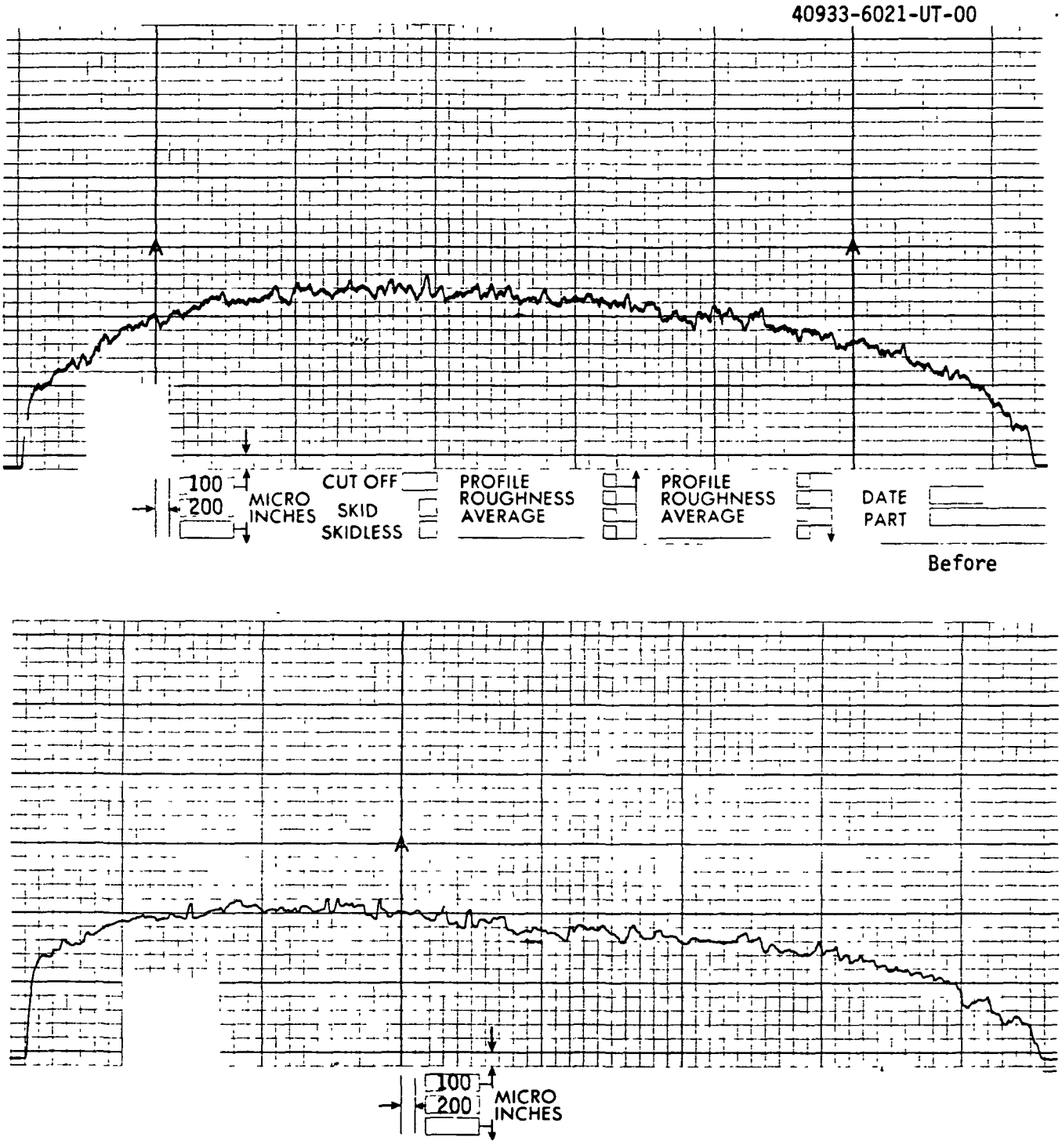

Figure C 8. Profiles of Molybdenum-based PTA Coating Before and After Wear Testing. This Coating Performed Poorly in Thermal Shock Testing.

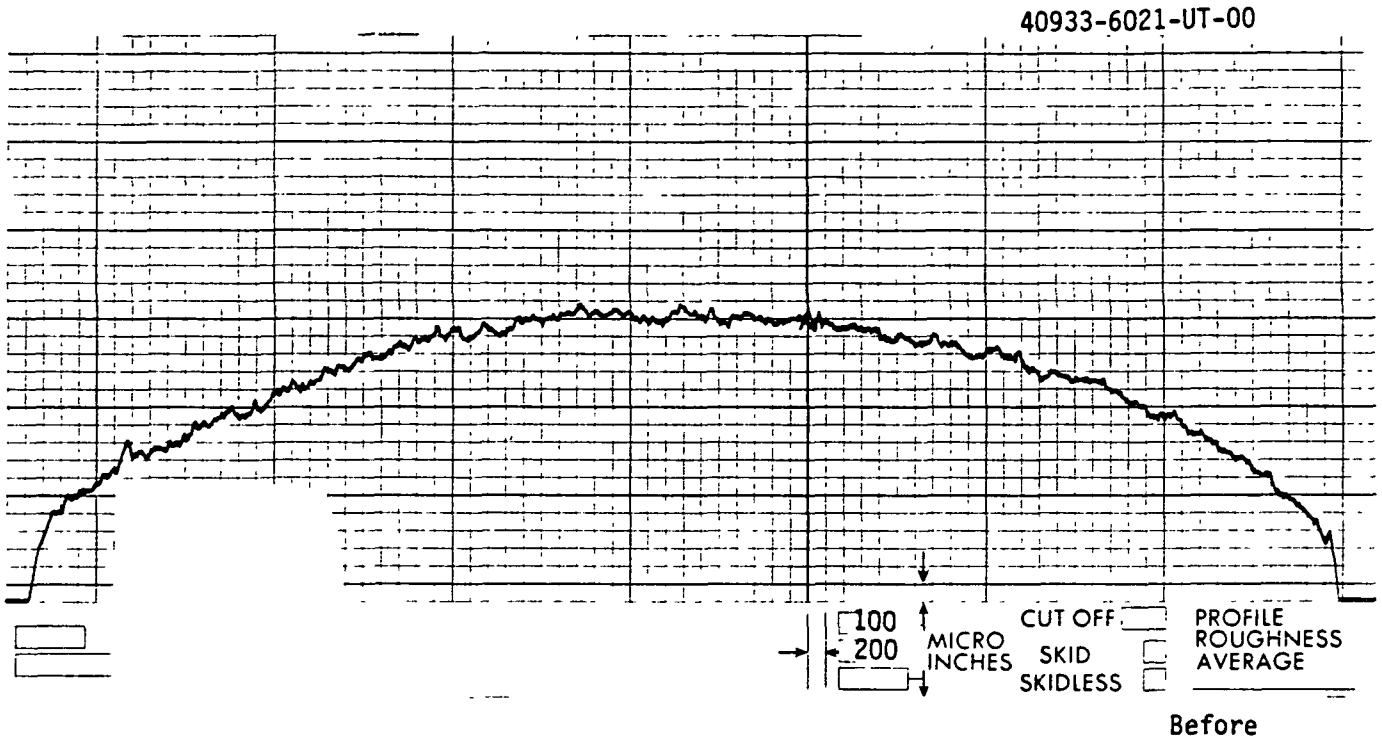

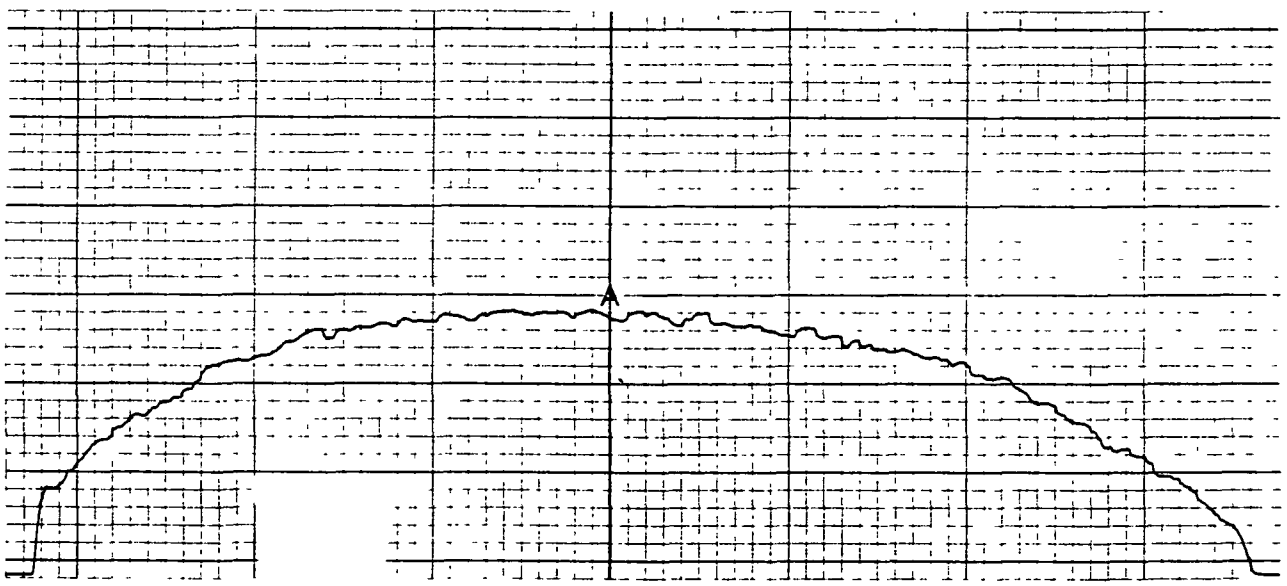

Figure C 9. Profiles of Tungsten Carbide PTA Coating Before and After Wear Testing. This Coating Performed Poorly in Thermal Shock Testing.

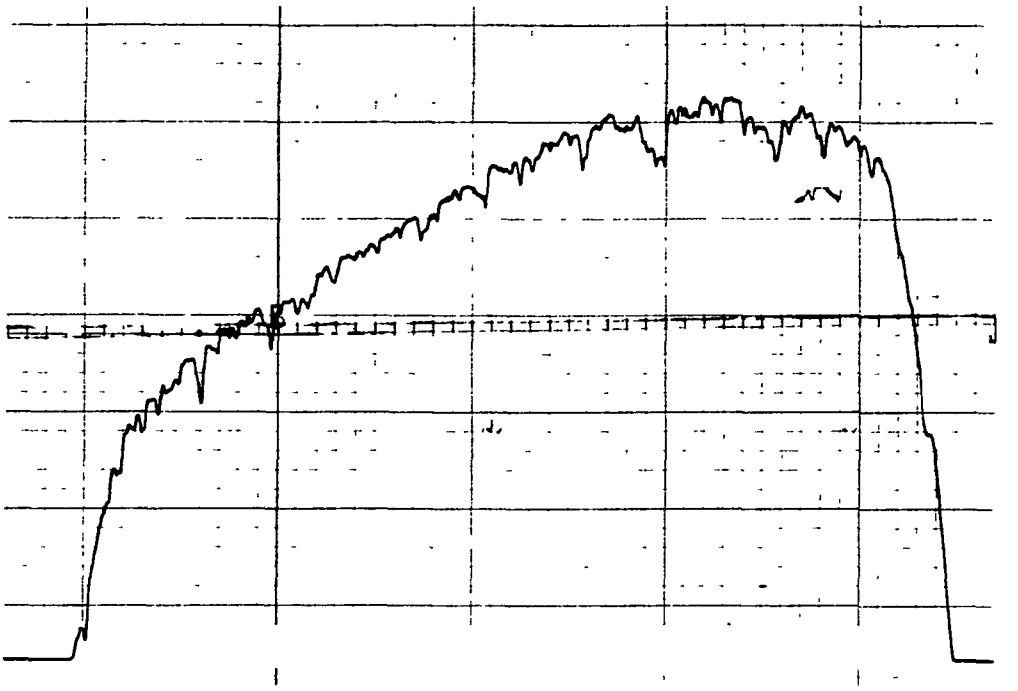

Before

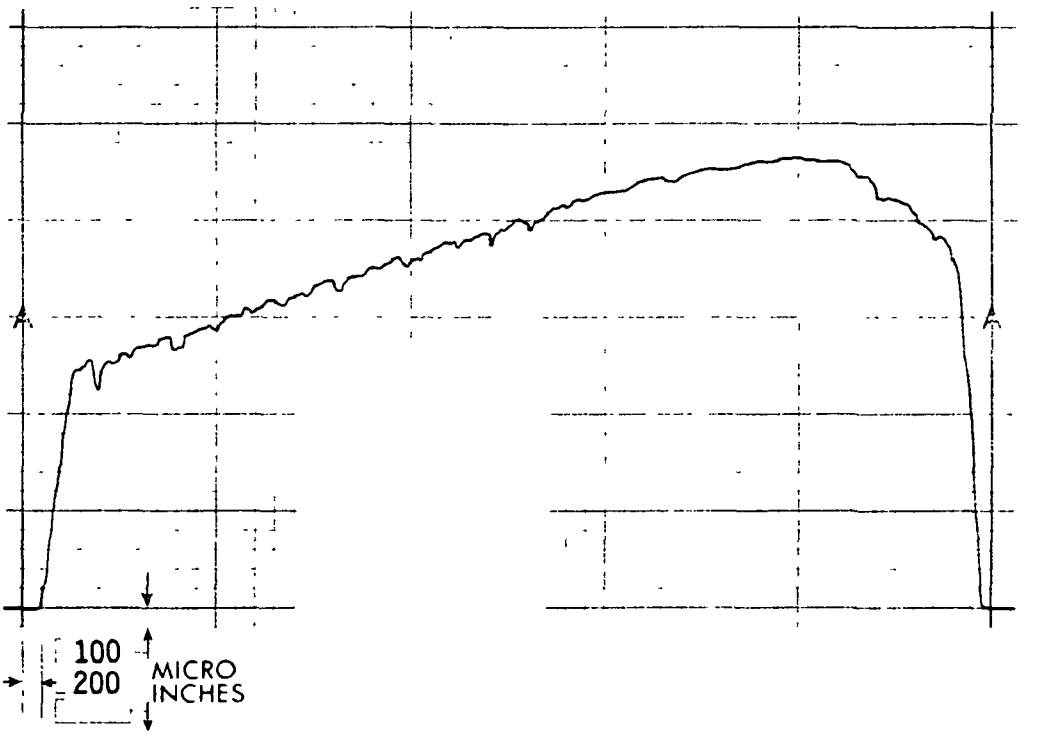

After

Figure C 10. Profiles of Non-graded $ZrO_2/TiO_2/Y_2O_3$ Coating Before and After Wear Testing Against a Si_3N_4 Cylinder Liner.

REFERENCES

1. Kamo, R., and Bryzik, W., "Ceramic for Adiabatic Turbocompound Deisel Engines," presented at International symposium on Ceramic Components for Engines, Hakone, Japan, Oct 1983.

2. Kingery, W. D., Bowen, H. K., and Uhlmann, D. R., Introduction to Ceramics, John Wiley and Sons, New York, (1976).

3. Gerdeman, D. A., and Hecht, N. L., Arc Plasma Technology in Materials Science, Springer - Verlag, New York, (1972).

4. Stott, F. H., Stevenson, C. W., and Wood, G. C., "Friction and Wear Properties of Stellite 31 at Temperatures from 293 to 1073°K," Metals Technology, February 1977, pp. 66-74.

1 Report No	2 Government Accession No	3 Recipient's Catalog No
CR-175058		

4 Title and Subtitle	5 Report Date
Improved Piston Ring Materials for 650°C Service	March 1985
	6 Performing Organization Code

7 Author(s)	8 Performing Organization Report No
W. D. Bjorndahl	40933-6021-UT-00
	10 Work Unit No

9 Performing Organization Name and Address	11 Contract or Grant No
Energy Division, TRW Inc. One Space Park Redondo Beach, CA 90278	DEN3-307
	13 Type of Report and Period Covered
	Contractor Report
12 Sponsoring Agency Name and Address	14 Sponsoring Agency Code
U.S. Department of Energy Office of Vehicle and Engine R&D Washington, DC 20585	DOE/NASA/0307-1

15 Supplementary Notes

Final Report. Prepared under Interagency Agreement DE-AI01-80CS50194. Project Manager, H. Yacobucci, Propulsion Systems Division, NASA Lewis Research Center, Cleveland, Ohio 44135.

16 Abstract

A program to develop piston ring material systems which will operate at 650°C was performed. In this program, two candidate high temperature piston ring substrate materials, Carpenter 709-2 and 440B, were hot formed into the piston ring shape and subsequently evaluated. In a parallel development effort ceramic and metallic piston ring coating materials were applied to cast iron rings by various processing techniques and then subjected to thermal shock and wear evaluation. Finally, promising candidate coatings were applied to the most thermally stable hot formed substrate. The results of evaluation tests of the hot formed substrate show that Carpenter 709-2 has greater thermal stability than 440B. Of the candidate coatings, plasma transferred arc (PTA) applied tungsten carbide and molybdenum based systems exhibit the greatest resistance to thermal shock. For the ceramic based systems, thermal shock resistance was improved by bond coat grading. Wear testing was conducted to 650°C (1202°F). For ceramic systems, the alumina/titania/zirconia/yttria composition showed highest wear resistance. For the PTA applied systems, the tungsten carbide based system showed highest wear resistance.

17 Key Words (Suggested by Author(s))	18 Distribution Statement
Piston ring coatings, ceramic coatings, Piston ring substrates, High Temperature Piston Ring Materials	Unclassified, unlimited

19 Security Classif (of this report)	20 Security Classif (of this page)	21 No of pages	22 Price*
Unclassified	Unclassified	106	

*For sale by the National Technical Information Service, Springfield, Virginia 22161